Title
The role of Mitofusin (Mfn) in the pathogenesis of Parkinson's disease and myopathy/frontotemporal dementia

Author
Zhang, Ting

Publication Date
2018

Peer reviewed|Thesis/dissertation

UNIVERISTY OF CALIFORNIA

Los Angeles

The role of Mitofusin (Mfn) in the pathogenesis of Parkinson's disease and myopathy/frontotemporal dementia

A dissertation submitted in partial satisfaction

of the requirements for the degree Doctor of Philosophy in

Molecular, Cellular, and Integrative Physiology

by

Ting Zhang

2018

ABSTRACT OF THE DISSERTATION

The role of Mitofusin (Mfn) in the pathogenesis of

Parkinson's disease and myopathy/frontotemporal dementia

by

Ting Zhang

Doctor of Philosophy in

Molecular, Cellular, and Integrative Physiology

University of California, Los Angeles, 2018

Professor Ming Guo, Chair

As life expectancy prolongs, the incidence of neurodegenerative diseases continues to rise. The pathogenesis of neurodegenerative diseases is poorly understood and there is no effective long-term therapy. This thesis focus on two neurodegenerative disease: Parkinson's disease (PD), the second most common neurodegenerative disease and inclusion body myopathy, Paget disease with frontotemporal dementia (IBMPFD) caused by Valosin-containing protein (VCP) mutants. Recent studies accentuate the key role of mitochondrial dysfunction in disease-onset. Mitochondrial fusion/fission is critical for mitochondrial integrity with Mitofusins (Mfn) control

the initial step of fusion. We found that Mitofusins are key targets in both Parkinson's disease and in disease by VCP mutants.

Mutations in *PTEN-induced putative kinase 1 (PINK1)* and *parkin* cause autosomal recessive PD. Genetic studies indicate *PINK1* and *parkin* function in a common pathway and negatively regulate Mfn. In chapter two, we identify VCP as a suppressor for *PINK1* and *parkin* mutants and its suppression is achieved through Mfn degradation. VCP missense mutations cause IBMPFD and other neurodegenerative disorders. The pathological mechanism of IBMPFD is not clear and there is no cure. we generated an *in vivo* IBMPFD model in *Drosophila*, which recapitulates disease pathologies in human patients; we demonstrated common VCP disease mutants act as hyperactive alleles and found that VCP inhibitors reverse the disease pathology in *in vivo* disease models as well as in patients' fibroblasts. Our results strongly suggest VCP inhibitors have therapeutic value.

Mitofusins are key substrates of ubiquitin E3 ligase Parkin. Yet the exact mechanism of the ubiquitination is not well-understood. In chapter three, we identified critical lysine sites for Mitofusin ubiquitination by Parkin in *Drosophila* as well as in mammalian cells. Flies harboring mutated lysine sites display severe tissue defects. Parkin-mediated mitophagy plays a major role in mitochondrial quality control. Lysine mutants delay Parkin-mediated degradation of Mitofusins and mitophagy. Our results uncover the important regulatory role of Mitofusins in mitochondrial quality control and tissue health.

Together, our work demonstrates that utilizing *Drosophila* and human cells, we could establish reliable *in vivo* and *in vitro* models of neurodegenerative disease, unravel novel disease mechanism and identify therapy for these devastating diseases.

The dissertation of Ting Zhang is approved.

Baljit S. Khakh

Michael Alan Teitell

Yibin Wang

Ming Guo, Committee Chair

University of California, Los Angeles

2018

TABLE OF CONTENT

LIST OF FIGURES

ACKNOWLEDGEMENTS

I would like to first thank my mentor, Dr. Ming Guo, for giving me tremendous guidance and support in my journey in science. Ming's willingness and skills in mentoring trainees impress me always. I was trained as a neurologist and did not have much experience in basic science when I finished my master's degree in China. Yet she took me in the lab, taught me the basic fly genetic skills, discussed the data I had and patiently led me into the field. During my Ph.D. study, she rigorously trained me in critical thinking and reasoning, high quality data production and presentation, and obtaining a vision of the big picture. More importantly, she always encourages me to my goal in study neurodegenerative disease in academia. Her devotion in patient care and enthusiasm in scientific discovery keeps inspiring me. She is always my role model.

I would like to thank my committee member Dr. Yibin Wang, Dr. Baljit S. Khakh and Dr. Michael A. Teitell for great advice and mentorship. I really appreciate their time, help and input to guide me in both science and career. I would also like to thank Dr. David C. Chan and Dr. Bruce A. Hay for input and guidance in my projects.

I would like to thank my husband, Thomas, for his love and support throughout my Ph.D. study. His encouragement for me to pursue my dream is invaluable to me. His willingness to share the responsibility of taking care of our children help me enormously every single day. Whatever happens, he is always there for me. I would like to thank my dearest sons, Seth and Leo. The ecstasy, the joy and the "chaos" they bring to me are irreplaceable. I would also like to thank my parents, Yuemin Zhou and Zhengqiang Zhang for their unconditioned love to support my decisions in life as well as in career. They will always be there for me when I need help. I couldn't thank them enough for what they have sacrificed to let me pursue my dream.

I could like to thank the previous and present Guo lab members, Mark W. Dodson, Haiqun Jia, Hansong Deng, Michael Lizzio, Prajal Patel, Lok Kwan Leung, Huan Yang, Junyi Zhu, Pallavi Lamba and Chak Lon Kuang for their help, support and friendship.

Last but not the least, I would like to thank UCLA dissertation year fellowship for funding the work.

Chapter two is a version of Ting Zhang, Prashant Mishra, Bruce Hay, David Chan and Ming Guo, "VCP inhibitors relieve Mitofusin-dependent mitochondrial defects due to VCP disease mutants" published in eLife, 2017 Mar 21, doi: 10.7554 PMID:28322724. We would like to thank HanSong Deng for first noting the suppression of *PINK1* mutant phenotype by VCP overexpression, Dr. Tzu Kang Sang from the National Tsing Hua University, Taiwan, for the VCP disease mutants allele flies, Dr. Hugo Bellen from the Baylor College of Medicine for the kind gift of pCasper-Mfn-HA flies and Dr. C.K. Yao from Academia Sinica, Taipei, for pCasper-Mfn-eGFP construct and Dr. Frank A. Laski for the microtome usage.

Chapter three is a version of manuscript prepared for submission. Ting Zhang, Moon Yong Cha, David Chan and Ming Guo, "A single Lysine is critical for Ubiquitination and Degradation of Mitofusion by Parkin". We would like to thank Dr. Hugo Bellen from the Baylor College of Medicine for *mfn* mutant flies, Dr. Alexander Whitworth for anti-Mfn antibody, Rainbow transgenic for generating transgenic fly strains, Dr. C. K. Yao from Academia Sinica, Taipei, for pCasper-Mfn-HA construct, Dr. David Chan for mouse Parkin CDS, human Mfn1 CDS, wildtype and Mfn1 Mfn2 double knockout MEFs, Dr. Mark Cookson for Hela cells, Dr. Richard Youle for the pCHAC-mitoKeima construct, Dr. Frank A. Laski for the microtome usage, Dr. Brue A. Hay for discussion and revising the manuscript.

BIOGRAPHIC SKETCH

Ting Zhang

Education

INSTITUTION AND LOCATION	DEGREE	MM/YY	FIELD OF STUDY
University of California, Los Angeles	Ph.D. Candidate	09/12-present	Molecular, Cellular & Integrative Physiology
Shanghai Jiao Tong University, China	M.S.	06/08	Neurology
Shanghai Jiao Tong University, China	M.D.	06/06	Clinical Medicine

Awards

2018 The Best Ph.D. Student Oral Presentation Award
UCLA Molecular, Cellular & Integrative Physiology Program Retreat

2017 The Best Oral Presentation (First Prize), Junior Research Talk Competition
UCLA Mitochondria Symposium, American Society for Cell Biology

2017 Dissertation Year Fellowship, UCLA Graduate Division

2016 Doctoral Student Travel Grants for Conferences, Professional Development and Off Campus Research, UCLA Graduate Division

2013 The Best Poster Award
UCLA Molecular, Cellular & Integrative Physiology Program Retreat

2013 Nonresident Tuition Scholarship, UCLA Graduate Division

2012 Nonresident Tuition Scholarship, UCLA Graduate Division

Publications

Zhang T, Cha MY, Chan D and Guo M. A single Lysine is critical for Ubiquitination and Degradation of Mitofusion by Parkin. In preparation.

Zhang T, Prashant M, Hay BA, Chan D and Guo M. (2017) VCP inhibitors relieve Mitofusin-dependent mitochondrial defects due to VCP disease mutants. **eLife**, 10.7554 PMID:28322724.

Zhang T, Guo M. In vivo *Drosophila* Model of IBMPFD. In preparation, **Bio-protocol**.

Kandul NP, **Zhang T**, Hay BA and Guo M. (2016) Selective removal of deletion-bearing mitochondrial DNA in heteroplasmic *Drosophila*. **Nature Communication**,7,13100. PMID: 27841259.

Dodson M, **Zhang T**, Jiang CA, Chen SD, and Guo M. (2011) Roles of the *Drosophila* LRRK2 homolog in Rab7-dependent lysosomal positioning. **Human Molecular Genetics**, 21:1350-1363. PMID: 22171073.

Cao L*, **Zhang T***, Xin Q, Wang Y, Bai L, Lu GQ, Ma JF, Zhang J, Ding JQ, and Chen SD. (2008). The Prevalence of LRRK2 Gly2385Arg Variant in Chinese Han Population with Parkinson's disease. **Movement Disorders**, 22(16): 2439-2443. *Co-first Author PMID: 17960808.

Conference Attendance

Zhang T, VCP inhibitors reverse pathology caused by VCP disease mutants. (2018.2) Winner of the Best Student Talk at UCLA Molecular, Cellular & Integrative Physiology Program Retreat.

Zhang T, VCP inhibitors relieve Mfn-dependent mitochondrial defects due to VCP disease mutants. (2017.11) Winner of the Best Presentation at Junior Research Competition, UCLA Mitochondria Symposium.

Zhang T, Prashant M, Hay BA, Chan D and Guo M. VCP inhibitors relieve defects in degenerative disease caused by VCP mutations. (2017.2) Poster Presentation at UCLA Molecular, Cellular & Integrative Physiology Program Retreat.

Zhang T and Guo M, VCP expression suppresses mitochondrial defects in *PINK1* and *parkin* null mutants in *Drosophila*. (2016.7) Poster Presentation at 57th Annual *Drosophila* Research and the Allied Genetics Conference (TAGC), Orlando, Florida.

Zhang T, Yun J and Guo M, *PINK1* and *parkin* regulate mitochondrial morphology and apoptosis in *Drosophila* female germline. (2013.2) Winner of the Best Poster Award. Poster Presentation at UCLA Molecular, Cellular & Integrative Physiology Program Retreat.

Teaching Experience

2015 Fall Teaching assistant for Life Science (LS23L) Laboratory and Scientific Methods
Department of Molecular, Cell and Developmental Biology, UCLA, CA

2014 Fall Teaching assistant for Life Science (LS23L) Laboratory and Scientific Methods
Department of Molecular, Cell and Developmental Biology, UCLA, CA

Clinical Experience

2006-2008 Resident Doctor, Department of Neurology, Ruijin Hospital, Shanghai, China.

CHAPTER ONE

INTRODUCTION

1. Neurodegenerative disease

Neurodegenerative disease is a heterogenous group of diseases featured by progressive structural and functional deterioration of neuronal cells in central and peripheral nervous system (Gitler, Dhillon et al. 2017). Common neurodegenerative diseases are Alzheimer's disease (AD), Parkinson's disease (PD), Amyotrophic lateral sclerosis (ALS), Huntington's disease (HD), Multiple sclerosis (MS) and Charcot-Marie-Tooth disease (CMT); Less common neurogenerative diseases include Spinocerebellar ataxia (SCA) and Hereditary spastic paraplegia (HSP) (Gitler, Dhillon et al. 2017) . Despite the difference in prevalence, all neurogenerative diseases are devastating to both patients and caretakers, especially at late stages of the diseases. Currently there is no cure for neurodegenerative diseases which carry high socioeconomic costs and consume large amount of medical resources. The pathogenesis of neurodegeneration is not well-understood. Recent studies on mitochondrial dysfunction have greatly advanced our understanding. My thesis focuses on two neurodegenerative disease, Parkinson's disease (PD) and myopathy/frontotemporal dementia caused by p97/VCP mutants.

1.1 Parkinson's Disease

Parkinson's disease is the second most common of neurodegenerative disease (PD), featured by motor symptoms including muscle rigidity, bradykinesia (slow movement), resting tremor. Besides the classic motor symptoms, patients also have non-motor symptoms including

cognitive impairments, mood disorders and disturbance of sleep-wake cycles, as well as autonomic systems defects, such as constipation (Poewe 2008). The typical pathological feature is neuronal protein aggregates composed of α-synuclein, or lewy body. Braak et al have proposed a stereotyped caudal to rostral spread of lewy body pathology from lower brain stem (Stage 1) to the neocortex (Stage 6). Loss of dopaminergic neurons at substantia nigra, which corresponds to the classic motor symptoms, occurs at Stage 3 (Braak, Del Tredici et al. 2003; Dickson 2012). The broad spectrum of symptoms of Parkinson's disease and progression of pathology in both central and peripheral nervous system suggesting a subpopulation of neurons are vulnerable to common or multiple pathological stimuli and susceptible to degenerate.

The cause of Parkinson's disease is multifactorial. The fact that there are both familial and sporadic forms of PD highly suggest both environmental assaults and genetic susceptibility contribute to the onset of the disease. Earlier studies focused on the environmental risk factors such as MPTP (1-methyl-4-phenyl-1,2,3,6-tetrahydropyridine), paraquat and rotenone exposure that leads to acute parkinsonism (Dauer and Przedborski 2003). In the past decade, studies of monogenic familial Parkinson's disease have greatly advanced our understanding on pathogenesis of the disease. Mutations in *SNCA, Leucine-rich repeat kinase 2 (LRRK2), Vacuolar protein sorting 35 (VPS35), Eukaryotic translation initiation factor 4-gamma 1 (EIF4G1)* and *coiled-coil-helix-coiled-coil-helix domain containing 2 (CHCHD2)* cause the autosomal dominant forms of familial PD; mutations in *PTEN-induced kinase 1 (PINK1)*, *Parkin, DJ-1, ATP13A2* and *F-box only protein 7(FBXO7)* cause autosomal recessive forms of familial PD (Spatola and Wider 2014). Mutations in *glucocerebrosidase (GBA)* and *SMPD1* associate with increased risk of PD (Spatola and Wider 2014). Further studies in functions of these genes reveal two major aspects that defects in which could cause PD: Mitochondrial

dysfunction and endolysosomal dysfunctions (Plotegher and Duchen 2017). This thesis focuses on the mitochondrial dysfunction in the pathogenesis in Parkinson's disease.

1.2. Myopathy/frontotemporal dementia by VCP mutants

Mutations of *p97/cdc48/Valosin-containing protein (VCP)* cause hereditary degeneration in multiple systems including brain, muscles and skeletons in an autosomal dominant fashion (Watts, Wymer et al. 2004). *VCP* mutations cause full penetrance of inclusion body myopathy, Paget disease of the bone and frontotemporal dementia (IBMPFD); associate with 1-2% of cases of sporadic amyotrophic lateral sclerosis (ALS), hereditary spastic paraplegia (HSP) and Charcot-Marie-Tooth 2 (CMT2) disease (Abramzon, Johnson et al. 2012; de Bot, Schelhaas et al. 2012; Gonzalez, Feely et al. 2014). 90% of IBMPFD patients display myopathy, the primary and earliest symptom (Weihl, Pestronk et al. 2009). With progression of the disease, 50% of patients develop Paget's disease of bone, affecting the skull, spine, hips and long bones of all four limbs. One-third of the patients develop frontotemporal dementia (Kimonis, Mehta et al. 2008; Weihl, Pestronk et al. 2009).

VCP encodes a highly conserved and abundant AAA+ ATPase which participates in multiple cellular processes (Meyer, Bug et al. 2012). VCP has three major domains: the regulatory N domain, and the D1 and D2 ATPase domains (Figure 1-1A). VCP hexameric rings utilize the energy from ATP hydrolysis to promote protein and RNA homeostasis, often by directly or indirectly modifying the fate of ubiquitin-labeled proteins (Meyer, Bug et al. 2012). VCP functions in multiple contexts that include protein quality control in the endoplasmic reticulum (Ye, Meyer et al. 2001; Shih and Hsueh 2016), chromatin modification (Dobrynin, Popp et al. 2011; Vaz, Halder et al. 2013; Puumalainen, Lessel et al. 2014), endolysosomal

sorting (Ritz, Vuk et al. 2011), membrane fusion (Zhang, Zhang et al. 2014), autophagosome/lysosome function (Ju, Fuentealba et al. 2009; Johnson, Shu et al. 2015), ER protein translocation (DeLaBarre, Christianson et al. 2006; Weihl, Dalal et al. 2006), formation of stress granules (Buchan, Kolaitis et al. 2013) and ciliogenesis (Raman, Sergeev et al. 2015). VCP interacts with a number of co-factors to regulate these processes (Meyer, Bug et al. 2012; Meyer and Weihl 2014), making it challenging to identify the molecular basis of phenotypes associated with disease mutations.

Disease-causing, single missense mutations of VCP locates in either the N domain or the D1 domain. Among them, the R155H mutation is the most frequently identified, while the A232E mutation associates with the most severe clinical manifestation (Kimonis, Fulchiero et al. 2008; Ritson, Custer et al. 2010). *In vitro* assays show that disease mutants have enhanced ATPase activity (Weihl, Dalal et al. 2006; Manno, Noguchi et al. 2010; Niwa, Ewens et al. 2012; Tang and Xia 2013; Zhang, Gui et al. 2015). However, because VCP assembles as a hexamer, it is controversial whether disease mutants with increased ATPase activity cause disease through a dominant-active (Chang, Hung et al. 2011) or dominant-negative mechanism (Ju, Fuentealba et al. 2009; Ritz, Vuk et al. 2011; Bartolome, Wu et al. 2013; Kim, Tresse et al. 2013; Kimura, Fukushi et al. 2013).

2. Mitochondria

Mitochondria are double-membrane intracellular organelles that generate ATP through oxidative phosphorylation and provide the major energy source for living organisms. The respiration complexes (I-IV) on the inner membrane transport the electron meanwhile pumping the proton into the intermembrane spaces which forms the proton gradients that drives influx of

proton to the matrix through complex V (ATP synthase) and generates ATP (Friedman and Nunnari 2014). Besides the major role of energy production, mitochondria play critical roles in maintaining cellular homeostasis such as cellular Ca^{2+} buffering, reactive oxygen species (ROS) generation and elimination and apoptosis (Friedman and Nunnari 2014; Nickel, Kohlhaas et al. 2014). The integrity of mitochondria is critical to tissue health and mitochondrial dysfunction is one of the central themes in human diseases pathogenesis.

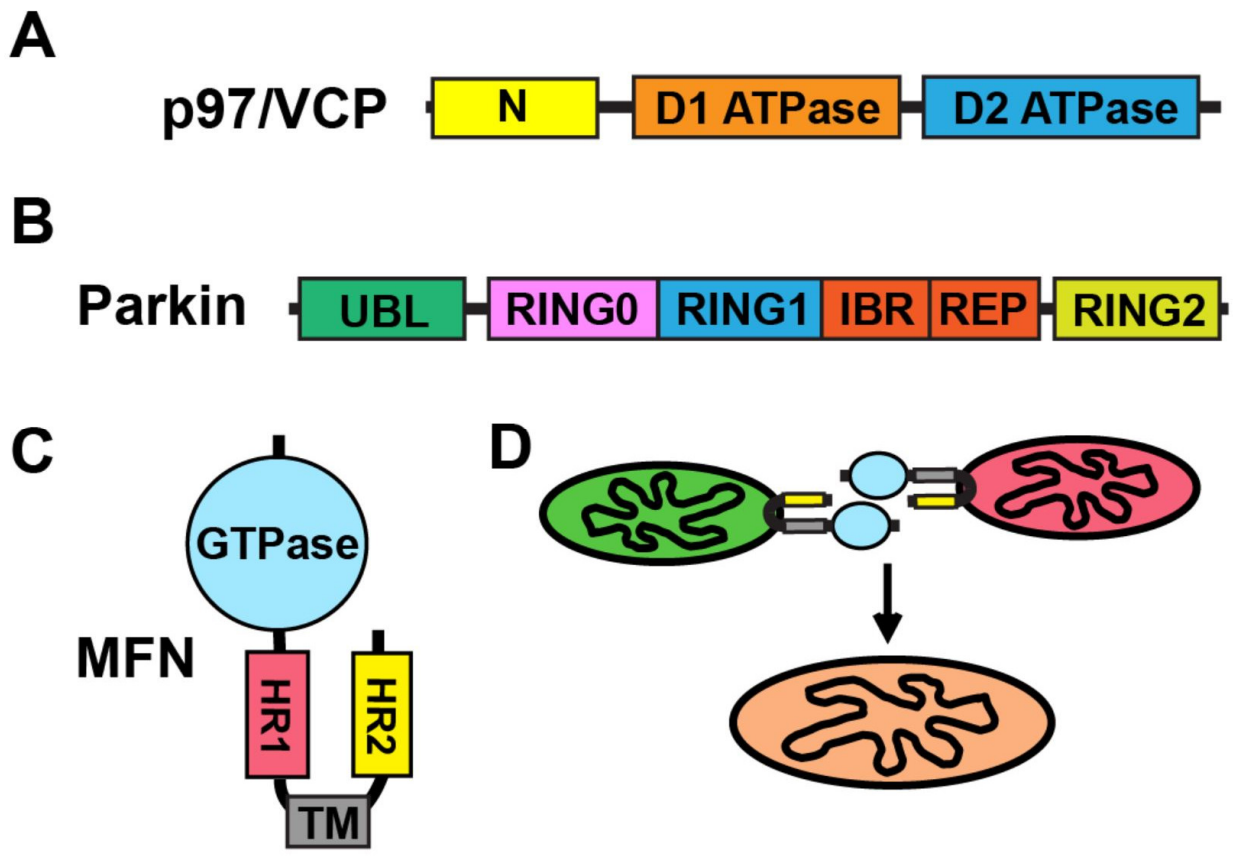

Figure 1-1: Diagrams of key molecules focused in the thesis. A) p97/VCP has a N-terminal protein interaction domain and two conserved ATPase domains. **B)** Parkin has an N-terminal Ubiquitin-like (UBL) domain, three RING domains, in-between ring domains (IBR) and repressor elements of Parkin (REP). **C)** Mitofusin is a highly conserved GTPase, with two heptad repeated domains and transmembrane domains. **D)** Two Mitofusin molecules form heterodimer and mediates mitochondrial fusion.

2.1. Mitochondrial DNA

Mitochondria is a unique cellular organelle as it is composed of proteins encoded by both mitochondrial DNA (mtDNA) and nuclear DNA. Human mitochondrial DNA is an approximately 16kb length genome, encodes 13 key proteins in oxidative phosphorylation, transfer RNAs and ribosomal RNAs. Mutations in the mitochondrial DNA or nuclear DNA encoding the mitochondrial proteins cause a variety of diseases affecting multiple organ systems in different age groups (Nunnari and Suomalainen 2012). Pathogenetic mitochondrial DNA mutations exists in the tissue as a heterogeneous state, a mixture of various copies numbers of wildtype and mutant mtDNA called heteroplasmy (Shoffner, Lott et al. 1990). Mitochondrial respiration functions are compromised when mutant mtDNA reache a certain threshold. Mutations in DNA polymeras gamma (*POLGA*) causes proofreading deficiency of mtDNA replication. Animals harboring POLGA mutants or mtDNA mutator mice accumulates both point mutations and deletion mutations and display premature aging phenotypes (Vermulst, Wanagat et al. 2008; Edgar, Shabalina et al. 2009). Accumulations of mtDNA deletions are detected in brain and heart of advanced aging population (Larsson 2010) as well as neurons in Parkinson's disease (Bender, Krishnan et al. 2006). However, further evidence is needed to establish the causality between mutant mtDNA and neurodegeneration.

2.2. Mitochondrial dynamics

Mitochondria constantly undergo morphology changes, a dynamic process called fusion and fission at physiological state and upon environmental stimuli. This process is intricately regulated by several highly conserved GTPases. Fusion is controlled by Mitofusin (Mfn) and Optic Atrophy gene1 (OPA1) proteins; Fission is controlled by Dynamin 1 like protein (DNML1 or DRP1)(Chan 2012). Mitofusins from two individual mitochondria form heterodimers controls

the initial steps of outermembrane fusion; OPA1 controls the fusion of inner membranes; Mitochondria fragment upon DRP1's translocation to mitochondria (Loson, Song et al. 2013).

Mitochondrial fusion and fission is essential to tissue health. Even Mild perturbation of fusion/fission balance has been associated with disease conditions. Loss of Mitofusins (Mfn1 and Mfn2, two homologues in mammals) leads to embryonic developmental defects (Chen, Detmer et al. 2003), skeletal muscle defects (Chen, Vermulst et al. 2010), neurodegeneration in cerebellum (Chen, McCaffery et al. 2007), cardiomyocyte defects (Song, Mihara et al. 2015) and cataract (Zhao, Wu et al. 2018); Mutations in Mfn2 causes Charcot-Marie-Tooth 2A (CMT2A), a hereditary peripheral neuropathy (Zuchner, Noureddine et al. 2005). Loss of OPA1 leads to embryo lethality (Song, Chen et al. 2007); Mutations in OPA1 causes autosomal dominant optic atrophy, a hereditary degeneration of retina ganglion cells (Alexander, Votruba et al. 2000). Loss of DRP1 leads to embryo lethality, synaptic formation defects in the brain and cardiomyopathy (Wakabayashi, Zhang et al. 2009; Song, Mihara et al. 2015); Mutations in DRP1 causes epileptic encephalopathy in child (Fahrner, Liu et al. 2016). All these findings suggest the key roles of mitochondrial fusion/fission balance in tissue developments, whereas how mitochondrial dynamics contributes to neurodegeneration requires further studies.

2.3. Mitochondrial quality control

Cells have evolved a delicate self-regulatory machinery to maintain mitochondrial homeostasis. Mitochondria fuse to exchange content and facilitate repair of their defective counterparts; If the damage is unrepairable, mitochondria will undergo asymmetric division to segregate the impaired mitochondria, which will be eliminated through a stepwise pathway, mitophagy(Shirihai, Song et al. 2015). The driving force for ATP synthesis, the proton gradient

generated through electron transport or membrane potential, is a sensitive marker for measuring mitochondrial health status. Uncoupler treatment (Carbonyl cyanide 3-chlorophenylhydrazone, CCCP) or inhibitions of respiration complexes (Oligomycin, Antimycin) directly dissipate the membrane potential; accumulation of mutant mtDNA, misfolded proteins, reactive oxidative species and iron depletion can cause mitochondrial dysfunction. Upon loss of mitochondrial membrane potential and stimuli mentioned above, PINK1, which is normally processed by mitochondrial protease PARL in the intermembrane space, stabilizes on the outermembrane; PINK1 undergoes autophosphorylation, phosphorylates ubiquitin and Parkin, recruit cytosolic Parkin to the mitochondria. Parkin ubiquitinates outermembrane proteins followed by their degradation through proteasome pathway. Ubiquitinated outermembrane proteins also recruits autophagosome though p62/SQSTM1, an adaptor protein and mediates autophagic-lysosomal degradation of mitochondria (Pickrell and Youle 2015; Rasool, Soya et al. 2018). Besides the PINK1-Parkin dependent pathway, dysfunctional mitochondria could be eliminated through PINK1-Parkin independent pathway. Loss of iron and overexpression AIRH1 cause mitophagy in the absence of PINK1 and Parkin (Allen, Toth et al. 2013; Villa, Proics et al. 2017). PINK1 overexpression is sufficient to induce mitophagy independent of Parkin (Lazarou, Sliter et al. 2015).

Mitochondrial dynamics is closely related with mitophagy machinery. Loss of DRP1, DRP1 dominant negative mutants or loss of Fis1, a DRP1 receptor on the mitochondria, significantly delay the basal level mitophagy process, but also mitophagy after CCCP treatment (Twig, Elorza et al. 2008; Kageyama, Hoshijima et al. 2014); Whereas in mitochondria proteotoxicity induced mitophagy, loss of DRP1 accelerate the process (Burman, Pickles et al. 2017). The inconsistency could be attributed to different stress conditions; therefore, more evidence is needed to clarify the

role DRP1 in mitophagy under stress conditions. On the other hand, the role of mitochondrial fusion, or Mitofusin 1 and 2 or OPA1 is not well understood (Twig and Shirihai 2011). Loss of Mfn1 and Mfn2 generates the heterogynous population of mitochondria with intact and defective membrane potentials. Parkin translocates to mitochondria with decreased membrane potentials without stress (Narendra, Tanaka et al. 2008). At 24 hours after CCCP treatment, loss of Mfn1 and Mfn2 does not show significant difference in term of mitophagy rate compared to wildtype (Tanaka, Cleland et al. 2010; Chan, Salazar et al. 2011). At chloroquine-induced mitophagy, OPA1 mutants and Mfn2 dominant negative mutants have enhanced mitophagic influx (Liao, Ashley et al. 2017). The inconsistency could also be attribute to difference in outside stimuli. In chapter two, we provide more evidence showing that loss of Mfn1 and Mfn2 enhances mitophagy under 6 hours CCCP treatment; delayed degradation of Mitofusins hinder the mitophagy process.

3.1. Mitochondrial dysfunction in Parkinson's disease

The initial finding that reveal the role of mitochondria in Parkinson's diseases was patients who have been exposed to environmental toxin (MPTPs) that inhibits mitochondrial complex I develop classic motor symptoms of PD (Langston, Ballard et al. 1983). Later on, injection of MPTP, paraquat, and rotenone, all of which inhibit mitochondrial complex I, in animals had specific dopaminergic neuronal loss at the substantia nigra and generates model for acute parkinsonism (Betarbet, Sherer et al. 2000; Dauer and Przedborski 2003). However, it is the discovery of pathogenic mutations in genes that affects mitochondria accentuate the critical role of mitochondrial dysfunction in pathogenesis of Parkinson's disease (Kondapalli, Kazlauskaite et al. 2012), especially the studies of *PINK1* (*Park6*) and *Parkin* (*Park2*), whose loss-of-function

mutations cause familial Parkinson's disease (Kitada, Asakawa et al. 1998; Valente, Abou-Sleiman et al. 2004). *PINK1* encodes a serine/threonine kinase, whereas *Parkin* encodes an E3 ligase. Our lab and others have shown that *in vivo* loss of *PINK1/parkin* cause severe mitochondrial damage; Parkin overexpression can compensate the mitochondrial defects in flies loss of PINK1; PINK1 and Parkin function in the same pathway with PINK1 functions upstream of Parkin; (Clark, Dodson et al. 2006; Park, Lee et al. 2006; Yang, Gehrke et al. 2006). Both PINK1 and Parkin are negative regulators of Mitofusion (Mfn) protein levels in *Drosophila* (Ziviani, Tao et al. 2010). The discovery of PINK1 and Parkin in mitochondrial quality control (discussed in detail above) strongly suggest the key role of mitochondria in tissue health. The following studies shows that a striking number of genes whose mutations cause monogenic PD significantly affect mitochondrial integrity. For example, pathogenic α-synuclein mutants inhibit mitochondrial respiration complex I (Martin, Pan et al. 2006); pathogenic LRRK2 G2019S mutants and ATP132A mutants depolarize mitochondrial membrane potential and decrease ATP generation (Grunewald, Arns et al. 2012; Papkovskaia, Chau et al. 2012). These findings set mitochondria as a key target for not only unravelling the disease pathology as well as developing therapy.

3.2. Mitochondrial dysfunction in myopathy/frontotemporal dementia caused by VCP mutants

VCP disease mutants predominantly affect organs that have a high level of energy expenditure, such as brain and muscle. Mitochondrial functional defects, including mitochondrial uncoupling and decreased ATP production, are observed in IBMPFD patient fibroblasts (Bartolome, Wu et al. 2013; Nalbandian, Llewellyn et al. 2015). Abnormal mitochondria are also

observed in transgenic VCP disease mutant R155H mice as well as VCP R155H knock-in mice (Custer, Neumann et al. 2010; Nalbandian, Llewellyn et al. 2012). These observations suggest that mitochondrial dysfunction is important for the pathogenesis of IBMPFD, but the mechanism by which VCP mutation alters mitochondrial function is not clear.

In Hela cells, VCP promotes Mfn 1 degradation (Xu, Peng et al. 2011). VCP also mediates Mfn degradation when mitophagy is stimulated in mammalian cells, and overexpression of VCP in *Drosophila* leads to significant downregulation of a tagged Mfn-transgene (Kim, Tresse et al. 2013; Kimura, Fukushi et al. 2013). These observations led us to investigate the mitochondrial basis and molecular mechanisms for VCP disease mutants function using both *Drosophila* and IBMPFD patient cell models. In chapter two, we generated *Drosophila* models of IBMPFD in muscle, which recapitulate disease pathologies. We provide evidence in both *Drosophila* and human patient cells that VCP disease mutants have an enhanced ability to promote Mfn degradation, behaving as a hyperactive allele as a novel disease mechanism. We also identified VCP inhibitors can significantly rescue reverse the disease pathology both *in vivo* in *Drosophila*, and patients' cells.

4. Ubiquitination of Mitofusin and Parkin

Parkin belongs to a family of RING-Between-RING E3 ligases. It has an N-terminus UBL (Ubiquitin-like) domain, three RING (really interesting new gene) domains, IBR (in-between RINGs domain and REP (repressor element of PARKIN domain) (Figure 1-1B). More than 120 disease-causing mutations have been reported in all the domains(Truban, Hou et al. 2017). Parkin is autoinhibited at resting condition; when PINK1 stabilizes on the outer membrane of mitochondria and initiates mitophagy, it phosphorylates Parkin at Serine 65 at UBL domain

(Kondapalli, Kazlauskaite et al. 2012). Cysteine 431 is the catalytic site of Parkin E3 ligase activity. Mutation of Cysteine 431 abolishes Parkin-mediated mitophagy (Riley, Lougheed et al. 2013). Upon Parkin's translocation to mitochondria, there are multiple outermembrane proteins are ubiquitinated. One of the key substrates is Mitofusins (Chan, Salazar et al. 2011; Sarraf, Raman et al. 2013).

Ubiquitination is a cellular process for protein quality control that includes three steps, ubiquitin activation by E1, ubiquitin conjugation by E2 and transfer of ubiquitin to target protein by E3 ligase. E3 ligase is the most selective for target protein in the ubiquitination process (Pickart and Eddins 2004). E3 ligase builds ubiquitin on the lysine sites of target proteins. Identification of the lysine sites on target protein is one of the key steps in understanding the significance of ubiquitination (Sadowski and Sarcevic 2010).

Mitofusins is a highly conserved GTPases through various species. They have GTPase domain at the N-terminus, coiled-coiled heptad repeat domain 1 (HR1), two transmembrane domains, and coiled-coiled heptad repeat domain 2 (HR2) at the C-terminus (Figure 1-1C). Two Mitofusin molecule from individual mitochondria forms a heterodimer and mediates outermembrane fusion (Figure 1-1D). Ubiquitination marks Mitofusion for degradation, suggesting the proteolytic role of the ubiquitination. Under certain conditions, ubiquitination of Mfn leads to mitochondrial fusion, suggesting the non-proteolytic or regulatory role of ubiquitinaton (Anton, Dittmar et al. 2013; Yue, Chen et al. 2014). Several E3 ligases have been identified that mediates ubiquitination of Mitofusions, Huwe1 for Mfn2 (Leboucher, Tsai et al. 2012), March5, GP78 for Mfn1 (Fu, St-Pierre et al. 2013; Park, Nguyen et al. 2014), SCF^{Mdm30} for yeast homologue of Mitofusin, Fzo1 (Cohen, Amiott et al. 2011) and aforementioned Parkin, the only E3 ligase that targets both Mfn1 and Mfn2 in mammals as well as Mfn in *Drosophila*. A

profile of ubiquitination lysine sites on Parkin-targeted mitochondria outer membrane proteins upon CCCP (uncoupler) depolarization are identified, including 8 sites on Mfn1 and 10 on Mfn2 respectively (Sarraf, Raman et al. 2013). The validity of these lysine sites requires further verification. Therefore, it is still unclear whether ubiquitination of Mitofusion regulates mitochondrial function, and more importantly, exerts biological consequences at the level of tissue health.

In chapter three, we identified a conserved lysine site in both *Drosophila* Mfn and human Mfn1 and Mfn2, that are critical for their ubiquitination and degradation by Parkin. Flies harboring mutant of the lysine site have stabilized Mfn protein levels and tissue defects. In mammalian cells, mutations of the same lysines in Mfn 1 and Mfn2 stabilize protein levels and delay Parkin-mediated degradation upon mitochondria depolarization and mitophagy process. These results provide direct evidences suggest that the lysine identified is critical for Mitofusin ubiquitination and protein stabilization; Mfn protein levels are critical for mitochondrial fusion/fission, mitophagy and tissue health.

Reference:

Abramzon, Y., J. O. Johnson, et al. (2012). "Valosin-containing protein (VCP) mutations in sporadic amyotrophic lateral sclerosis." Neurobiology of aging **33**(9): 2231 e2231-2231 e2236.

Alexander, C., M. Votruba, et al. (2000). "OPA1, encoding a dynamin-related GTPase, is mutated in autosomal dominant optic atrophy linked to chromosome 3q28." Nat Genet **26**(2): 211-215.

Allen, G. F., R. Toth, et al. (2013). "Loss of iron triggers PINK1/Parkin-independent mitophagy." EMBO Rep **14**(12): 1127-1135.

Anton, F., G. Dittmar, et al. (2013). "Two deubiquitylases act on mitofusin and regulate mitochondrial fusion along independent pathways." Molecular cell **49**(3): 487-498.

Bartolome, F., H. C. Wu, et al. (2013). "Pathogenic VCP mutations induce mitochondrial uncoupling and reduced ATP levels." Neuron **78**(1): 57-64.

Bender, A., K. J. Krishnan, et al. (2006). "High levels of mitochondrial DNA deletions in substantia nigra neurons in aging and Parkinson disease." Nat Genet **38**(5): 515-517.

Betarbet, R., T. B. Sherer, et al. (2000). "Chronic systemic pesticide exposure reproduces features of Parkinson's disease." Nat Neurosci **3**(12): 1301-1306.

Braak, H., K. Del Tredici, et al. (2003). "Staging of brain pathology related to sporadic Parkinson's disease." Neurobiol Aging **24**(2): 197-211.

Buchan, J. R., R. M. Kolaitis, et al. (2013). "Eukaryotic stress granules are cleared by autophagy and Cdc48/VCP function." Cell **153**(7): 1461-1474.

Burman, J. L., S. Pickles, et al. (2017). "Mitochondrial fission facilitates the selective mitophagy of protein aggregates." J Cell Biol **216**(10): 3231-3247.

Chan, D. C. (2012). "Fusion and fission: interlinked processes critical for mitochondrial health." Annual review of genetics **46**: 265-287.

Chan, N. C., A. M. Salazar, et al. (2011). "Broad activation of the ubiquitin-proteasome system by Parkin is critical for mitophagy." Hum Mol Genet **20**(9): 1726-1737.

Chang, Y. C., W. T. Hung, et al. (2011). "Pathogenic VCP/TER94 alleles are dominant actives and contribute to neurodegeneration by altering cellular ATP level in a Drosophila IBMPFD model." PLoS genetics **7**(2): e1001288.

Chen, H., S. A. Detmer, et al. (2003). "Mitofusins Mfn1 and Mfn2 coordinately regulate mitochondrial fusion and are essential for embryonic development." The Journal of cell biology **160**(2): 189-200.

Chen, H., J. M. McCaffery, et al. (2007). "Mitochondrial fusion protects against neurodegeneration in the cerebellum." Cell **130**(3): 548-562.

Chen, H., M. Vermulst, et al. (2010). "Mitochondrial fusion is required for mtDNA stability in skeletal muscle and tolerance of mtDNA mutations." Cell **141**(2): 280-289.

Clark, I. E., M. W. Dodson, et al. (2006). "Drosophila pink1 is required for mitochondrial function and interacts genetically with parkin." Nature **441**(7097): 1162-1166.

Cohen, M. M., E. A. Amiott, et al. (2011). "Sequential requirements for the GTPase domain of the mitofusin Fzo1 and the ubiquitin ligase SCFMdm30 in mitochondrial outer membrane fusion." Journal of cell science **124**(Pt 9): 1403-1410.

Custer, S. K., M. Neumann, et al. (2010). "Transgenic mice expressing mutant forms VCP/p97 recapitulate the full spectrum of IBMPFD including degeneration in muscle, brain and bone." Hum Mol Genet **19**(9): 1741-1755.

Dauer, W. and S. Przedborski (2003). "Parkinson's disease: mechanisms and models." Neuron **39**(6): 889-909.

de Bot, S. T., H. J. Schelhaas, et al. (2012). "Hereditary spastic paraplegia caused by a mutation in the VCP gene." Brain **135**(Pt 12): e223; author reply e224.

DeLaBarre, B., J. C. Christianson, et al. (2006). "Central pore residues mediate the p97/VCP activity required for ERAD." Molecular cell **22**(4): 451-462.

Dickson, D. W. (2012). "Parkinson's disease and parkinsonism: neuropathology." Cold Spring Harb Perspect Med **2**(8).

Dobrynin, G., O. Popp, et al. (2011). "Cdc48/p97-Ufd1-Npl4 antagonizes Aurora B during chromosome segregation in HeLa cells." Journal of cell science **124**(Pt 9): 1571-1580.

Edgar, D., I. Shabalina, et al. (2009). "Random point mutations with major effects on protein-coding genes are the driving force behind premature aging in mtDNA mutator mice." Cell Metab **10**(2): 131-138.

Fahrner, J. A., R. Liu, et al. (2016). "A novel de novo dominant negative mutation in DNM1L impairs mitochondrial fission and presents as childhood epileptic encephalopathy." Am J Med Genet A **170**(8): 2002-2011.

Friedman, J. R. and J. Nunnari (2014). "Mitochondrial form and function." Nature **505**(7483): 335-343.

Fu, M., P. St-Pierre, et al. (2013). "Regulation of mitophagy by the Gp78 E3 ubiquitin ligase." Molecular biology of the cell **24**(8): 1153-1162.

Gitler, A. D., P. Dhillon, et al. (2017). "Neurodegenerative disease: models, mechanisms, and a new hope." Dis Model Mech **10**(5): 499-502.

Gonzalez, M. A., S. M. Feely, et al. (2014). "A novel mutation in VCP causes Charcot-Marie-Tooth Type 2 disease." Brain : a journal of neurology **137**(Pt 11): 2897-2902.

Grunewald, A., B. Arns, et al. (2012). "ATP13A2 mutations impair mitochondrial function in fibroblasts from patients with Kufor-Rakeb syndrome." Neurobiol Aging **33**(8): 1843 e1841-1847.

Johnson, A. E., H. Shu, et al. (2015). "VCP-dependent muscle degeneration is linked to defects in a dynamic tubular lysosomal network in vivo." Elife **4**.

Ju, J. S., R. A. Fuentealba, et al. (2009). "Valosin-containing protein (VCP) is required for autophagy and is disrupted in VCP disease." The Journal of cell biology **187**(6): 875-888.

Kageyama, Y., M. Hoshijima, et al. (2014). "Parkin-independent mitophagy requires Drp1 and maintains the integrity of mammalian heart and brain." EMBO J **33**(23): 2798-2813.

Kim, N. C., E. Tresse, et al. (2013). "VCP is essential for mitochondrial quality control by PINK1/Parkin and this function is impaired by VCP mutations." Neuron **78**(1): 65-80.

Kimonis, V. E., E. Fulchiero, et al. (2008). "VCP disease associated with myopathy, Paget disease of bone and frontotemporal dementia: review of a unique disorder." Biochimica et biophysica acta **1782**(12): 744-748.

Kimonis, V. E., S. G. Mehta, et al. (2008). "Clinical studies in familial VCP myopathy associated with Paget disease of bone and frontotemporal dementia." American journal of medical genetics. Part A **146A**(6): 745-757.

Kimura, Y., J. Fukushi, et al. (2013). "Different dynamic movements of wild-type and pathogenic VCPs and their cofactors to damaged mitochondria in a Parkin-mediated mitochondrial quality control system." Genes to cells : devoted to molecular & cellular mechanisms **18**(12): 1131-1143.

Kitada, T., S. Asakawa, et al. (1998). "Mutations in the parkin gene cause autosomal recessive juvenile parkinsonism." Nature **392**(6676): 605-608.

Kondapalli, C., A. Kazlauskaite, et al. (2012). "PINK1 is activated by mitochondrial membrane potential depolarization and stimulates Parkin E3 ligase activity by phosphorylating Serine 65." Open Biol **2**(5): 120080.

Langston, J. W., P. Ballard, et al. (1983). "Chronic Parkinsonism in humans due to a product of meperidine-analog synthesis." Science **219**(4587): 979-980.

Larsson, N. G. (2010). "Somatic mitochondrial DNA mutations in mammalian aging." Annu Rev Biochem **79**: 683-706.

Lazarou, M., D. A. Sliter, et al. (2015). "The ubiquitin kinase PINK1 recruits autophagy receptors to induce mitophagy." Nature **524**(7565): 309-314.

Leboucher, G. P., Y. C. Tsai, et al. (2012). "Stress-induced phosphorylation and proteasomal degradation of mitofusin 2 facilitates mitochondrial fragmentation and apoptosis." Molecular cell **47**(4): 547-557.

Liao, C., N. Ashley, et al. (2017). "Dysregulated mitophagy and mitochondrial organization in optic atrophy due to OPA1 mutations." Neurology **88**(2): 131-142.

Loson, O. C., Z. Song, et al. (2013). "Fis1, Mff, MiD49, and MiD51 mediate Drp1 recruitment in mitochondrial fission." Mol Biol Cell **24**(5): 659-667.

Manno, A., M. Noguchi, et al. (2010). "Enhanced ATPase activities as a primary defect of mutant valosin-containing proteins that cause inclusion body myopathy associated with Paget disease of bone and frontotemporal dementia." Genes to cells : devoted to molecular & cellular mechanisms **15**(8): 911-922.

Martin, L. J., Y. Pan, et al. (2006). "Parkinson's disease alpha-synuclein transgenic mice develop neuronal mitochondrial degeneration and cell death." J Neurosci **26**(1): 41-50.

Meyer, H., M. Bug, et al. (2012). "Emerging functions of the VCP/p97 AAA-ATPase in the ubiquitin system." Nat Cell Biol **14**(2): 117-123.

Meyer, H., M. Bug, et al. (2012). "Emerging functions of the VCP/p97 AAA-ATPase in the ubiquitin system." Nature cell biology **14**(2): 117-123.

Meyer, H. and C. C. Weihl (2014). "The VCP/p97 system at a glance: connecting cellular function to disease pathogenesis." Journal of cell science **127**(Pt 18): 3877-3883.

Nalbandian, A., K. J. Llewellyn, et al. (2015). "In vitro studies in VCP-associated multisystem proteinopathy suggest altered mitochondrial bioenergetics." Mitochondrion **22**: 1-8.

Nalbandian, A., K. J. Llewellyn, et al. (2012). "The homozygote VCP(R(1)(5)(5)H/R(1)(5)(5)H) mouse model exhibits accelerated human VCP-associated disease pathology." PLoS One **7**(9): e46308.

Narendra, D., A. Tanaka, et al. (2008). "Parkin is recruited selectively to impaired mitochondria and promotes their autophagy." J Cell Biol **183**(5): 795-803.

Nickel, A., M. Kohlhaas, et al. (2014). "Mitochondrial reactive oxygen species production and elimination." J Mol Cell Cardiol **73**: 26-33.

Niwa, H., C. A. Ewens, et al. (2012). "The role of the N-domain in the ATPase activity of the mammalian AAA ATPase p97/VCP." The Journal of biological chemistry **287**(11): 8561-8570.

Nunnari, J. and A. Suomalainen (2012). "Mitochondria: in sickness and in health." Cell **148**(6): 1145-1159.

Papkovskaia, T. D., K. Y. Chau, et al. (2012). "G2019S leucine-rich repeat kinase 2 causes uncoupling protein-mediated mitochondrial depolarization." Hum Mol Genet **21**(19): 4201-4213.

Park, J., S. B. Lee, et al. (2006). "Mitochondrial dysfunction in Drosophila PINK1 mutants is complemented by parkin." Nature **441**(7097): 1157-1161.

Park, Y. Y., O. T. Nguyen, et al. (2014). "MARCH5-mediated quality control on acetylated Mfn1 facilitates mitochondrial homeostasis and cell survival." Cell death & disease **5**: e1172.

Pickart, C. M. and M. J. Eddins (2004). "Ubiquitin: structures, functions, mechanisms." Biochimica et biophysica acta **1695**(1-3): 55-72.

Pickrell, A. M. and R. J. Youle (2015). "The roles of PINK1, parkin, and mitochondrial fidelity in Parkinson's disease." Neuron **85**(2): 257-273.

Plotegher, N. and M. R. Duchen (2017). "Crosstalk between Lysosomes and Mitochondria in Parkinson's Disease." Front Cell Dev Biol **5**: 110.

Poewe, W. (2008). "Non-motor symptoms in Parkinson's disease." Eur J Neurol **15 Suppl 1**: 14-20.

Puumalainen, M. R., D. Lessel, et al. (2014). "Chromatin retention of DNA damage sensors DDB2 and XPC through loss of p97 segregase causes genotoxicity." Nature communications **5**: 3695.

Raman, M., M. Sergeev, et al. (2015). "Systematic proteomics of the VCP-UBXD adaptor network identifies a role for UBXN10 in regulating ciliogenesis." Nature cell biology.

Rasool, S., N. Soya, et al. (2018). "PINK1 autophosphorylation is required for ubiquitin recognition." EMBO Rep **19**(4).

Riley, B. E., J. C. Lougheed, et al. (2013). "Structure and function of Parkin E3 ubiquitin ligase reveals aspects of RING and HECT ligases." Nat Commun **4**: 1982.

Ritson, G. P., S. K. Custer, et al. (2010). "TDP-43 mediates degeneration in a novel Drosophila model of disease caused by mutations in VCP/p97." The Journal of neuroscience : the official journal of the Society for Neuroscience **30**(22): 7729-7739.

Ritz, D., M. Vuk, et al. (2011). "Endolysosomal sorting of ubiquitylated caveolin-1 is regulated by VCP and UBXD1 and impaired by VCP disease mutations." Nat Cell Biol **13**(9): 1116-1123.

Sadowski, M. and B. Sarcevic (2010). "Mechanisms of mono- and poly-ubiquitination: Ubiquitination specificity depends on compatibility between the E2 catalytic core and amino acid residues proximal to the lysine." Cell Div **5**: 19.

Sarraf, S. A., M. Raman, et al. (2013). "Landscape of the PARKIN-dependent ubiquitylome in response to mitochondrial depolarization." Nature **496**(7445): 372-376.

Shih, Y. T. and Y. P. Hsueh (2016). "VCP and ATL1 regulate endoplasmic reticulum and protein synthesis for dendritic spine formation." Nature communications **7**: 11020.

Shirihai, O. S., M. Song, et al. (2015). "How mitochondrial dynamism orchestrates mitophagy." Circ Res **116**(11): 1835-1849.

Shoffner, J. M., M. T. Lott, et al. (1990). "Myoclonic epilepsy and ragged-red fiber disease (MERRF) is associated with a mitochondrial DNA tRNA(Lys) mutation." Cell **61**(6): 931-937.

Song, M., K. Mihara, et al. (2015). "Mitochondrial fission and fusion factors reciprocally orchestrate mitophagic culling in mouse hearts and cultured fibroblasts." Cell Metab **21**(2): 273-286.

Song, M., K. Mihara, et al. (2015). "Mitochondrial fission and fusion factors reciprocally orchestrate mitophagic culling in mouse hearts and cultured fibroblasts." Cell metabolism **21**(2): 273-285.

Song, Z., H. Chen, et al. (2007). "OPA1 processing controls mitochondrial fusion and is regulated by mRNA splicing, membrane potential, and Yme1L." J Cell Biol **178**(5): 749-755.

Spatola, M. and C. Wider (2014). "Genetics of Parkinson's disease: the yield." Parkinsonism Relat Disord **20 Suppl 1**: S35-38.

Tanaka, A., M. M. Cleland, et al. (2010). "Proteasome and p97 mediate mitophagy and degradation of mitofusins induced by Parkin." J Cell Biol **191**(7): 1367-1380.

Tang, W. K. and D. Xia (2013). "Altered intersubunit communication is the molecular basis for functional defects of pathogenic p97 mutants." The Journal of biological chemistry **288**(51): 36624-36635.

Truban, D., X. Hou, et al. (2017). "PINK1, Parkin, and Mitochondrial Quality Control: What can we Learn about Parkinson's Disease Pathobiology?" J Parkinsons Dis **7**(1): 13-29.

Twig, G., A. Elorza, et al. (2008). "Fission and selective fusion govern mitochondrial segregation and elimination by autophagy." EMBO J **27**(2): 433-446.

Twig, G. and O. S. Shirihai (2011). "The interplay between mitochondrial dynamics and mitophagy." Antioxid Redox Signal **14**(10): 1939-1951.

Valente, E. M., P. M. Abou-Sleiman, et al. (2004). "Hereditary early-onset Parkinson's disease caused by mutations in PINK1." Science **304**(5674): 1158-1160.

Vaz, B., S. Halder, et al. (2013). "Role of p97/VCP (Cdc48) in genome stability." Frontiers in genetics **4**: 60.

Vermulst, M., J. Wanagat, et al. (2008). "DNA deletions and clonal mutations drive premature aging in mitochondrial mutator mice." Nat Genet **40**(4): 392-394.

Villa, E., E. Proics, et al. (2017). "Parkin-Independent Mitophagy Controls Chemotherapeutic Response in Cancer Cells." Cell Rep **20**(12): 2846-2859.

Wakabayashi, J., Z. Zhang, et al. (2009). "The dynamin-related GTPase Drp1 is required for embryonic and brain development in mice." J Cell Biol **186**(6): 805-816.

Watts, G. D., J. Wymer, et al. (2004). "Inclusion body myopathy associated with Paget disease of bone and frontotemporal dementia is caused by mutant valosin-containing protein." Nat Genet **36**(4): 377-381.

Weihl, C. C., S. Dalal, et al. (2006). "Inclusion body myopathy-associated mutations in p97/VCP impair endoplasmic reticulum-associated degradation." Human molecular genetics **15**(2): 189-199.

Weihl, C. C., A. Pestronk, et al. (2009). "Valosin-containing protein disease: inclusion body myopathy with Paget's disease of the bone and fronto-temporal dementia." Neuromuscular disorders : NMD **19**(5): 308-315.

Xu, S., G. Peng, et al. (2011). "The AAA-ATPase p97 is essential for outer mitochondrial membrane protein turnover." Mol Biol Cell **22**(3): 291-300.

Yang, Y., S. Gehrke, et al. (2006). "Mitochondrial pathology and muscle and dopaminergic neuron degeneration caused by inactivation of Drosophila Pink1 is rescued by Parkin." Proceedings of the National Academy of Sciences of the United States of America **103**(28): 10793-10798.

Ye, Y., H. H. Meyer, et al. (2001). "The AAA ATPase Cdc48/p97 and its partners transport proteins from the ER into the cytosol." Nature **414**(6864): 652-656.

Yue, W., Z. Chen, et al. (2014). "A small natural molecule promotes mitochondrial fusion through inhibition of the deubiquitinase USP30." Cell research **24**(4): 482-496.

Zhang, X., L. Gui, et al. (2015). "Altered cofactor regulation with disease-associated p97/VCP mutations." Proceedings of the National Academy of Sciences of the United States of America **112**(14): E1705-1714.

Zhang, X., H. Zhang, et al. (2014). "Phosphorylation regulates VCIP135 function in Golgi membrane fusion during the cell cycle." Journal of cell science **127**(Pt 1): 172-181.

Zhao, J., X. Wu, et al. (2018). "Embryonic Surface Ectoderm-specific Mitofusin 2 Conditional Knockout Induces Congenital Cataracts in Mice." Sci Rep **8**(1): 1522.

Ziviani, E., R. N. Tao, et al. (2010). "Drosophila parkin requires PINK1 for mitochondrial translocation and ubiquitinates mitofusin." Proceedings of the National Academy of Sciences of the United States of America **107**(11): 5018-5023.

Zuchner, S., M. Noureddine, et al. (2005). "Mutations in the pleckstrin homology domain of dynamin 2 cause dominant intermediate Charcot-Marie-Tooth disease." Nat Genet **37**(3): 289-294.

CHAPTER TWO

VCP inhibitors relieve Mitofusin-dependent mitochondrial defects due to VCP disease mutants

Ting Zhang[1], Prashant Mishra[3, #], Bruce Hay[3], David Chan[3] and Ming Guo[1, 2 *]

[1]Department of Neurology, [2]Department of Molecular and Medical Pharmacology, UCLA David Geffen School of Medicine, University of California, Los Angeles, CA 90095;

[3]Division of Biology and Biological Engineering, California Institute of Technology, Pasadena, CA 91125

*To whom correspondence should be addressed: mingfly@g.ucla.edu

[#]Current address:

Children's Medical Center Research Institute, University of Texas Southwestern Medical Center, Dallas, TX 75390

Published in Elife. 2017 Mar 21, doi: 10.7554 PMID:28322724

Abstract:

Missense mutations of *valosin-containing protein* (*VCP*) cause an autosomal dominant disease known as inclusion body myopathy, Paget disease with frontotemporal dementia (IBMPFD) and other neurodegenerative disorders. The pathological mechanism of IBMPFD is not clear and there is no treatment. We show that endogenous VCP negatively regulates Mitofusin, which is required for outer mitochondrial membrane fusion. Because 90% of IBMPFD patients have myopathy, we generated an *in vivo* IBMPFD model in adult *Drosophila* muscle, which recapitulates disease pathologies. We show that common VCP disease mutants act as hyperactive alleles with respect to regulation of Mitofusin. Importantly, VCP inhibitors suppress mitochondrial defects, muscle tissue damage and cell death associated with IBMPFD models in *Drosophila*. These inhibitors also suppress mitochondrial fusion and respiratory defects in IBMPFD patient fibroblasts. These results suggest that VCP disease mutants cause IBMPFD through a gain-of-function mechanism, and that VCP inhibitors have therapeutic value.

Introduction

IBMPFD is an autosomal dominant disease that afflicts multiple body systems (Kimonis, Fulchiero et al. 2008). 90% of IBMPFD patients display skeletal muscle weakness (myopathy), the primary and earliest symptom of IBMPFD (Weihl, Pestronk et al. 2009). With progression of the disease, 50% of patients will develop Paget's disease of bone, affecting the skull, spine, hips and long bones of all four limbs. One-third of the patients will also develop frontotemporal dementia (Kimonis, Mehta et al. 2008; Weihl, Pestronk et al. 2009). Single missense mutations of *p97/cdc48/Valosin-containing protein (VCP)* cause fully penetrant IBMPFD (Watts, Wymer et al. 2004). *VCP* mutations are also associated with 1-2% of cases of amyotrophic lateral

sclerosis (ALS), familial hereditary spastic paraplegia (HSP) and Charcot-Marie-Tooth 2 (CMT2) disease (Abramzon, Johnson et al. 2012; de Bot, Schelhaas et al. 2012; Gonzalez, Feely et al. 2014).

VCP encodes a highly conserved and abundant AAA+ ATPase which participates in multiple cellular processes (Meyer, Bug et al. 2012). Human p97/VCP and its *Drosophila* homologue have 85% identity and 93% similarity in protein sequence. VCP has three major domains: the regulatory N domain, and the D1 and D2 ATPase domains. VCP hexameric rings utilize the energy from ATP hydrolysis to promote protein and RNA homeostasis, often by directly or indirectly modifying the fate of ubiquitin-labeled proteins (Meyer, Bug et al. 2012). VCP functions in multiple contexts that include protein quality control in the endoplasmic reticulum (Ye, Meyer et al. 2001; Shih and Hsueh 2016), chromatin modification (Dobrynin, Popp et al. 2011; Vaz, Halder et al. 2013; Puumalainen, Lessel et al. 2014), endolysosomal sorting (Ritz, Vuk et al. 2011), membrane fusion (Zhang, Zhang et al. 2014), autophagosome/lyosome function (Ju, Fuentealba et al. 2009; Johnson, Shu et al. 2015), ER protein translocation (DeLaBarre, Christianson et al. 2006; Weihl, Dalal et al. 2006), formation of stress granules (Buchan, Kolaitis et al. 2013) and ciliogenesis (Raman, Sergeev et al. 2015). VCP interacts with a number of co-factors to regulate these processes (Meyer, Bug et al. 2012; Meyer and Weihl 2014), making it challenging to identify the molecular basis of phenotypes associated with disease mutations.

Disease-causing, single missense mutations of VCP are mainly located in the N-terminal half of the protein, either in the N domain or the D1 domain. Among them, the R155H mutation is the most frequently identified in IBMPFD patients, while the A232E mutation is associated with the most severe clinical manifestation (Kimonis, Fulchiero et al. 2008; Ritson, Custer et al.

2010). *In vitro* assays show that disease mutants have enhanced ATPase activity (Weihl, Dalal et al. 2006; Manno, Noguchi et al. 2010; Niwa, Ewens et al. 2012; Tang and Xia 2013; Zhang, Gui et al. 2015). However, because VCP assembles as a hexamer, it is controversial whether disease mutants with increased ATPase activity cause disease through a dominant-active (Chang, Hung et al. 2011) or dominant-negative mechanism (Ju, Fuentealba et al. 2009; Ritz, Vuk et al. 2011; Bartolome, Wu et al. 2013; Kim, Tresse et al. 2013; Kimura, Fukushi et al. 2013).

VCP disease mutants predominantly affect organs that have a high level of energy expenditure, such as brain and muscle. Mitochondria provide the bulk of the ATP to these tissues through oxidative phosphorylation and mitochondrial functional defects, including mitochondrial uncoupling and decreased ATP production, are observed in IBMPFD patient fibroblasts (Bartolome, Wu et al. 2013; Nalbandian, Llewellyn et al. 2015). Abnormal mitochondria are also observed in transgenic VCP disease mutant R155H mice as well as VCP R155H knock-in mice (Custer, Neumann et al. 2010; Nalbandian, Llewellyn et al. 2012). These observations suggest that mitochondrial dysfunction is important for the pathogenesis of IBMPFD, but the mechanism by which VCP mutation alters mitochondrial function is not clear.

Mitochondrial morphology is controlled by dynamic cycles of fusion, controlled by Mitofusin (Mfn), and fission, regulated by DRP1 (Chan 2012). Recent studies have uncovered roles of mitochondria fusion and fission defects in the pathogenesis of multiple neurodegenerative disorders (Chen, Detmer et al. 2003; Davies, Hollins et al. 2007; Wakabayashi, Zhang et al. 2009), particularly Parkinson's disease, the second most common neurodegenerative disorder (Yang, Gehrke et al. 2006; Deng, Dodson et al. 2008; Poole, Thomas et al. 2008; Yang, Ouyang et al. 2008; Park, Lee et al. 2009; Poole, Thomas et al. 2010; Guo 2012; Pickrell and Youle 2015). In mammals, homologous proteins Mitofusin 1 and 2 (Mfn1 and

Mfn2) mediate mitochondrial outer membrane fusion, with loss of function of Mfn 1 and 2 resulting in fragmented mitochondria and multiple defects in mitochondrial function (Chen, Detmer et al. 2003). In Hela cells, VCP promotes Mfn 1 degradation (Xu, Peng et al. 2011). VCP also mediates Mfn degradation when mitophagy is stimulated in mammalian cells, and overexpression of VCP in *Drosophila* leads to significant downregulation of a tagged Mfn-transgene (Kim, Tresse et al. 2013; Kimura, Fukushi et al. 2013). These observations led us to investigate the mitochondrial basis and molecular mechanisms for VCP disease mutants function using both *Drosophila* and IBMPFD patient cell models. As IBMPFD show the highest penetrance in muscle, with 90% of patients manifesting phenotypes in this tissue, we generated *Drosophila* models of IBMPFD in muscle, which recapitulate disease pathologies. We provide evidence in both *Drosophila* and human patient cells that VCP disease mutants have an enhanced ability to promote Mfn degradation, loss of which is associated with defects in mitochondrial fusion and physiology. Consistent with the hypothesis that VCP disease phenotypes are due to increased activity on substrates we find that VCP ATPase activity inhibitors such as NMS-873 and ML240 can significantly rescue the mitochondrial defects, disrupted muscle integrity and muscle cell death *in vivo* in *Drosophila*, and mitochondrial fusion and respiration defects in IBMPFD patient fibroblasts.

Results

Endogenous VCP regulates mitochondrial fusion via negative regulation of Mfn protein levels.

Since VCP disease mutants have dramatic muscle phenotypes in humans and mouse models, and these are associated with defects in mitochondrial structure and function, we first examined the consequences of manipulating VCP levels. The *Drosophila* adult indirect flight

muscle (IFM) is a non-essential, post-mitotic, and energy-intense tissue containing a high density of mitochondria. It also shows strong and consistent phenotypes in response to altered expression of genes required for mitochondrial fusion, fission and quality control (Clark, Dodson et al. 2006; Deng, Dodson et al. 2008; Poole, Thomas et al. 2008; Yang, Ouyang et al. 2008; Park, Lee et al. 2009; Poole, Thomas et al. 2010; Yun, Puri et al. 2014). Using the UAS-Gal4 system (Brand and Perrimon 1993), we expressed VCP under the control of an IFM promoter derived from the *flightin* gene we previously generated (Yun, Puri et al. 2014). While expression of VCP under the control of the pan-muscle Gal4 drivers 24B-Gal4 or Mef2-Gal4 resulted in 100% adult lethality, expression of wildtype VCP under IFM control, which provides a pulse of expression in late pupal stages and early adulthood, gave rise to viable flies with intact and healthy muscle following adult eclosion. We utilized mitochondrially targeted GFP (mitoGFP) as a mitochondrial marker, as well as transmission electron microscopy (EM) at the ultrastructual levels for enhanced resolution particularly for cristae morphology. In 2-day old flies, expression of VCP results in muscle with small mitochondria with intact cristae (Figure 2-1-figure supplement 1A-B'). Similar phenotypes are also observed in muscle from 6-day old VCP-expressing flies (Figure 2-1A-B''). Conversely, expression of UAS-VCP RNAi under IFM control (VCP RNAi flies) results in mitochondria with an elongated phenotype (Figure 2-1C-C'', Figure 2-1-figure supplement 1C and C'). Two independent VCP RNAi lines were utilized and both showed significant knockdown (Figure 2-1-figure supplement 2).

To explore the generality of VCP's ability to regulate mitochondrial morphology we also examined mitochondrial morphology phenotypes of a *vcp* loss-of-function mutation. *vcp* null mutants in *Drosophila* are embryonic lethal (Ruden, Sollars et al. 2000). The indirect flight muscle is a cellular syncytium and therefore cannot be used for mosaic analysis. As an

alternative, we focused on the *Drosophila* female germline, in which a *vcp* loss-of-function mutant can be monitored in individual cells, which are relatively large and offer great resolution for examining mitochondrial morphology. vcp^{K15502} is a strong loss-of-function allele that has a P element insertion at the 5'-UTR of *Drosophila VCP* gene (Ruden, Sollars et al. 2000; Chang, Hung et al. 2011) and has been used to generate *vcp* loss-of-function clones in imaginal discs (Zhang, Lv et al. 2013). The *Drosophila* ovary consists of numerous developing egg chambers. Each egg chamber develops from stage 1 to stage 14 and has three types of cells, follicle cells, nurse cells and the oocyte (Frydman and Spradling 2001). The germline complement of each egg chamber (15 nurse cells and the oocyte) derives from four sequential divisions of a single daughter of a stem cell. We utilized the FLP/FRT system (Theodosiou and Xu 1998) to create mitotic recombinants in which nurse cells were either wildtype (+/+), heterozygous (vcp^{K15502}/+) or homozygous ($vcp^{K15502}/vcp^{K15502}$) for the *vcp* loss-of-function mutation (Figure 2-1D). In this system wildtype and heterozygous *vcp* loss-of-function mutant cells carry 2 or 1 copies of ubi-mRFP.NLS (RFP) respectively, whereas the homozygous *vcp* mutant cells are RFP negative (Figure 2-1E). Anti-ATP5A antibody is used to visualize mitochondrial morphology in nurse cells (Figure 2-1E'). Mitochondria in wildtype and heterozygous *vcp* mutant cells have a punctate morphology (Figure 2-1F and G). In contrast, in homozygous *vcp* loss-of-function mutants mitochondria are more tubular and clumped (Figure 2-1H and I). Together these results suggest that endogenous VCP negatively regulates mitochondrial fusion or positively regulates fission.

Next, we investigated how *vcp* loss-of-function leads to elongated mitochondria. First, we examined the expression levels of Mfn in the female germline, using mosaic analysis, as above. We used a tagged genomic rescue transgene (pCasper-Mfn-eGFP, a transgene construct with a

GFP tagged Mfn under the control of its endogenous promoter) to monitor the endogenous Mfn level (a kind gift from Dr. C.K. Yao) as the existing anti-Mfn antibody lacked sufficient sensitivity. As expected, the genomic rescue Mfn-eGFP signal colocalizes with the mitochondria marker ATP5A in the nurse cells (Figure 2-1-figure supplement 3A). This signal is eliminated following Mfn RNAi, indicating that genomic rescue Mfn-eGFP is a reliable marker for endogenous Mfn (Figure 2-1-figure supplement 3B). In each egg chamber, as *vcp* loss-of-function mosaic cells are next to the wildtype cells, this provides an excellent opportunity to unambiguously compare the levels of Mfn. As shown in Figure 2-1J-J'', nurse cells homozygous for a *vcp* loss-of-function mutant have greatly increased Mfn levels compared to wildtype and heterozygous *vcp* loss-of-function cells. The findings that endogenous VCP regulates Mfn *in vivo* are unexpected and important, as VCP is a highly abundant cytosolic protein with many targets and VCP does not show appreciable localization to mitochondria in unstressed cells.

Second, we examined whether alteration of *vcp* can regulate Mfn levels in tissue lysate. Overexpression of wildtype VCP (VCP OE) in the flight muscle resulted in a decrease in endogenous Mfn levels (Figure 2-2A). VCP overexpression also caused a decrease in the levels of Mfn when Mfn was overexpressed (Mfn OE) using the IFM promoter, suggesting that VCP regulates Mfn post transcriptionally (Figure 2-2A). Conversely, VCP RNAi resulted in an increase in endogenous Mfn levels in a wildtype background, and an increase in total Mfn levels in the presence of Mfn OE (Figure 2-2B). In contrast, VCP overexpression does not alter the levels of pro-fission protein DRP1 (Figure 2-2C). In addition, VCP's regulation of Mfn is specific and not part of a general mitophagy response since the levels of other mitochondrial proteins, the outer membrane protein Porin, the inner membrane protein NDUSF3, and the matrix protein MnSOD, are not altered (Figure 2-2D).

VCP physically interacts with Mfn via the N and D1 domains.

To explore the possibility that Mfn is a direct target for VCP, we asked if Mfn could physically interact with VCP in immunoprecipitation assays from S2 cells. Indeed, Full length VCP strongly interacts with Mfn (Figure 2-2E). This is consistent with previous findings [30]. VCP has been shown to interact with substrate through the D1 ATPase domain, with the presence of the N domain being essential for the interaction (Meyer, Bug et al. 2012). As shown in Figure 2-2A, this is also the case with VCP-Mfn interactions. When the N domain of VCP is deleted, the strength of VCP-Mfn interaction is decreased, and it is undetectable when N and D1 are both deleted. In contrast, removal of the D2 domain has no effect on interaction between VCP and Mfn. Interestingly, Mfn levels in the input blot are decreased under conditions when VCP and Mfn interact, but not under conditions in which interactions are not observed, consistent with the hypothesis that direct interactions between VCP and Mfn are required for Mfn degradation. Together these observations suggest that Mfn is a specific, direct target of VCP.

VCP suppresses PINK1/parkin mutant mitochondrial phenotypes in muscle.

Mutations in *PINK1* and *parkin* lead to autosomal recessive forms of Parkinson's disease (PD). (Kitada, Asakawa et al. 1998; Valente, Abou-Sleiman et al. 2004). We and other have first shown that *PINK1* and *parkin* function in the same pathway, with *PINK1* positively regulating *parkin* to control mitochondrial integrity and quality control in *Drosophila* (Clark, Dodson et al. 2006; Park, Lee et al. 2006; Yang, Gehrke et al. 2006). Importantly, levels of Mfn are significantly increased in *PINK1* and *parkin* null mutants and downregulation of Mfn protein

levels suppresses phenotypes in both mutants (Deng, Dodson et al. 2008; Yang, Ouyang et al. 2008; Park, Lee et al. 2009; Yu, Sun et al. 2011). The results presented above suggest that expression of VCP, by decreasing the level of Mfn, could also suppress *PINK1/parkin* phenotypes. Kim et al have argued that VCP expression suppresses *PINK1*, but not *parkin* loss-of-function phenotypes. This, along with their observation that VCP levels at mitochondria increased following expression of Parkin in the presence of CCCP, suggested a model in which VCP action on mitochondria requires recruitment by Parkin (Kim, Tresse et al. 2013). Because the EDTP-Gal4 driver used in these earlier experiments does not express at significant levels in flight muscle (Seroude, Brummel et al. 2002) (Figure 2-3J, see GFP signals), we reexamined this issue. We expressed VCP in the flight muscle of *PINK1* and *parkin* mutants. As previously shown (Clark, Dodson et al. 2006; Park, Lee et al. 2006; Yang, Gehrke et al. 2006), *PINK1* and *parkin* null mutants show mitochondrial defects and tissue disintegration with vacuolation in muscle (Figure 2-3A-B'' and D-D''). At the ultrastructural level, *PINK1* and *parkin* mutants display swollen mitochondria with broken cristae (Figure 2-3A''', B''' and D'''). VCP OE completely suppressed tissue damage and mitochondrial defects (Figure 2-3C-C''' and E-E'''). The thorax indentation phenotype in *PINK1/parkin* mutants are also completely suppressed by VCP overexpression under the control of the IFM-Gal4 driver, but not the EDTP-Gal4 driver (Figure 2-3-figure supplement 1). The suppression observed by Kim, et al is probably due to non-disjunction of the *PINK1* null flies. As predicted for a mechanism of VCP action that occurs through regulation of Mfn, VCP OE significantly reduced the accumulation of Mfn normally observed in both mutants (Figure 2-3F).

To further substantiate the finding that overexpression of *VCP* suppresses *parkin* null mutants, we also examined VCP's ability to suppress mitochondrial phenotypes associated with

loss of both *parkin* and *Mul1*. MUL1 (MULAN/MAPL) is a RING-containing E3 ligase that acts as a negative regulator of Mfn in both *Drosophila* and mammals (Yun, Puri et al. 2014). When overexpressed, it suppresses *PINK1* and *parkin* null mutant phenotypes by degrading Mfn, while loss of *mul1* leads to increased levels of Mfn. Thus, *parkin mul1* double null mutants have strikingly more severe mitochondrial phenotypes than those observed in flies lacking *parkin* alone (Yun, Puri et al. 2014). Remarkably, expression of VCP resulted in a dramatic rescue of mitochondrial morphology due to lack of both *parkin* and *mul1* (Figure 2-3G-I'). Together, these results suggest that VCP-dependent suppression of *PINK1* null, *parkin* null and *parkin mul1* double phenotypes occurs through downregulaton of Mfn levels (Figure 2-3K). Together, our observations argue that VCP regulates Mfn levels under non-stress conditions. They also show that VCP-dependent regulation of Mfn does not require PINK1 or Parkin. However, these results do not exclude the possibility that Parkin activation further promotes VCP-dependent Mfn degradation under some situations.

Expression of VCP disease mutants in muscle recapitulates pathological features of IBMPFD.

To explore the basis of myopathy induced by VCP disease mutants we sought to create a model of IBMPFD in *Drosophila* muscle, as 90% of the IBMPFD patients show muscle phenotypes. Since *VCP* disease mutations are autosomal dominant, we characterized the consequences of disease mutant overexpression. The pathologies observed in IBMPFD patient muscle, and in muscle from VCP disease mutant transgenic and mouse knock-in models, include muscle cell death, changes in mitochondrial morphology, damaged tissue integrity, TAR DNA-binding protein 43 (TDP43) mislocalization to the cytosol, and formation of autophagic marker p62 and ubiquitin aggregates, signs of multisystem proteinopathy (Ju, Fuentealba et al. 2009;

Ritson, Custer et al. 2010; Ritz, Vuk et al. 2011; Weihl 2011; Nalbandian, Llewellyn et al. 2012; Nalbandian, Llewellyn et al. 2015; Ahmed, Machado et al. 2016). Previous studies of VCP disease mutants in Drosophila muscle showed effects on tissue integrity and mitochondria cristae structure (Chang, Hung et al. 2011; Kim, Tresse et al. 2013), but not other pathologies. We thus investigated the pathologies due to mutant VCP expression. We focused on expression of VCP R152H and A229E (corresponding to Human VCP R155H and A232E, hereafter referred to as VCP RH and VCP AE), as they are the most frequent and the most severe mutations identified, respectively (Figure 2-4A). Anti-VCP antibody blotting shows that VCP WT, VCP RH and VCP AE are expressed at comparable level in the fly thorax (Figure 2-4B). In wildtype flies, flies with IFM-Gal4 insertion, and flies with VCP WT expression, the muscle structure was healthy and intact 6 days after eclosion. No cell death was observed and mitochondria were densely packed and contained high levels of MitoGFP (Figure 2-4C, D and D'). Muscles also displayed a well-aligned myofibril structure (Figure 2-4E and E'). Together these observations indicate that increased expression of VCP is not overtly toxic. In contrast, muscle from flies expressing VCP RH or VCP AE under IFM-Gal4 control (thereafter called VCP RH or VCP AE flies) showed extensive cell death (97±3.6% and 95.7±5.1% muscle are TUNEL-positive), defective MitoGFP signals (Figure 2-4D'' and D'''), and severely disrupted muscle integrity (Figure 2-4E'' and E'''). In addition, while in wildtype and VCP WT flies TDP43 was found in IFM nuclear and sarcoplasmic compartments, IFMs from VCP RH and AE flies showed a decrease in the intensity of the nuclear signal, and an increase in the intensity of staining associated with puncta in the sarcoplasmic area (Figure 2-4C, F-F'''). Muscle from VCP RH and AE flies also contained large aggregates of anti-p62 and anti-Ubiquitin staining. These were not observed in wildtype or VCP WT flies (Figure 2-4G-H'''). Importantly, the pathologies observed in flight muscle at day 6 post

eclosion were not present at day 2 (Figure 2-4-figure supplement 1), suggesting the degenerative nature of the pathology, as with the human disease and mouse models (Kimonis, Fulchiero et al. 2008; Custer, Neumann et al. 2010; Nalbandian, Llewellyn et al. 2012). Together these observations indicate that IFM-specific expression of VCP RH and AE recapitulates a broad spectrum of IBMPFD disease pathologies and forms the strong basis for further investigation of disease mechanisms and treatment studies.

VCP disease mutants are hyperactive with respect to downregulation of Mfn protein levels and inhibition of mitochondrial fusion.

Next, we investigated the cellular basis of mitochondrial defects in our IBMPFD flies using electron microscopy. Flies expressing VCP WT have smaller mitochondria as compared with control flies, but with intact cristae (Figure 2-5A-B'). In VCP RH and AE muscle, however, mitochondria are smaller in size, and more fragmented than in VCP WT flies. In addition, they also have severe ultrastructural defects under EM studies with broken cristae (Figure 2-5C-D'). This phenotype is similar to that of flies with a muscle-specific Mfn knock down (Figure 2-5E and E') (Deng, Dodson et al. 2008). Muscle from VCP RH and VCP AE flies show similar phenotypes to Mfn knock down (Figure 2-5-figure supplement 1).

The strong mitochondrial phenotypes observed in VCP RH or VCP AE predicts that expression of VCP RH or VCP AE may result in a greater decrease in Mfn levels as compared with expression of VCP WT. This is indeed what we observed (Figure 2-5F). This raises the possibility that VCP RH and AE are hyperactive alleles. To further substantiate these findings, we compared the Mfn levels in flies expressing VCP E2Q, a well-established ATPase defective mutant containing two mutations (fly or human residues by number E305Q and E578Q) that

abolish ATPase activity of the D1 and D2 domains. Expression of E2Q did not significantly change the Mfn levels (Figure 2-5F). As a control, expression of any of the above forms of VCP did not alter expression levels of another mitochondrial protein Hsp60 (Figure 2-5F). These results suggest that VCP disease mutants are hyperactive with respect to promoting downregulation of Mfn levels.

Based on these observations, we hypothesized that VCP disease mutants should also rescue mitochondrial phenotypes in *parkin* and *parkin mul1* double mutants. As shown in Figure 2-5G-J, expression of VCP RH and AE mutants, but not VCP E2Q or VCP RNAi, robustly restored mitochondrial structure, as indicated by MitoGFP fluorescence, in the *parkin* null mutant (Figure 2-5K and L). Moreover, corresponding to the mitochondrial phenotypes, the accumulation of Mfn in *parkin* mutants was significantly reduced in the presence of VCP WT, RH and AE, with VCP RH and AE causing greater decreases in Mfn levels than VCP WT (Figure 2-5S). In addition, VCP RH and AE expression also robustly rescued the mitochondrial defects in the *parkin mul1* double null mutants, but expression of VCP E2Q or VCP RNAi did not (Figure 2-5M-R). Taken together, these results indicate that VCP RH and AE disease mutants do not behave as ATPase defective or loss-of-function mutants, and instead are hyperactive with respect to regulation of Mfn.

Mfn downregulation is important to the muscle pathology in IBMPFD flies.

A prediction from our finding that Mfn downregulation is important for IBMPFD pathology is that downregulation of Mfn should results in phenotypes similar to those observed with expression of VCP disease mutants. Indeed, *mfn* muscle-specific knockdown flies have fragmented mitochondria (Figure 2-4I-I'), TDP43 mislocalization (Figure 2-4J-J'), vacuole

formation (Figure 2-4K-K'), p62 and Ubiquitin accumulation (Figure 2-4L-L' and M-M'), as with the VCP disease mutants. Next we asked if *mfn* overexpression could rescue the phenotypes due to VCP RH and AE. Since *mfn* overexpression results in significant mitochondrial phenotypes, tissue disintegration and cell death on its own (Yun, Puri et al. 2014), we are unable to address this question completely due to a technical limitation. We were, however, able to bring about a mild increase in Mfn levels through addition of 2 copies of an *mfn* genomic rescue transgene in the background of VCP RH and AE expressing flies. Interestingly, this resulted in a suppression of the mitochondrial fragmentation and cristae phenotypes in 2-day old VCP RH and AE flies (Figure 2-5-figure supplement 2) but not the pathology observed in VCP RH and AE fly muscles at 8 days (Figure 2-5-figure supplement 3). Together, our data suggest that downregulation of Mfn is an important contributor to IBMPFD muscle pathology.

IBMPFD patient fibroblasts with the VCP R155H mutation have mitochondrial respiratory chain and mitochondrial fusion defects.

Next, we extended our studies in IBMPFD patient fibroblasts. We focused our studies on $VCP^{R155H/+}$ cells (thereafter called RH cells), as fibroblasts harboring the $VCP^{A232E/+}$ mutation are not available. First, we characterized mitochondrial respiration in control and immortalized patient fibroblasts. As shown in Figure 2-6A, the basal level Oxygen Consumption Rate (OCR) in the VCP RH patient cells is slightly decreased compared to the healthy control, suggesting that baseline mitochondrial respiratory chain function is compromised in patient cells. Maximum OCR, measured in the presence of the uncoupler FCCP, is significantly decreased in VCP RH IBMPFD patient cells. The spare OCR, which is calculated by subtracting the basal OCR from the maximum OCR, provides a measure of reserve mitochondrial capacity for ATP generation.

The spare OCR in IBMPFD patient cells is significantly decreased as compared with controls. Others have recently reported similar observations (Nalbandian, Llewellyn et al. 2015).

Disruption of mitochondrial fusion can result in defects in respiration similar to those observed in patient cells (Chen, Detmer et al. 2003). Mfn 1 and 2 levels in VCP RH cells were reduced to 0.66±0.14 and 0.60±0.14 respectively, as compared with age and gender matched healthy control cells (set as 1, Figure 2-6B). To explore the functional significance of this decrease, we carried out mitochondrial fusion assays using fibroblasts from healthy controls and patients. Both cell populations were transfected with a plasmid encoding a mitochondrial matrix targeted, photoactivated GFP (PA-GFP). Following photoactivation of GFP within a region of the cell, the GFP fluorescence signal spreads and the intensity decreases as these mitochondria fuse with non-activated neighboring mitochondria. Thus, in this assay an increased rate of fluorescence loss corresponds to increased mitochondrial fusion activity (Mishra, Carelli et al. 2014). In control cells, PA-GFP gradually decreases after photoactivation; in the VCP RH IBMPFD patient cells, the GFP signal decrease is significantly delayed (Figure 2-6C-D', E). These data suggest that VCP RH mutation results in a decrease in Mfn 1 and 2 levels that lead to impaired mitochondrial fusion. In addition, the VCP mutant impairs both basal and maximal mitochondrial respiratory function.

The VCP inhibitors NMS-873 and ML240 generate elongated mitochondria, block VCP disease mutant phenotypes, and VCP-dependent suppression of PINK1 mutant mitochondrial defects.

It has been controversial in the field whether VCP disease mutants with increased ATPase activity behave as dominant-active or dominant-negative mutants. Some studies show

that VCP RH and AE, with enhanced ATPase activity (Weihl, Dalal et al. 2006; Manno, Noguchi et al. 2010; Niwa, Ewens et al. 2012; Tang and Xia 2013; Zhang, Gui et al. 2015), results in hyperactivity in animal disease models (Chang, Hung et al. 2011). However, other cell-based studies suggest they behave in a dominant negative fashion (Ju, Fuentealba et al. 2009; Ritz, Vuk et al. 2011; Bartolome, Wu et al. 2013; Kim, Tresse et al. 2013; Kimura, Fukushi et al. 2013). Understanding how VCP disease mutants behave is critical for understanding the disease process and finding possible therapies. We hypothesize that if abnormally enhanced ATPase activity causes pathology, disease severity should ameliorate if ATPase activity is decreased through the use of VCP ATPase inhibitors. To test this hypothesis, we characterized the effects of VCP inhibitors *in vivo*.

Multiple VCP ATPase activity inhibitors have recently been described (Chapman, Maksim et al. 2015). NMS-873, 3-[3-Cyclopentylsulfanyl-5-(4'-methanesulfonyl-2-methyl-biphenyl-4-yloxymethyl)-[1, 2, 4] triazol-4-yl]-pyridine, an allosteric inhibitor of VCP ATPase activity, is a highly specific and robust VCP ATPase inhibitor (Magnaghi, D'Alessio et al. 2013). ML240, 2-(2-Amino-1H-benzimidazol-1-yl)-8-methoxy-N-(phenylmethyl)-4-quinazolinamine is another potent inhibitor, which competitively blocks ATP binding to VCP (Chou, Li et al. 2013). These drugs and their derivatives were developed for treatment of cancers (Chou, Li et al. 2013; Magnaghi, D'Alessio et al. 2013; Deshaies 2014; Zhou, Wang et al. 2015). The ability of these compounds to rescue defects in IBMPFD models has not been reported.

We first examined the effects of VCP inhibitors delivered to *Drosophila* through feeding. Various concentrations of drug or DMSO were included in food during the first to third larval instars, and muscle mitochondrial morphology was characterized at 2 and 6 days after eclosion. NMS-873 or ML240 feeding resulted in dramatic mitochondrial elongation in wildtype animals

as visualized with MitoGFP using light microscopy (Figure 2-7A-A'') and at the ultrastructural level using EM (Figure 2-7B-B'''). These phenotypes are similar to those observed following VCP RNAi (Figure 2-1C-C''). In other respect drug treated animals developed normally (data not shown). The smaller mitochondria phenotype associated with overexpression of VCP WT was also significantly suppressed following feeding with 30 μM NMS-873 or 30 μM ML240 (Figure 2-7C-C'''). Feeding with NMS-873 and ML240 also reversed the phenotypic rescue of mitochondrial defects caused by expression of VCP WT, RH and AE in *PINK1* mutants (Figure 2-7-figure supplement 1). Supporting these results, feeding with NMS-873 also resulted in a dose-dependent increase in the levels of Mfn (Figure 2-7D). Together these observations suggest that NMS-873 and ML240 inhibit endogenous VCP *in vivo*, resulting in a phenocopy of loss of VCP function.

We then fed NMS-873 and ML240 to VCP RH and AE disease mutant flies and analyzed mitochondrial phenotypes, muscle viability and integrity in 6 days old flies. Flies were fed with 30 μM NMS-873 or 30 μM ML240 from 1st instar larvae until 6 days after eclosion. In control and VCP WT expressing flies, NMS-873 and ML240 feeding resulted in normal development to adulthood (data not shown) and did not cause muscle death or tissue damage; all muscles were TUNEL negative and had intact tissue structure (Figure 2-8-figure supplement 1). Strikingly, NMS-873 and ML240 feeding largely prevented muscle cell death caused by expression of VCP RH or AE (Figure 2-8A-B''). It also significantly rescued disrupted muscle integrity (Figure 2-8C-D''). Rescue of mitochondrial size, cristae structure, and myofibril organization was also observed at the ultrastructural level (Figure 2-8E-F''). It is interesting to note that in the VCP disease mutants feeding groups (Figure 2-8E', E'', F' and F''), mitochondria remained somewhat smaller as compared to wildtype in Figure 2-7B. Elongated mitochondria, such as

those observed in the wildtype and VCP WT feeding groups (Figure 2-7B', B'', C' and C''), were never observed in the VCP RH and VCP AE groups even though all were fed the same concentration of inhibitors. This partial suppression further suggests that these mutants are hyperactive. Finally, we note that VCP inhibitor feeding also resulted in significant rescue of a number of other phenotypes in VCP RH and AE expressing flies, including those associated with p62, ubiquitin and TDP43 (Figure 2-8G-L''). Together these observations suggest that VCP disease mutants are hyperactive in multiple aspects, and that disease phenotypes can be suppressed by inhibition of VCP ATPase activity.

Low level of VCP inhibitor treatment suppresses mitochondrial fusion and respiration defects in IBMPFD patient's fibroblasts.

The above data demonstrated a decrease in Mfn 1 and 2 levels, mitochondrial fusion defects and impaired mitochondrial respiratory function in IBMPFD patient cells. Next, we explored the effects of these drugs on these changes in IBMPFD patient fibroblasts. In patient cells, a high concentration of ML240 (10 μM, with IC50 of 110 nM) or NMS-873 (10 μM, with IC50 of 30 nM) led to cell death, and NMS-873 directly inhibits mitochondrial respiration (data not shown). However, when lower concentrations of ML240 are used, robust rescue effects are observed (Figure 2-9). As shown in Figure 2-9A, immortalized IBMPFD patient fibroblasts have decreased Mfn 1 levels, and these are increased by treatment with 250 nM ML240 for 6 hours. Overall mitochondrial morphology of IBMPFD fibroblasts does not change in response to inhibitor treatment (Figure 2-9-figure supplement 1). However, in a more sensitive assay in which rates of fusion are measured directly, mitochondrial fusion defects in IBMPFD patient fibroblasts were significantly rescued after 6 hours of treatment with 250 nM ML240 (Figure 2-

9B). Finally, 50 nM and 100 nM ML240 treatment for 4 days also significantly enhanced the basal and maximal oxygen consumption rate (OCR) in patient fibroblasts (Figure 2-9C). Similarly, 1 nM and 10 nM NMS-873 treatment for 6 days significantly enhanced the maximal oxygen consumption rate (OCR) in patient fibroblasts as well (Figure 2-9D). Together, these data strongly support the effects of VCP inhibitors as potential therapeutic tools for IBMPFD disease.

Discussion:

Missense mutations of VCP lead to the autosomal dominant disease IBMPFD. However, it is controversial whether these mutations cause disease through a dominant active or dominant negative manner. Moreover, the molecular mechanisms by which VCP mutations alter mitochondrial function are unclear. Here, we have investigated the endogenous function of VCP, cellular effects of expression of VCP disease mutants, and the ability of VCP inhibitors to suppress VCP disease pathology in *Drosophila* and patient fibroblasts. In summary we have made the following findings:

Endogenous VCP regulates mitochondrial fusion (Figure 2-10A). Loss of VCP function leads to increased Mfn levels and increased mitochondrial size in multiple tissues. Conversely, VCP overexpression results in reduced Mfn levels and decreased mitochondrial size. VCP physically interacts with Mfn via domains that are also used to bind its substrates in other contexts. Thus, it is likely that Mfn is an endogenous VCP substrate. Previously, Kim et al showed that VCP RNAi increased resulted in an increase in ubiquinated HA-tagged Mfn in an overexpression setting in the fly eye (Kim, Tresse et al. 2013). Here we provide the first *in vivo* evidence in muscle, the major disease tissue in IBMPFD, that Mfn is a specific endogenous

target of VCP. Regulation of endogenous Mfn by VCP is unexpected, given that VCP is an abundant protein implicated in multiple cellular processes, but has not been shown to localize to mitochondria that are not depolarized by CCCP. We show that VCP-dependent removal of Mfn does not require Parkin or Mul1, E3 ligases known to ubiquitinate Mfn. How VCP brings about Parkin and Mul1-independent removal of Mfn requires future investigation.

IBMPFD is 100% penetrant, and myopathy is the most prevalent (affecting 90% of patients) and primary symptom of IBMPFD patients. We generated an IBMPFD disease model in adult *Drosophila* muscle, and used this system to monitor tissue pathology, and investigate molecular mechanisms by which VCP disease mutants function. We show that compared to VCP WT, expression of VCP disease mutants results in tissue damage, mitochondrial fusion defects and decreased levels of Mfn (Figure 2-10B). These phenotypes are opposite to those associated with decreased levels of VCP, or expression of an ATPase defective mutant version of VCP. Expression of VCP disease mutants, but not a VCP ATPase defective mutant or VCP RNAi, also suppress the mitochondrial defects mediated by accumulation of Mfn in *PINK1* null*, parkin* null*,* and *parkin mul1* double null mutants. Taken together, these results suggest that VCP disease mutants do not function as loss-of-function or dominant negative mutants, but rather as dominant activated mutants in regulating Mfn levels and bringing about mitochondrial fusion defects. This conclusion is further supported by our findings that mitochondrial fusion and Mfn levels are also decreased in VCP disease mutant fibroblasts.

Our finding that VCP overexpression suppresses a *parkin* null mutant in addition to a *PINK1* null stands in contrast to what was reported in Kim et al., who proposed that VCP-dependent degradation of Mfn required recruitment by Parkin. In addition, we also find that VCP overexpression suppresses phenotypes due to double mutants of *parkin* and *mul1*, which acts in a

parallel pathway to degrade Mfn (Yun, Puri et al. 2014). Together these observations show that VCP-dependent regulation of Mfn does not require *PINK1* or *parkin*. The VCP-dependent degradation of Mfn we observe is also specific and unlikely to be mediated through a more general process such as mitophagy, as levels of several other mitochondrial proteins are not altered by VCP overexpression. However, these results do not exclude models in which Parkin activation further promotes VCP-dependent Mfn degradation, which may or may not involve mitophagy, under some conditions.

Regarding the mechanisms of VCP disease mutant action, *in vitro* biochemistry studies suggest that they have increased ATPase activities, thus favoring a dominant active model (Weihl, Dalal et al. 2006; Manno, Noguchi et al. 2010; Niwa, Ewens et al. 2012; Tang and Xia 2013; Zhang, Gui et al. 2015). In addition, *in vivo* data from *Drosophila* shows that eye phenotypes caused by VCP disease mutant expression can be alleviated through loss of one copy of wildtype VCP. This also is consistent with models in which VCP mutants have increased activity (Chang, Hung et al. 2011). In contrast, in cell culture studies Bartolome, et al showed that VCP disease mutant expression led to mitochondria respiratory chain defects, as did VCP RNAi (Bartolome, Wu et al. 2013); Ritz, et al showed that VCP disease mutant expression impaired endocytosis to the same extent as that of VCP ATPase defective mutants (Ritz, Vuk et al. 2011). While the above studies can be interpreted as showing that VCP disease mutants function as loss-of-function or dominant negative mutants, these results do not rule out the possibility that disease mutants are hyperactive alleles. For example, an alternative interpretation of the impairment of respiratory chain function observed following VCP disease mutant expression or following VCP RNAi is that either an increase or a decrease in the levels of VCP activity leads to mitochondrial defects, which is what we observed in this study.

Currently there is no treatment that can halt the progression of IBMPFD. Our findings that VCP disease mutants are hyperactive provide important therapeutic implications. Indeed, we find VCP inhibitors potently rescue multiple VCP disease phenotypes in flies and patient cells (Figure 2-10C). Importantly, suppression includes phenotypes beyond mitochondria (Figure 2-10C), involving TDP43, p62 and ubiquitin, suggesting that these inhibitors are likely to be effective in therapeutic settings. Of course, in order for VCP inhibitors to be useful as therapeutics, it will be necessary to inhibit mutant forms of VCP to an extent sufficient to suppress disease without bringing about a deleterious decrease in the activity of wildtype VCP. Our observation that *Drosophila* fed inhibitors are suppressed with respect to VCP disease phenotypes, but otherwise develop normally, suggests that this therapeutic goal may be possible. Finally, VCP disease mutants are associated with sporadic amyotrophic lateral sclerosis (Abramzon, Johnson et al. 2012) and hereditary spastic paraplegia (de Bot, Schelhaas et al. 2012). Our findings suggest possible therapeutic values of VCP inhibitors for these diseases.

Figures and Figure legends:

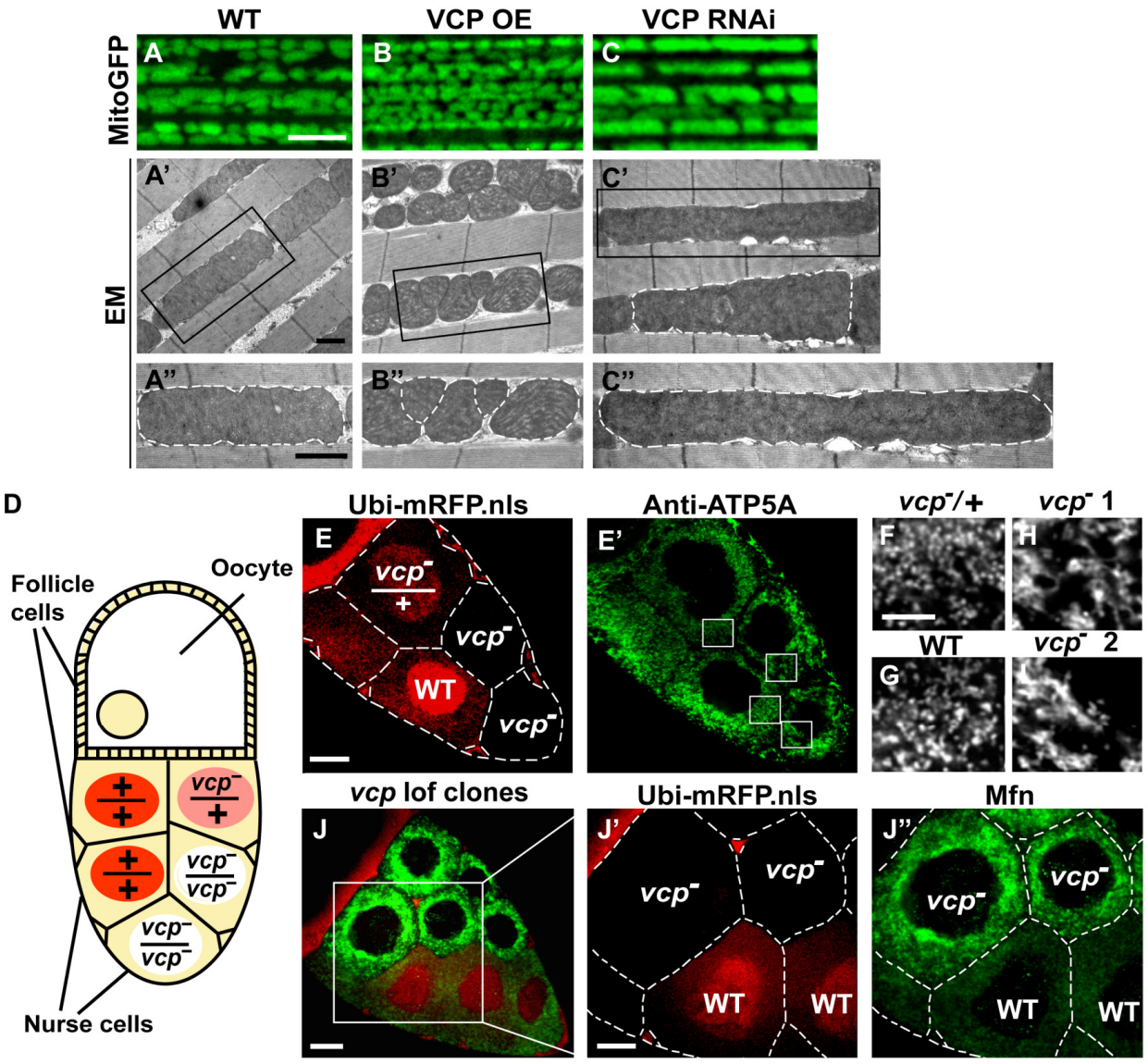

Figure 2-1: Endogenous VCP regulates mitochondrial fusion via negative regulation of Mfn protein levels.

(A-C): MitoGFP localization to mitochondria serves as a marker for healthy mitochondria and their morphology in the indirect flight muscle. VCP overexpression (VCP OE, B) results in small mitochondria compared to wildtype (WT) flies (A); VCP RNAi expression results in elongated mitochondria (C). Scale Bar: 5µm. **(A'-C'')**: Electronic microscopic (EM) images show that

VCP OE (B'-B'') results in smaller mitochondria as compared with WT (A'-A''). VCP RNAi generates elongated mitochondria with intact cristae (outlined with white dashed lines in C' and C''). A'-C': Lower magnification; A''-C'': Higher magnification of mitochondria outlined with black solid lines in A'-C'. Scale bar: 1µm. **(D)**: Schematic diagram of nurse cell mosaic analysis in *Drosophila* female germline. A stage 10A egg chamber has three types of cells. The monolayer follicle cells coat the surface of the egg chamber; 15 nurse cells provide proteins and RNAs to the oocyte during oogenesis. Heat shock induction of mitotic recombination during larvae stages results in the creation of a mosaic pattern in the adult nurse cells. Ubi-mRFP.NLS (Red) is used as clone marker. Wildtype (WT) cells are labeled with two copies of RFP, +/+; heterozygous mutant cells have one copy of RFP and one copy of the *vcp* loss-of-function mutant, vcp^{K15502}/+; homozygous mutant cells are RFP negative and have two copies of *vcp* lof mutant, $vcp^{K15502}/vcp^{K15502}$. **(E)**: A stage 10A egg chamber with a mosaic pattern of nurse cells. Red signal is Ubi-mRFP.NLS. Scale bar: 20µm. **(E')**: Anti-ATP5A antibody staining is used to visualize mitochondrial morphology in nurse cells. Scale bar: 20µm. **(F-I)**: Higher magnification view of mitochondrial morphology in E' (outlined in white solid lines). Mitochondria appear as discrete and punctate structures in wildtype (G) and heterozygous *vcp* mutant cells (F), but becomes elongated and clumped in homozygous *vcp* loss-of-function mutant cells (H and I). Scale bar: 5µm. **(J)**: A stage 10B egg chamber with a mosaic pattern of nurse cells. Red signal is Ubi-mRFP.NLS; Green signal is anti-GFP staining of pCasper-Mfn-eGFP. Scale bar: 20µm. **(J'-J'')**: Higher magnification of the egg chamber in J (outlined in white solid lines). Wildtype cells are RFP positive and homozygous *vcp* loss-of-function mutant cells are RFP negative (J'). pCasper-Mfn-eGFP levels significantly increase in homozygous *vcp* loss-of-function mutant cells (J''). Scale bar: 10µm.

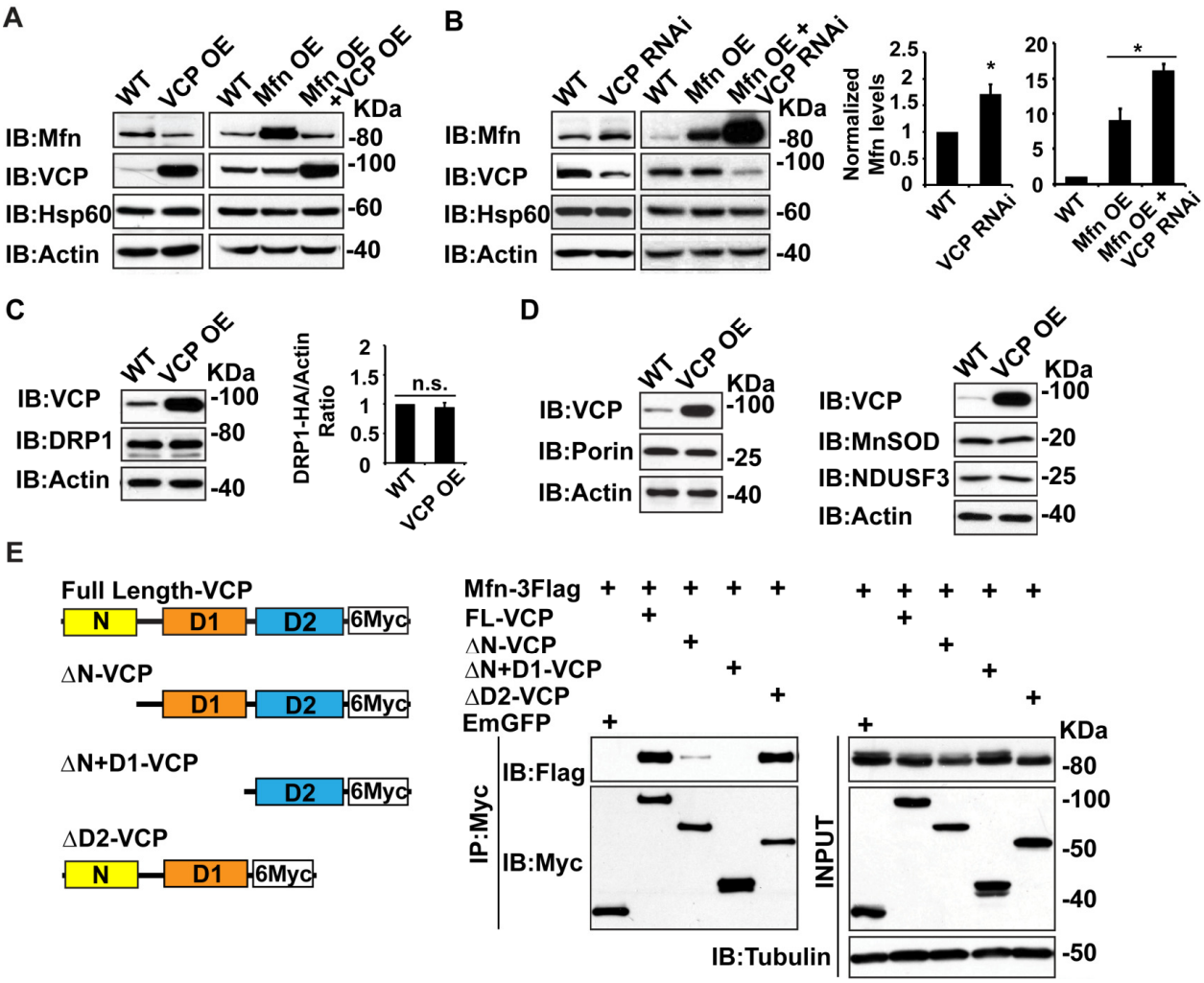

Figure 2-2: Mfn is a specific target of VCP.

(A): In fly thoraxes, VCP OE in wildtype (IFM-Gal4 control) and Mfn OE background results in a significant decrease in Mfn levels. Hsp60 was used as a mitochondria control; Actin was used as loading control. **(B)**: VCP RNAi leads to enhanced Mfn levels (1.72±0.37 compared to wildtype, set as 1; p=0.021, independent t-test, N=4). VCP RNAi results in accumulation of Mfn in the Mfn OE background (16.15±0.85 as compared to Mfn OE alone, 9.02±1.63, wildtype set as 1, p=0.0101, independent t test, N=3). *: $p<0.05$. Mfn levels are normalized with Hsp60 and are displayed as mean±½SD. **(C)**: VCP OE also does not result in changes in the levels of the

pro-fission protein DRP1 level (p=0.088, independent t test, N=3). DRP1 was detected using an HA tagged genomic rescue transgene expressed under the control of the endogenous DRP1 promoter (pCasper-DRP1-HA). n.s.: no statistical difference. **(D)**: Markers for various mitochondrial compartments, including Porin (outer membrane), MnSOD (Matrix), and NDUSF3 (inner membrane) were not altered by VCP WT expression. **(E)**: Schematic diagram of full length and truncated VCP forms used in protein interaction assays in S2 cells. Protein interactions are assayed between full length and truncated VCP forms and Mfn. N and D1 domains are essential domains for the VCP/Mfn interaction.

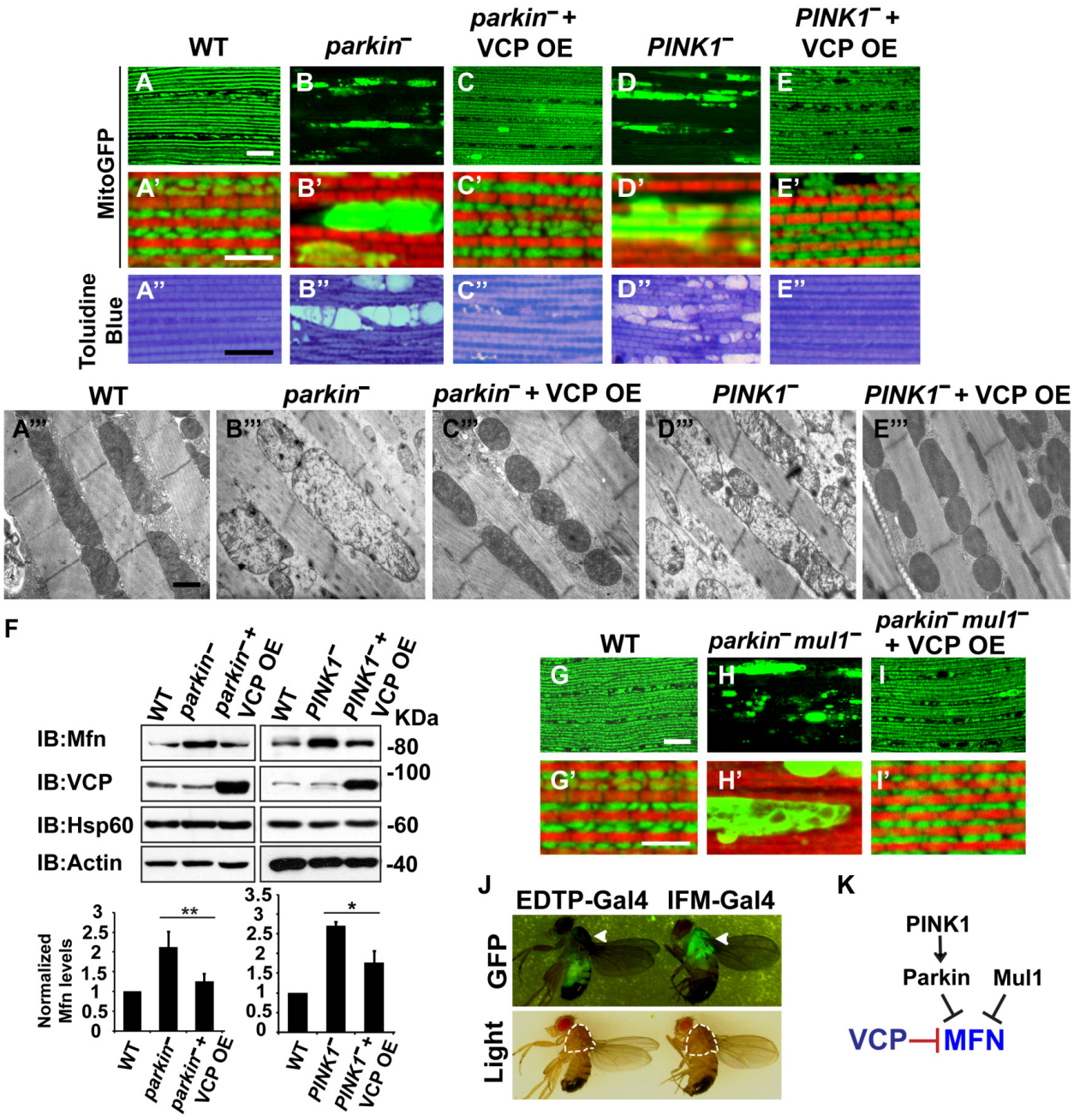

Figure 2-3: VCP overexpression suppresses mitochondrial defects in *PINK1* null, *parkin* null and *parkin mul1* double null mutants.

(A-E'): Compared to wildtype (A and A'), *parkin* and *PINK1* mutants lose MitoGFP staining and accumulate large aggregates. VCP OE (IFM-Gal4>UAS-VCP) significantly rescues the MitoGFP phenotype in both mutants. Filamentous actin is stained with Rhodamine Phalloidin

(Red). A-E: Lower magnification. Scale bar: 20µm. A'-E': Higher magnification. Scale bar: 5µm. **(A''-E'')**: Toluidine Blue shows that vacuole formation in the muscle tissue in *parkin* and *PINK1* mutants are robustly suppressed by VCP OE. Thoraxes are assayed 2 days after eclosion. Scale bar: 30µm. **(A'''-E''')**: At the ultrastructural level, wildtype (WT, IFM-Gal4 control) mitochondria are well aligned with compact cristae (A'''). *parkin* and *PINK1* mutants display swollen mitochondria with broken cristae (B''' and D'''). VCP OE (IFM-Gal4>UAS-VCP) completely rescued the mitochondrial defects in both mutants (C''' and E'''). Thoraxes are sectioned at 2 days after eclosion. Scale bar: 1µm. **(F)**: VCP OE caused a decrease in Mfn accumulation in *parkin* and *PINK1* mutants. Mfn protein levels in the *parkin* mutant increased to 2.12±0.69 as compared with wildtype (set as 1). VCP OE caused a decrease in Mfn levels in the *parkin* mutant to 1.26±0.34 as compared with *parkin* ($p=0.005$, independent t test, N=3. **: $p<0.01$). In *PINK1* mutants, Mfn levels increased to 2.69±0.11 as compared with wildtype, while VCP OE in *PINK1* mutant caused Mfn levels to decrease (1.77±0.29 as compared with *PINK1*, $p=0.023$, independent t test, N=3, *: $p<0.05$). Normalized Mfn levels are shown as mean±½SD. **(G-I')**: Compared to wildtype, the *parkin mul1* mutant lacks most MitoGFP signal and large aggregates are present (G-H'). VCP OE (IFM-Gal4>UAS-VCP) rescues MitoGFP phenotype in *parkin mul1* mutants (I and I'). Myofibrils are stained with Rhodamine Phalloidin (Red). G-I: Lower Magnification, Scale bar: 20µm; G'-I': Higher Magnification, Scale bar: 5µm. **(J)**: Expression pattern of EDTP-Gal4 and IFM-Gal4 in 3-day old flies. EDTP-Gal4 driven UAS-MitoGFP signal is barely detected in the thorax, where the indirect flight muscle is located, suggesting that EDTP-Gal4 does not have sufficient flight muscle specific expression. MitoGFP is present at high levels in the thoraxes of IFM-Gal4 driven flies. Thorax structure is outlined with dashed white lines in white light and indicated with a white arrowhead in GFP field. **(K)**:

Schematic diagram showing that PINK/Parkin in parallel with Mul1 negatively regulates Mfn protein levels; VCP negatively regulates Mfn protein levels independent of these modifiers.

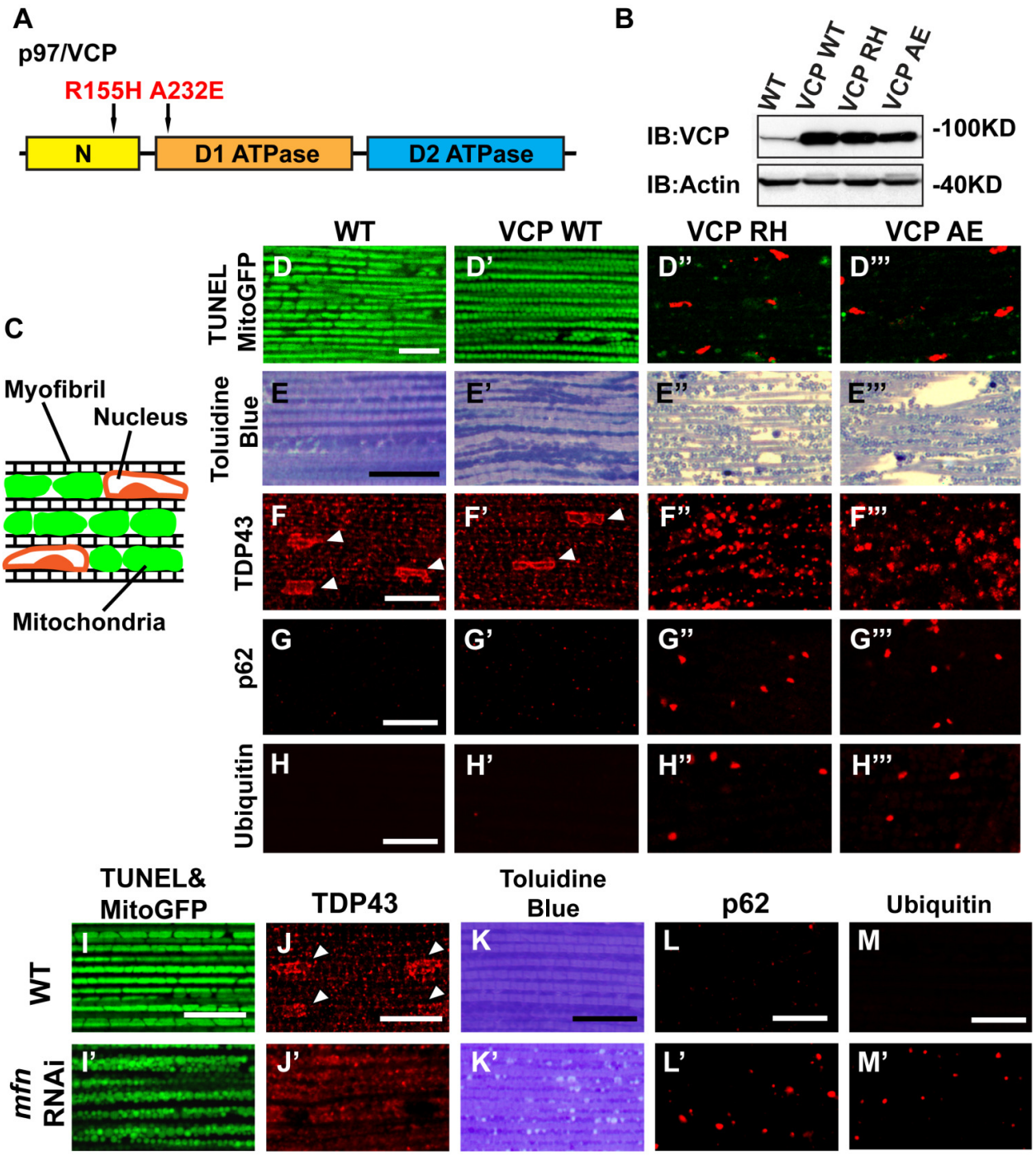

Figure 2-4: Expression of VCP disease mutants and *mfn* RNAi knocking down lead to pathology in adult muscle tissue.

(A): Diagram of Human p97/VCP protein domains and two disease mutants, VCP R155H and A232E. Their corresponding *Drosophila* homologues are VCP R152H and A229E, hereafter

referred to as VCP RH and AE. **(B)**: Expression levels of UAS-VCP WT, RH and AE disease mutants expressed under IFM-Gal4 are comparable. **(C)**: Diagram of *Drosophila* indirect flight muscle structure. Mitochondria (Green) and nuclei (Orange) are densely packed in between myofibrils (which contain large amounts of actin, Black). **(D-D''')**: MitoGFP (Green) and TUNEL staining (Red). 6-day old WT (IFM-Gal4 control) flies and VCP WT flies have healthy muscles (no TUNEL staining) and are MitoGFP positive (**D** and **D'**). 6-day old VCP RH and AE expressing flies show high levels of TUNEL staining. 97±3.6% and 95.7±5.1% of RH (p=0.03. RH v.s. WT, independent t test) and AE (p=0.015, AE v.s. WT, independent t test) and are MitoGFP negative (**D''** and **D'''**). Scale bar: 10µm. **(E-E''')**: Toluidine Blue staining of muscle in WT, VCP WT, RH and AE flies. Myofibrils are well aligned with densely packed mitochondria in WT and VCP WT flies 6 days after eclosion (**E** and **E'**). In VCP RH and AE flies fiber structure is disrupted, and mitochondria are misaligned and lightly stained, with empty spaces in between (**E''** and **E'''**). Scale bar: 40µm. **(F-F''')**: Anti-TDP43 antibody staining shows nuclear (white arrowhead) and sarcoplasmic localization of TDP-43 in WT and VCP WT adult fly muscle (**F** and **F'**). In VCP RH and AE flies the nuclear signal disappears and signal is increased in muscle sarcoplasm (**F''** and **F'''**). Scale bar: 5µm. **(G-G''')**: Anti-Ref(2)P/p62 antibody staining. Signal is weak and uniform in WT and VCP WT flies (**G** and **G'**), and punctate in VCP RH and AE flies (**G''** and **G'''**). Scale bar: 5µm. **(H-H''')**: Anti-P4D1 ubiquitin antibody staining. Signal is weak and uniform in WT and VCP WT flies (**H'** and **H'**), and punctate in VCP RH and AE flies (**H''** and **H'''**). Scale bar: 5µm. **(I-M)** Effects of Mfn RNAi in adult muscle tissue. (I-M) Wildtype muscle visualized with TUNEL and mitoGFP (I), anti-TDP43 (J), Toluidine blue (K), anti-p62 (L), and anti-ubiquitin (M). (I'-M') Mfn RNAi muscle visualized with the same probes as above. Scale bar: 30µm in K-K', 5µm in the rest.

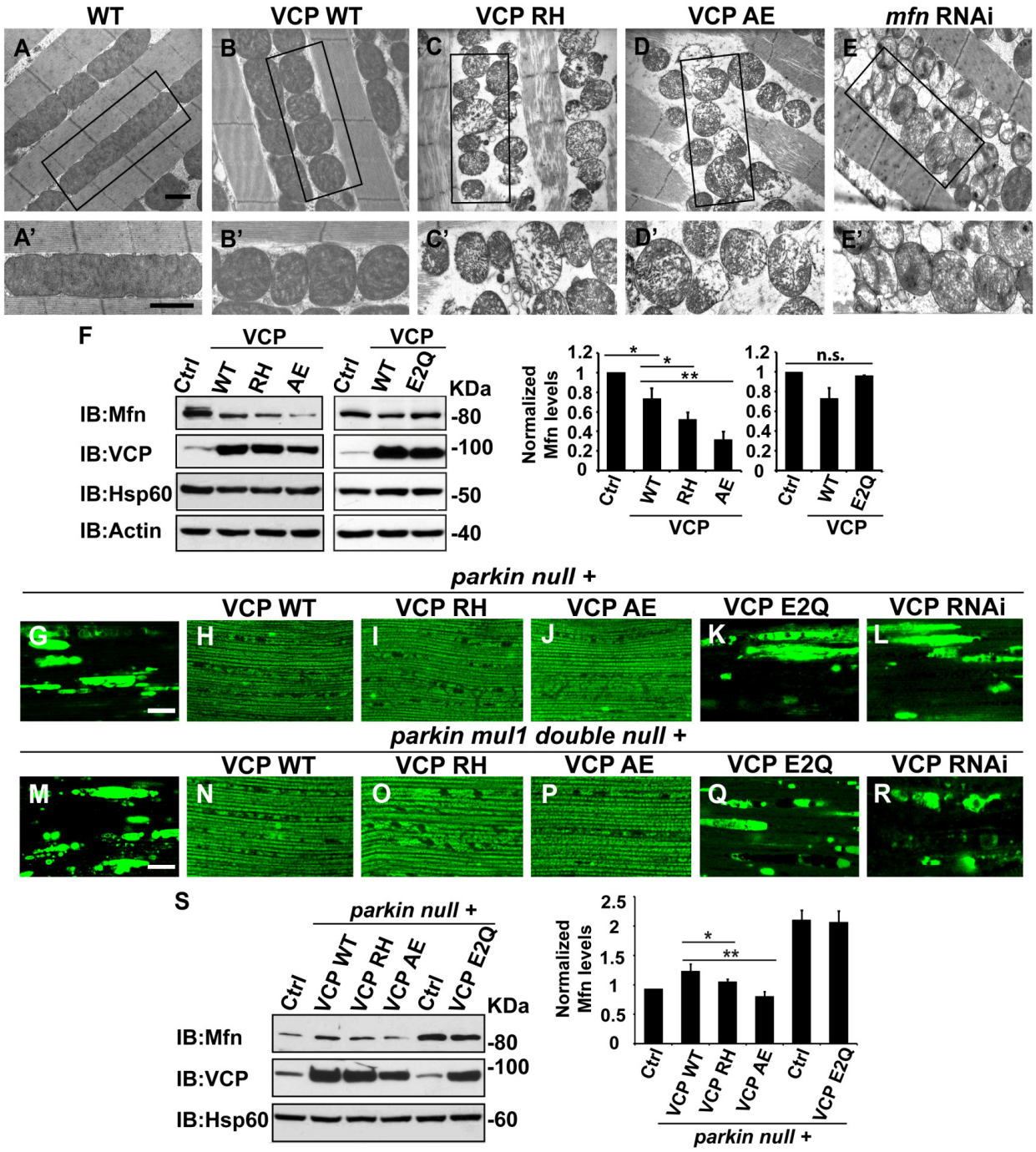

Figure 2-5: VCP disease mutants are hyperactive in downregulating Mfn protein levels and inhibiting mitochondrial fusion.

(A-B'): Electronic microscopic images of muscle of different genotypes. Compared to WT (IFM-Gal4 control, A and A'), mitochondria are smaller with intact cristea in VCP WT (B and

B') 6 days after eclosion. Scale bar: 1μm. **(C-E')**: Expression of VCP RH and AE leads to distorted fiber structure, and small mitochondria with broken or empty cristae. Mfn RNAi flies have similar morphological defects in mitochondria (E and E'). Scale bar: 1μm. **(F):** Expression of VCP RH and AE lead to a further reduction in Mfn as compared to VCP WT. Mfn levels in VCP WT are reduced to 0.73±0.21 as compared with Gal4 control, which is set as 1 ($p=0.037$, independent t test, N=3). Mfn levels in VCP RH and AE are reduced to 0.52±0.14 ($p=0.037$, independent t test, N=3) and 0.32±0.16 ($p=0.003$, independent t test, N=3) as compared with Gal4 control. Mfn levels are normalized with those of Hsp60, a mitochondria marker. Expression of VCP ATPase defective mutant E2Q ($p=0.097$, independent t test, N=3) does not significantly change the Mfn level in fly thoraxes as compared with Gal4 control. n.s.: no statistical significance, $p>0.05$. Normalized Mfn levels are shown as mean±½SD. **(G-L)**: MitoGFP localization assay shows expression of VCP WT (H), RH (I) and AE (J) potently rescues the mitochondrial defects in *parkin* mutant (G). Expression of the ATPase defective mutant E2Q (K) or VCP RNAi (line 1, L) does not. Scale bar: 20μm. **(M-R)**: MitoGFP assay shows expression of VCP WT (N), RH (O) and AE (P) potently rescues the mitochondrial defects in *parkin mul1* double mutants (M). Expression of VCP E2Q (Q) and VCP RNAi (line 1, R) do not. Scale bar: 20μm. **(S)**: Western blot shows that increased Mfn levels normally present in a *parkin* null mutant are significantly decreased in VCP WT, RH and AE flies, but not in VCP E2Q flies. Mfn levels are further decreased in a *parkin* mutant expressing VCP RH ($p=0.0228$, independent t test, N=3) or AE ($p=0.00565$, independent t test, N=3), as compared to VCP WT. Samples are from 2-day old fly thoraces. Normalized Mfn levels are shown as mean±½SD. *: $p<0.05$; **: $p<0.01$.

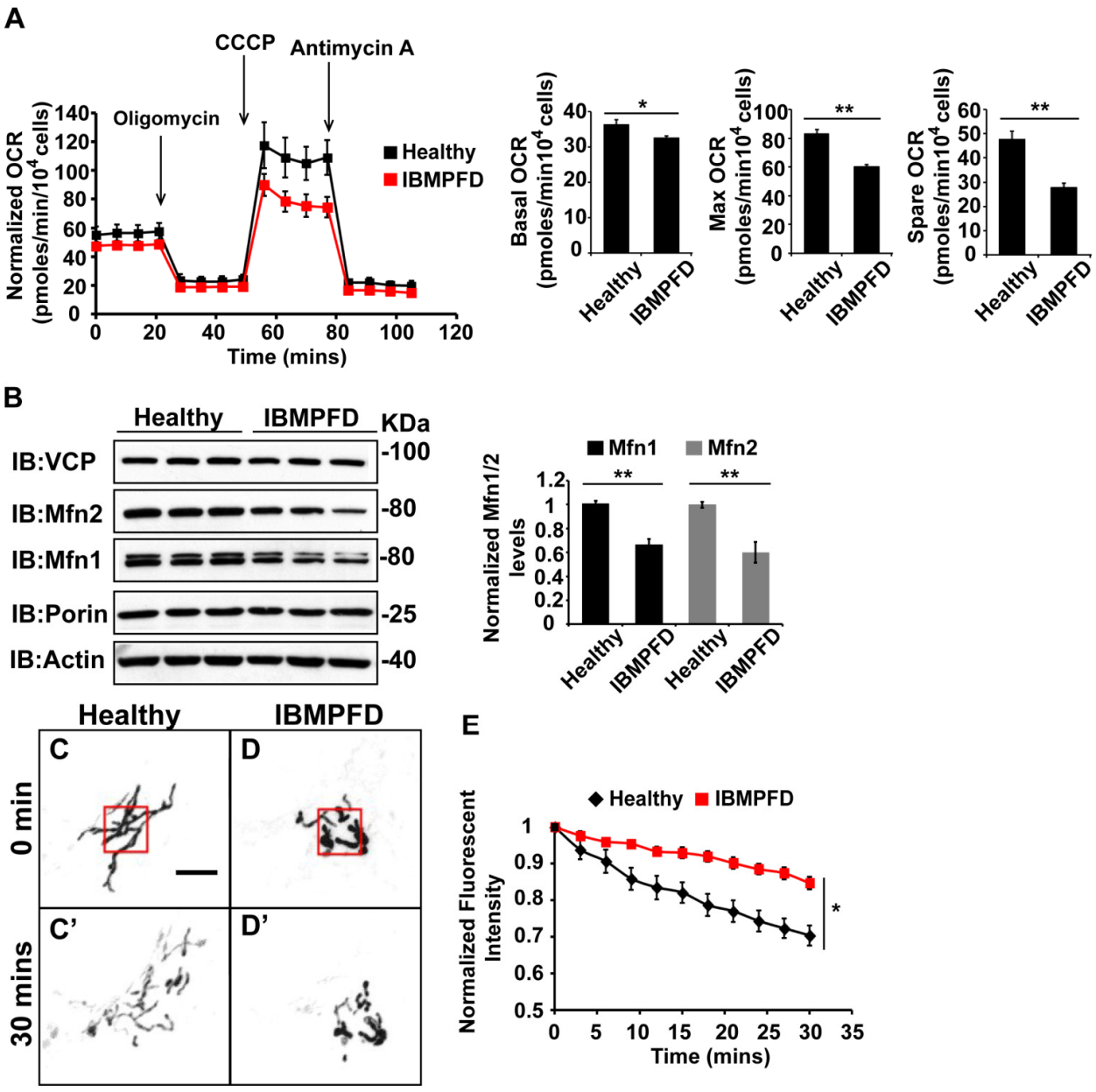

Figure 2-6: IBMPFD patient cells carrying the *VCP*$^{R155H/+}$ mutation have decreased Mfn 1 and Mfn 2 levels and reduced mitochondrial fusion.

(**A**): Oxygen consumption rates (OCR) in healthy control and IBMPFD patient fibroblasts. Inhibitory drugs were added at the time points indicated. Basal levels of OCR (p=0.026, independent t test, N=8) and maximum (CCCP-stimulated) OCR (p=3.74E-06, independent t test, N=8) are both decreased in the IBMPFD patient fibroblasts. The spare OCR is also

significantly decreased (p=0.000024, independent t test, N=8). **(B)**: Mfn 1 and 2 levels are consistently decreased in three independent lysates from the IBMPFD patient fibroblasts when compared to the healthy control. Mfn 1 levels in patient fibroblasts are reduced to 0.66±0.14 of controls (p=0.001, independent t test, N=5); Mfn 2 levels are reduced to 0.60±0.14 of controls (p=0.008, independent t test, N=5). **: p<0.01. Normalized Mfn 1 and 2 levels are shown as mean±½SD. **(C-D')**: Mitochondrial fusion assay utilizing photoactivatable mitoGFP (PA-GFP) in healthy control and IBMPFD patient fibroblasts. After laser photoactivation of a region (Red hollow square in C and D), cells were tracked for 30 minutes. **(E)** PA-GFP signal intensity (throughout the whole cell) is recorded every 3 minutes, and the rate of decrease of average GFP signal is a measure of mitochondrial fusion. Fusion rates are significantly decreased in the IBMPFD patient fibroblasts when compared to the healthy control (C', D' and E, independent t test, *: p<0.05).

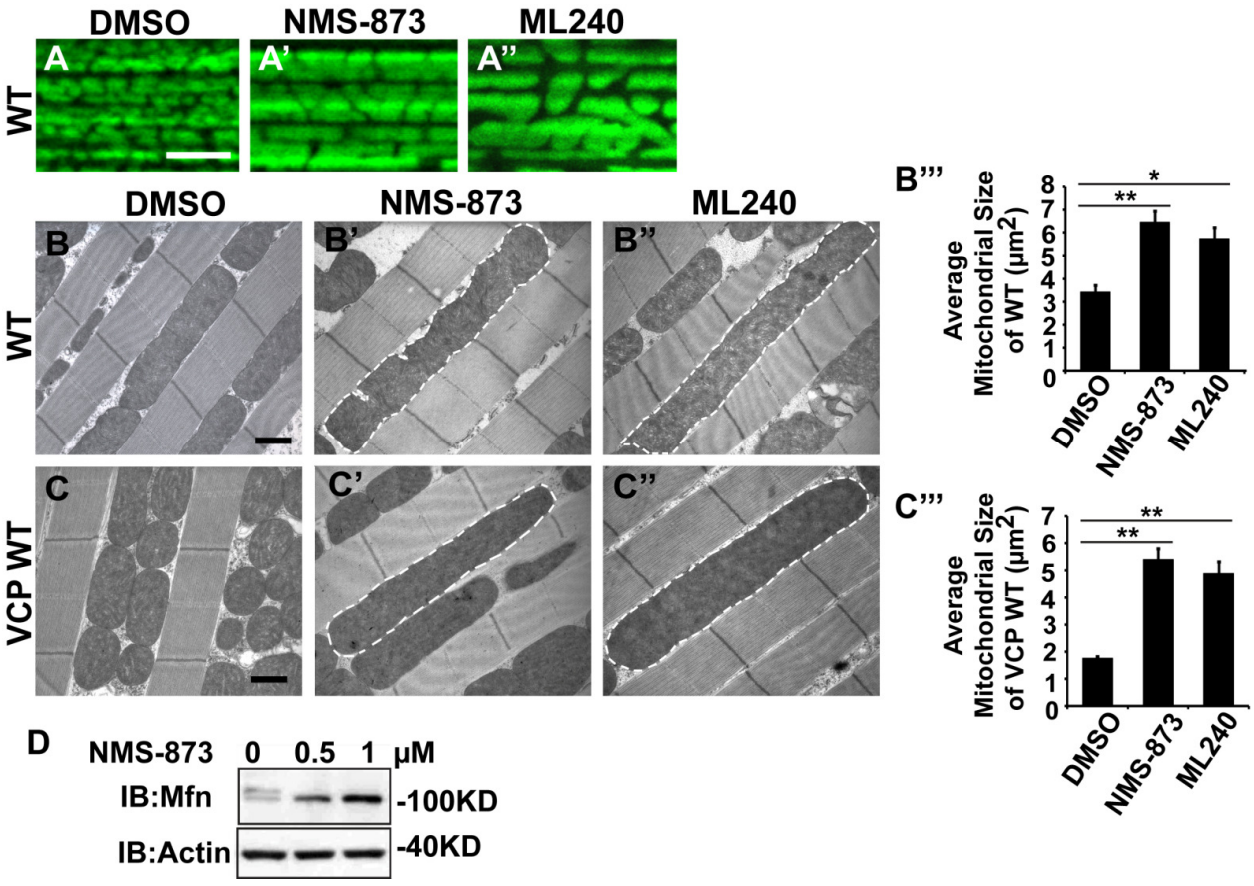

Figure 2-7: VCP inhibitors promote mitochondrial elongation.

(A-A''): MitoGFP assay for mitochondrial morphology. Compared to DMSO fed flies, 10μM NMS-873 or ML240 feeding results in more fused mitochondria in 2-day old flies. Scale bar: 5μm. **(B-B'' and C-C'')**: In 6-day old flies fed with 30μM NMS-873 (B') or 30μM ML240 (B''), elongated mitochondria (outlined in dashed white lines) are observed in muscle. Mitochondria are small in VCP WT flies (C) as compared with WT (IFM-Gal4 control, B). This phenotype is reversed by 30μM NMS-873 (C') or 30μM ML240 (C'') feeding and shifted towards a pro-fusion direction, as the mitochondria are also elongated as compared with WT (B). **(B''' and C''')**: Statistical analysis of mitochondrial size in EM cross sections. In wildtype flies, 30μM NMS-873 or ML240 feeding results in a mitochondrial size increase to 6.46±0.44μm^2 (p=0.007, independent t test, N=45) or 5.75±0.48μm^2 (p=0.032, independent t test, N=39) as

compared to the DMSO group (3.45±0.27μm^2, N=47). VCP WT expression results in small mitochondria (1.78±0.05μm^2, N=68) as compared with WT (B). Feeding of 30μM NMS-873 (5.41±0.40μm^2, p=0.000, independent t test, N=44) or ML240 (4.90±0.42μm^2, p=0.000, independent t test, N=45) reverses these effects. Mitochondria size is shown as mean±½SEM. **(D)**: pCasper-Mfn-eGFP levels accumulate in a dose dependent manner when treated with NMS-873 at 0.5μM and 1μM for 14 hours.

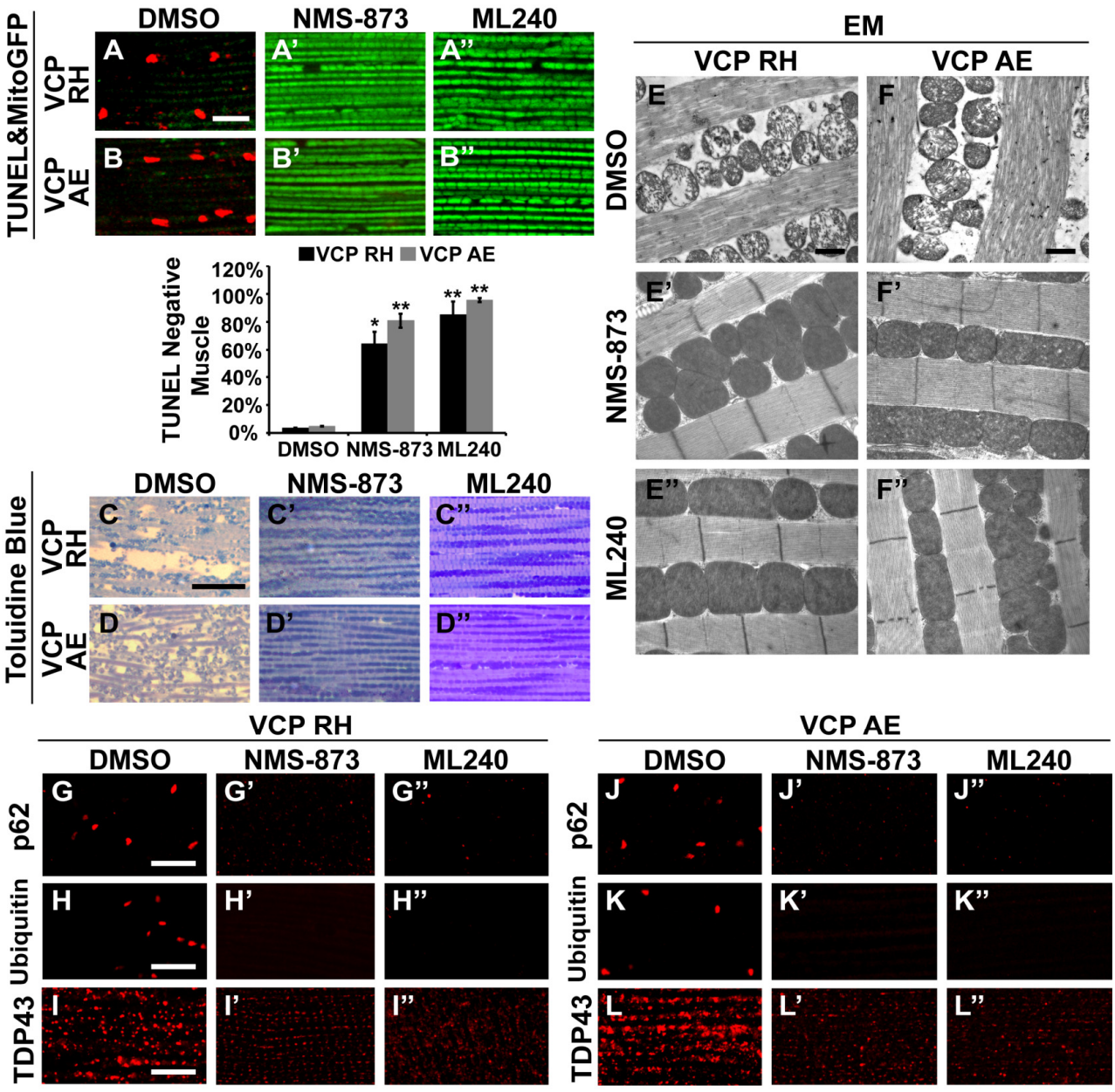

Figure 2-8: VCP inhibitors block mitochondrial defects, muscle tissue damage and muscle cell death in VCP disease mutant flies.

(**A-B''**): Expression of VCP RH and AE leads to muscle cell death by 6 days after eclosion, as visualized through loss of MitoGFP and TUNEL positive signal in nuclei. In the DMSO feeding groups 3.4±0.5% of VCP RH and 4.8±0.6% of VCP AE flies are TUNEL negative. 30μM NMS-873 or ML240 feeding since 1st instar larvae till 6 days after eclosion significantly blocks the

muscle cell death, with 64.3±17.0% (p=0.017) and 85.1±19.0% (p=0.000) of VCP RH, and 80.9±10.1% (p=0.002) and 95.6±3.1% (p=0.000) of VCP AE muscles TUNEL negative. Data are shown as mean±½SD. Independent t test is used. Three independent rounds are performed, 15-20 flies are used each round. *: p<0.05;**: p<0.01. Scale bar: 10µm. **(C-D'')**: Toluidine Blue staining shows that 30µM NMS-873 or ML240 feeding significantly rescue the disrupted muscle structure in VCP RH and AE flies. Scale bar: 40µm. **(E-F'')**: EM shows that 30µM NMS-873 or ML240 feeding significantly rescue the broken myofibril structure and small mitochondria with broken cristae phenotypes in VCP RH and AE flies. Scale bar: 1µm. Note that the mitochondria are still smaller than those from WT flies (Fig. 6B). **(G-L'')**: In 6-day old flies, 30µM NMS-873 (G', H', J' and K') or ML240 (G'', H'', J'' and K'') treatments result in a significant decrease in Ref(2)P/p62 (G and J) and Ubiquitin (H and K) aggregates in VCP RH and AE expressing flies; TDP43 mislocalization (I and L) is partially rescued as the large sarcoplasmic signal decreases, but no nuclear signal is observed (I', I'', L' and L''). Scale bar: 5µm.

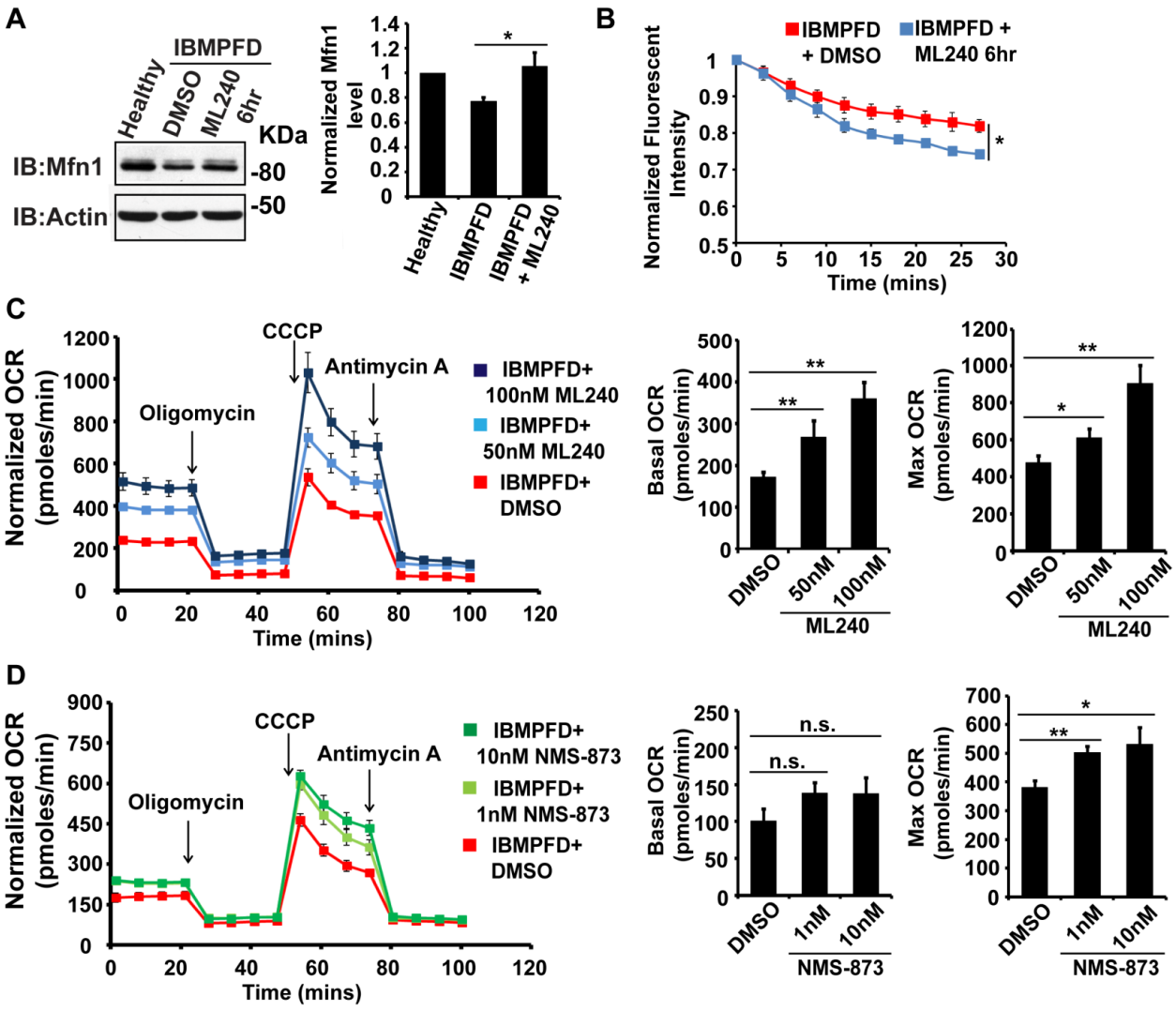

Figure 2-9: VCP inhibitor treatment significantly suppresses mitochondrial respiratory chain and fusion defects in *VCP*$^{R155H/+}$ IBMPFD patient fibroblasts.

(**A**): After treatment of 250nM ML240 for 6 hours, Mfn 1 level of *VCP*$^{R155H/+}$ IBMPFD patient fibroblasts are elevated from 0.77±0.02 to 1.05±0.11 (p=0.037, independent t test, N=3), as compared with healthy controls, for which values are set as 1. (**B**): After treatment with 250nM ML240 for 6 hours, the mitochondria fusion assay shows that the decreased mitochondrial fusion observed in IBMPFD patient's fibroblasts is significantly reversed (independent t test, *: p<0.05). (**C**): 50nM and 100nM ML240 treatment for 4 days significantly increases basal

(p=0.0001, DMSO v.s. 50nM ML240; p=0.0027, DMSO v.s. 100nM ML240, Welch's unpaired t test, N=8) and maximal oxygen consumption rate (p=0.0415, DMSO v.s. 50nM ML240; p=0.0028, DMSO v.s. 100nM ML240, Welch's unpaired t test, N=8) in the IBMPFD patient fibroblasts harboring $VCP^{R155H/+}$ mutation. **(D):** 1nM and 10nM NMS-873 treatment for 6 days significantly increases maximal oxygen consumption rate (p=0.0021, DMSO v.s. 1nM NMS-873; p=0.0395, DMSO v.s. 10nM NMS-873, N=8), but not basal oxygen consumption rate (p=0.0994, DMSO v.s. 1nM NMS-873; p=0.1804, DMSO v.s. 10nM NMS-873, N=8). Welch's unpaired t test is used. *: $p<0.05$, **: $p<0.01$, n.s, no statistical significance.

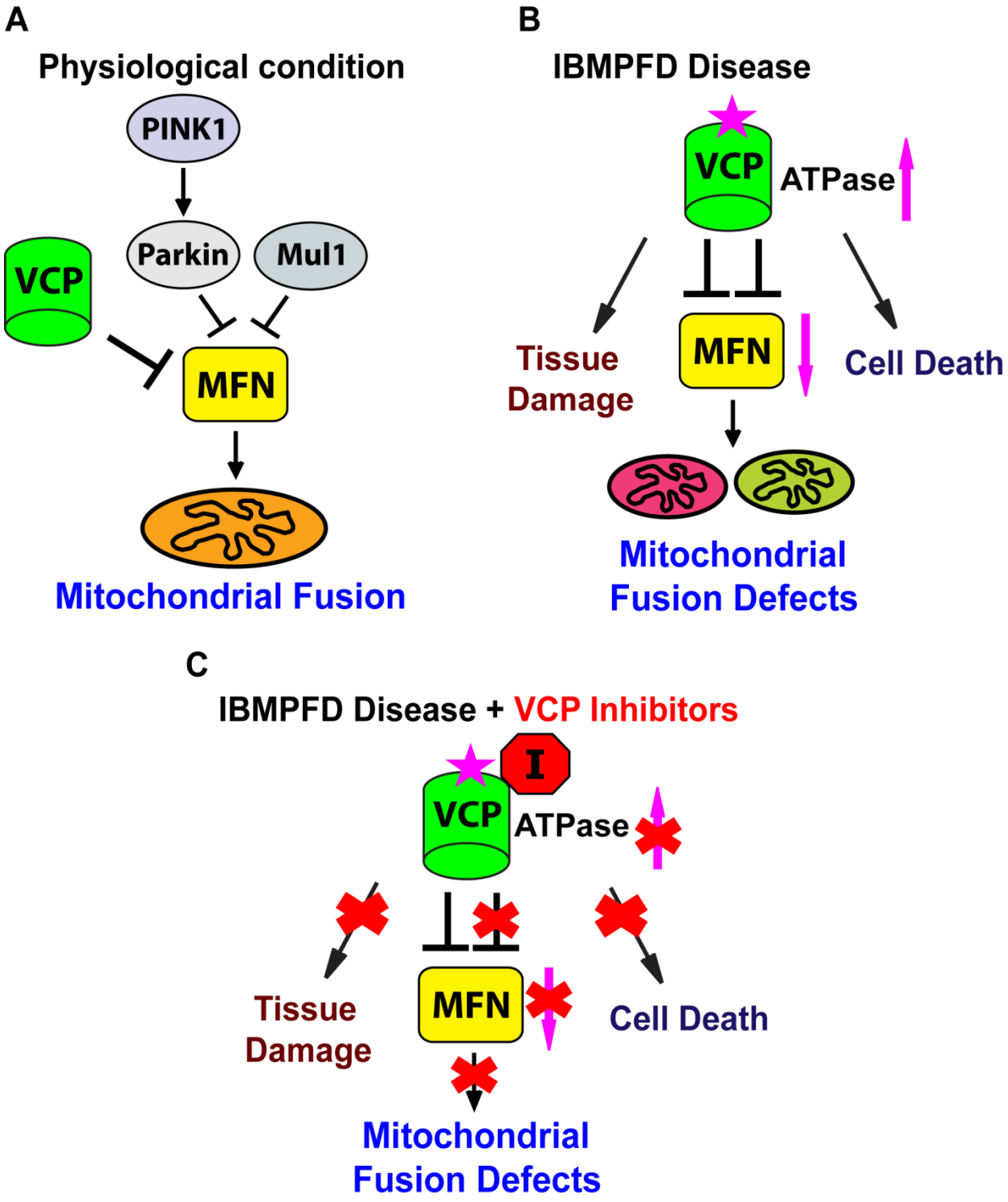

Figure 2-10: Proposed mechanisms of VCP disease mutants mediated mitochondrial defects and potential therapeutic role of VCP inhibitors.

(A): Under physiological conditions, VCP, independent of PINK1/parkin and Mul1, negatively regulates Mfn protein levels, which are critical for the proper balance of mitochondrial fusion and fission. **(B)**: In the IBMPFD disease, enhanced ATPase activity of a VCP disease mutant protein results in excessive loss of Mfn and mitochondrial fusion, leading to mitochondrial fusion defects. Besides the mitochondrial defects, VCP disease mutants also generate pathology including adult muscle tissue damage and muscle cell death. **(C)**: VCP ATPase inhibitors robustly relieves the pathology caused by VCP disease mutants associated with hyperactive VCP activity while leaving normal VCP-dependent functions intact.

Supplementary Figures and Figure Legends:

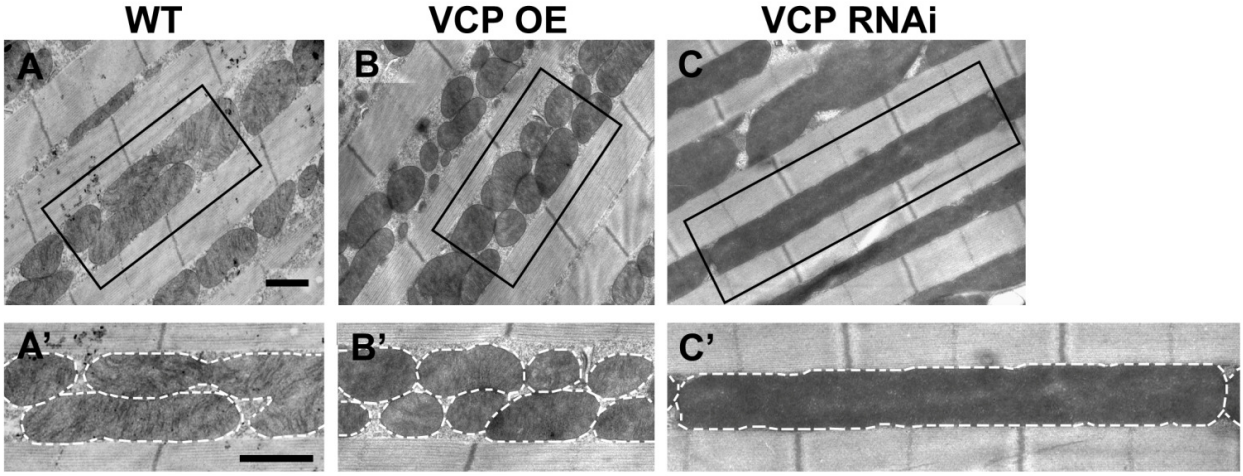

Figure 2-1-figure supplement 1: VCP overexpression leads to smaller mitochondria, while VCP RNAi leads to elongated mitochondria in 2-day old indirect flight muscles.

(A-C'): EM shows that compared to WT (IFM-Gal4 control, A and A'), VCP WT has smaller mitochondrial with intact cristae (B and B'). VCP RNAi results in mitochondrial elongation (C and C') in 2-day old flies. Scale bar: 1µm.

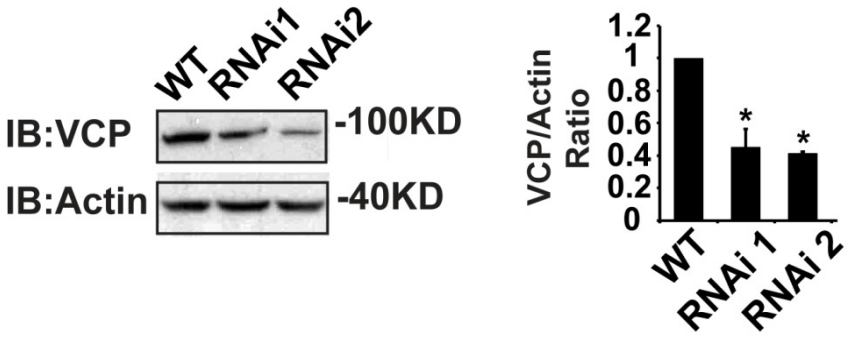

Figure 2-1-figure supplement 2: IFM-Gal4 driven UAS-VCP RNAi results in a significant decrease in VCP levels.

Expression of VCP RNAi line 1 and RNAi line 2 result in a decrease in VCP levels to 45.06±11.17% (p=0.014) and 42.29±1.12% (p=0.037) of those present in WT. Independent t test is used for statistical analysis, N=3. Normalized VCP levels are shown as mean±½SD.

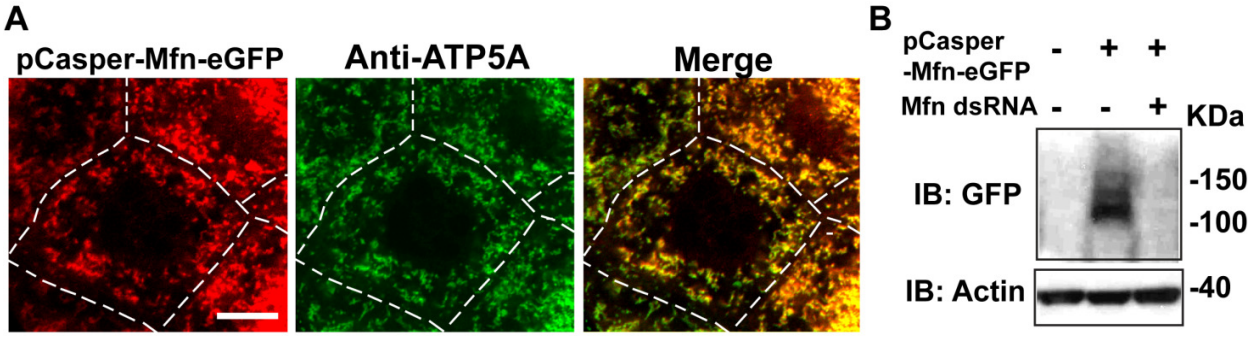

Figure 2-1-figure supplement 3: pCasper-Mfn-eGFP colocalizes with the mitochondria marker ATP5A and is silenced by expression of dsRNA targeting endogenous Mfn.

(A): One nurse cell of a stage 10B egg chamber in transgenetic flies carrying the genomic rescue of Mfn (pCasper-Mfn-eGFP). The pCasper-Mfn-eGFP construct expresses Mfn-eGFP under the control of the endogenous Mfn promoter. GFP signal colocalizes with anti-ATP5A staining, indicating mitochondrial localization. Scale bar: 20μm. **(B)**: S2 cells were transfected with pCasper-Mfn-eGFP and blotted and probed with anti-GFP antibody. Mfn dsRNA treatment (corresponding to the Mfn RNAi construct used in the text) results in loss of Mfn-eGFP expression.

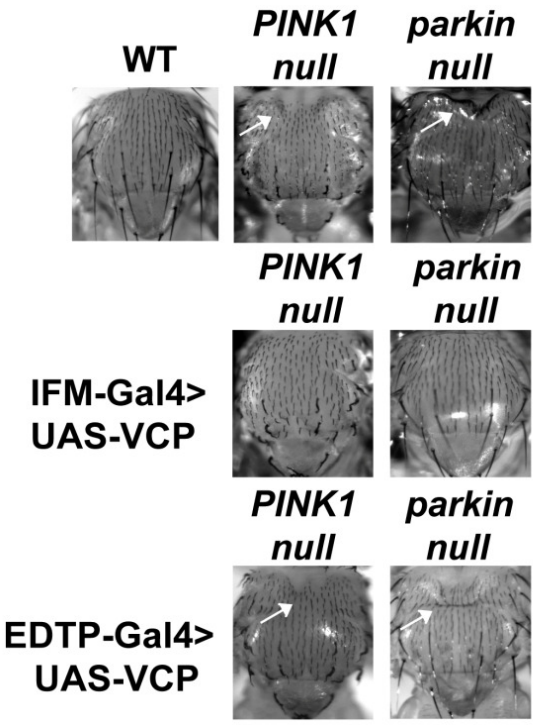

Figure 2-3-figure supplement 1: IFM-Gal4 driven UAS-VCP expression but not EDTP-Gal4 driven UAS-VCP rescues mitochondrial defects in *PINK1* and *parkin* mutants in *Drosophila.*

Thorax indentation is observed in both *PINK1* and *parkin* mutants, indicative of muscle tissue damage. EDTP-Gal4 driven UAS-VCP does not rescue this defect in *PINK1* and *parkin* mutants. IFM-Gal4 driven UAS-VCP completely rescues the thorax indentation in both mutants.

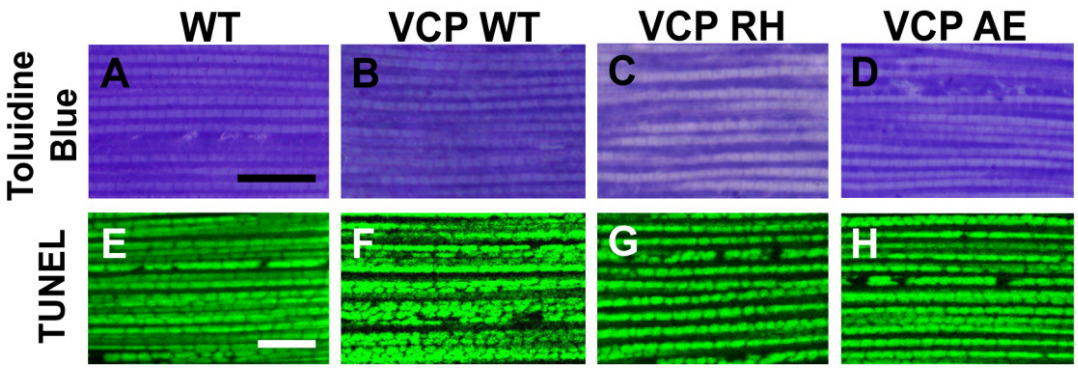

Figure 2-4-figure supplement 1: Muscle isolated from flies expressing VCP disease mutants does not show gross defects at 2 days post eclosion.

(A-D): Toluidine Blue staining of overall muscle morphology shows that VCP RH and AE expression does not result in tissue damage. Scale bar: 40µm. **(E-H)**: Cell death, as visualized using TUNEL/MitoGFP assay, is absent (No Red Signal) and MitoGFP localization (Green) is normal in VCP RH and AE. Scale bar: 10µm.

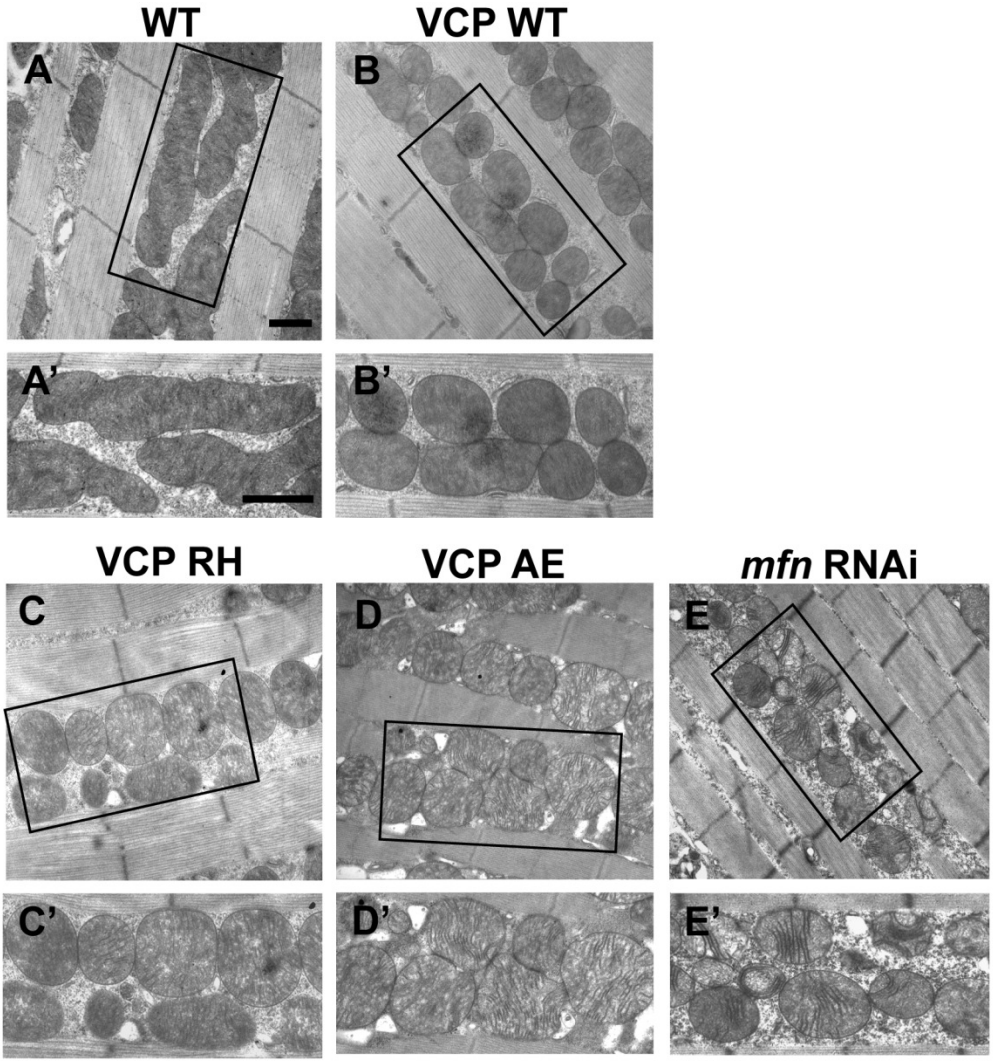

Figure 2-5-figure supplement 1: Expression of VCP disease mutants leads to small mitochondria with abnormal cristae, phenotypes similar to *mfn* RNAi knocking down.

(A-B'): 2 days after eclosion, EM shows that compared to WT (IFM-Gal4 control, A and A'), VCP WT expression results in smaller mitochondrial with intact cristae (B and B'). **(C-E')**: VCP RH and AE also have smaller and fragmented mitochondria, but the cristae are abnormal (C-D'), similar to the phenotype of *mfn* RNAi flies (E and E'). Scale bar: 1μm.

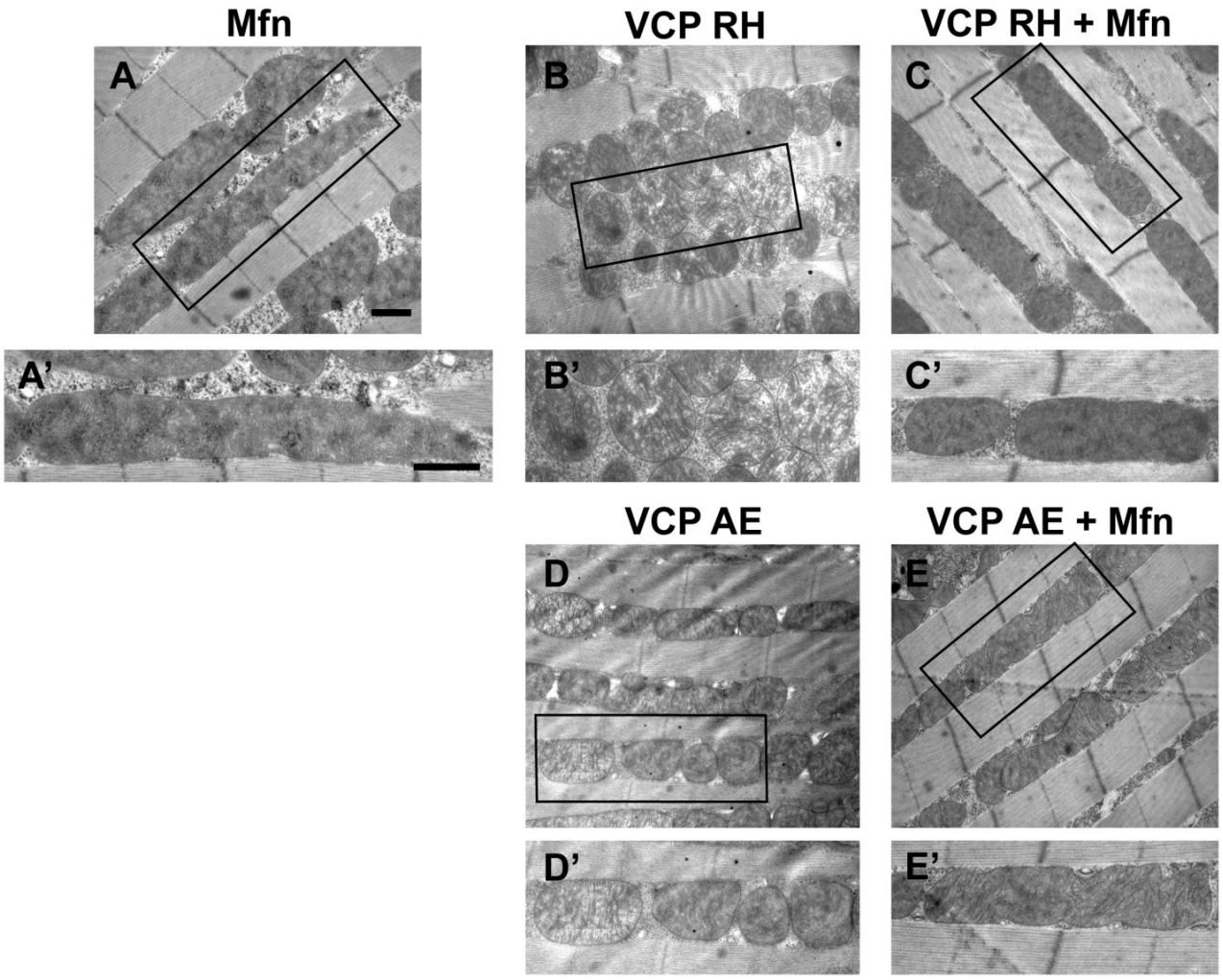

Figure 2-5-figure supplement 2: Mfn expression can suppress mitochondrial defects observed in VCP RH and AE flies.

(A): 2 copies of genomic rescue Mfn-HA (pCasper-Mfn-HA) lead to a heterogeneous mitochondrial phenotype in which some mitochondria are elongated. A' shows a typical elongated mitochondrion. **(B-E')**: In 2-day old flies, expression of 2 copies pCasper-Mfn-HA (C, C' and E, E') results in suppression of mitochondrial defects (fragmented mitochondrial with abnormal cristae) in VCP RH (B and B') and AE (D and D') flies. Scale bar: 1µm.

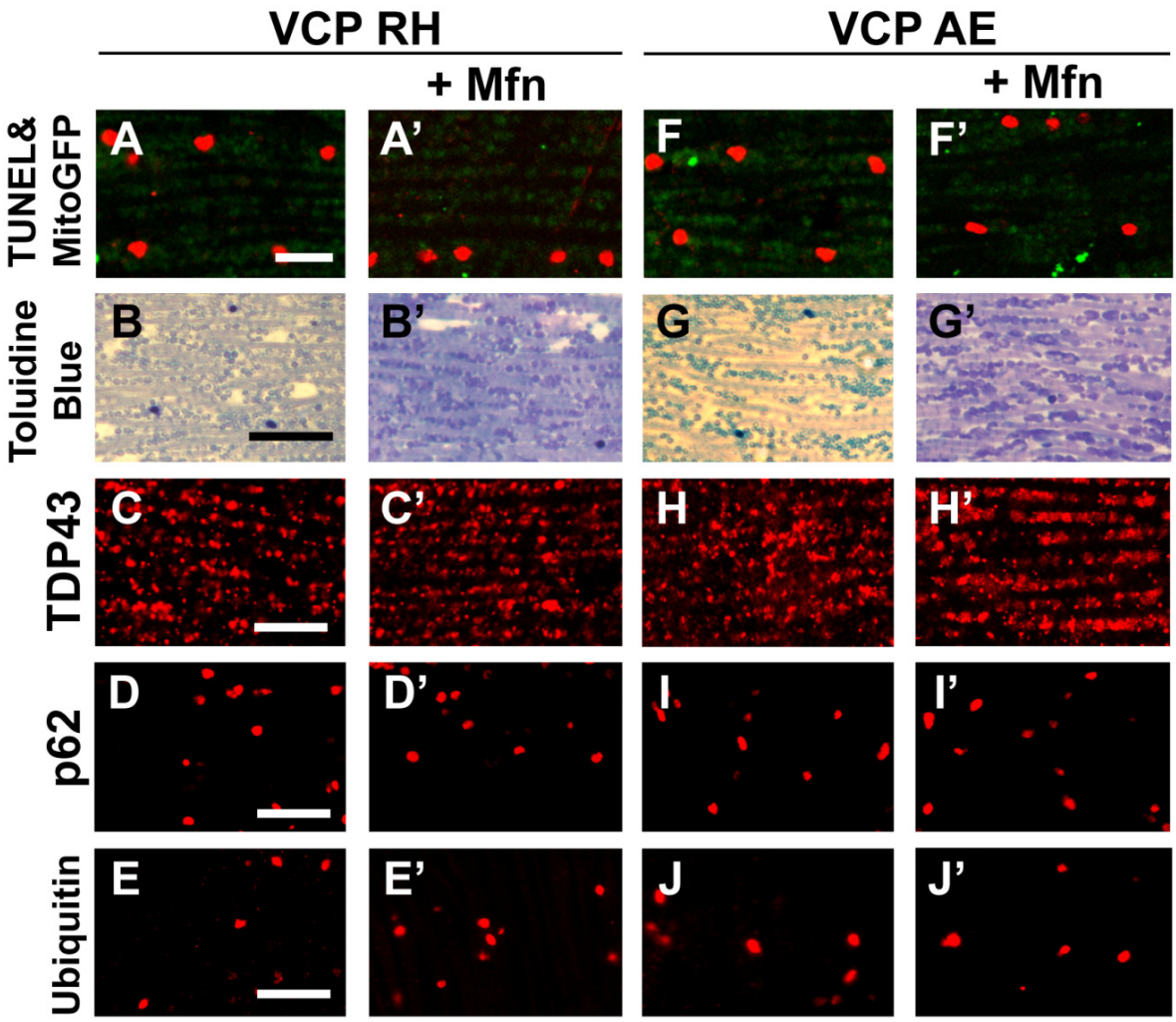

Figure 2-5-figure supplement 3: Mfn expression does not significantly rescue the pathology in VCP RH and AE fly muscles.

2 copies of the pCasper-Mfn-HA/eGFP transgene in VCP RH and AE flies at 8 days of age does not significantly alter muscle cell death assayed by TUNEL/MitoGFP (A,A' and F, F', Scale bar: 10µm), overall tissue disintegration (B, B' and G, G', Scale bar: 40µm), TDP43 mislocalization (C, C' and H, H' Scale bar: 5µm), or the frequency of p62 and Ubiquitin positive aggregates (E, E' and J-J', Scale bar: 5µm).

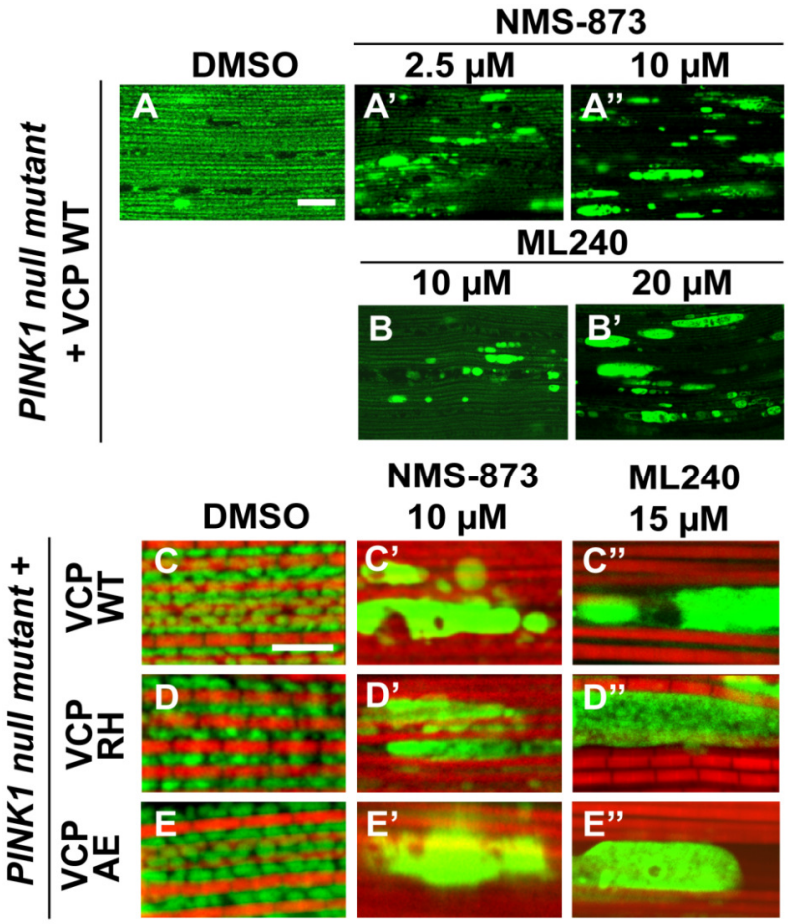

Figure 2-7-figure supplement 1: VCP inhibitor treatment blocks VCP WT and disease mutant rescue of mitochondrial defects in a *PINK1* mutant.

(A-B'): MitoGFP assay shows that NMS-873 and ML240 feeding blocks the ability of VCP WT to rescue *PINK1* mutant mitochondrial phenotypes in a dose-dependent manner. 2.5µM NMS-873 (A) and 10µM ML240 (B) partially inhibit the rescue effect. The rescue effect is significantly blocked with 10µM NMS-873 (A') and 20µM ML240 (B'). Scale bar: 20µm. **(C-E'')**: 10µM NMS-873 blocks VCP WT (C'), RH (D') and AE (E') rescue of *PINK1* mutant mitochondrial phenotypes (C-E) as does feeding with 15µM ML240: VCP WT (C''), RH (D'') and AE (E''). Scale bar: 5µm.

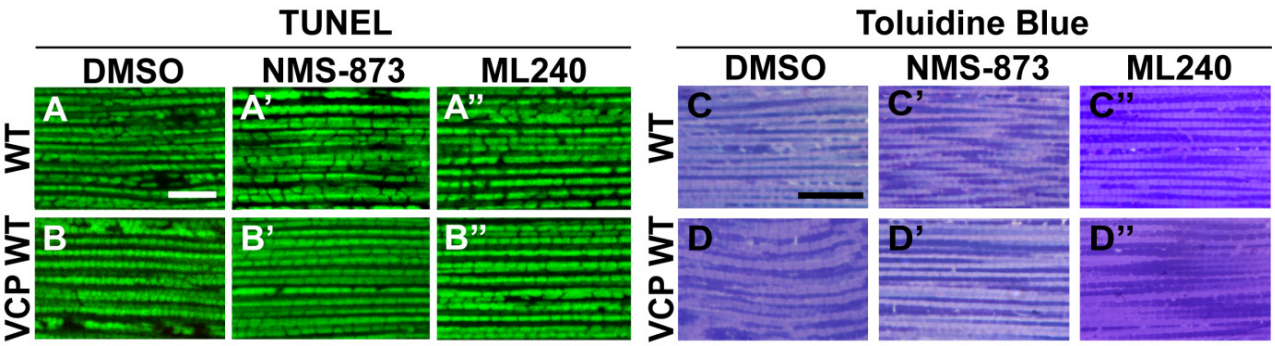

Figure 2-8-figure supplement 1: VCP inhibitor feeding does not affect muscle viability and tissue integrity in 6-day old flies.

(A-B''): TUNEL/MitoGFP assay shows that feeding of 30µM NMS-873 or ML240 does not cause muscle cell death in WT (IFM-Gal4 control, A-A'') and VCP WT flies (B-B''). Scale bar: 10µm. **(C-D'')**: Toluidine Blue assay shows that feeding of 30µM NMS-873 or ML240 does not disrupt muscle integrity in WT (IFM-Gal4 control, C-C'') and VCP WT flies (D-D''). Scale bar: 40µm.

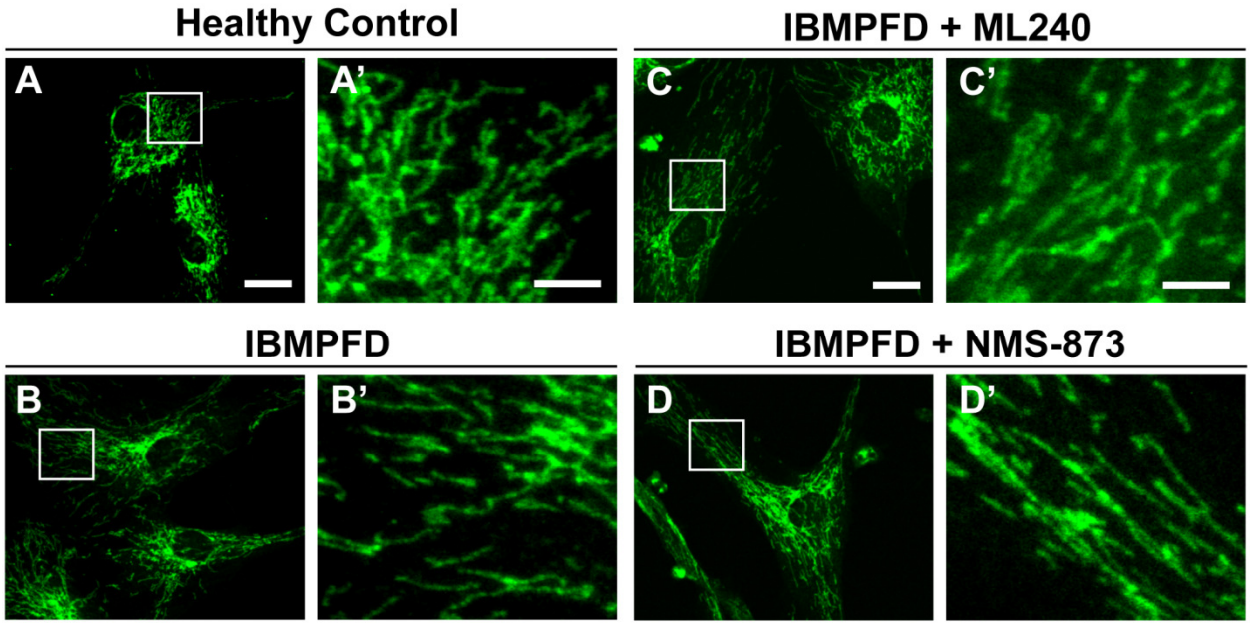

Figure 2-9-figure supplement 1: ML240 and NMS-873 treatments do not significantly change the mitochondrial morphology in IBMPFD patients.

In healthy control fibroblasts mitochondria display an elongated and interconnected phenotype (A-A'). IBMPFD patient's fibroblasts harboring *VCP*$^{R155H/+}$ mutation do not show a significant mitochondrial morphological difference (B-B'). Treatment of these cells with 100nM ML240 treatment for 4 days (C-C') or 10nM NMS-873 treatment for 6 days (D-D') also does not result in a change in mitochondrial morphology (though see Figure 2-9 for evidence that rates of fusion are altered). Scale bar: A-D: 20µm; Scale bar: A'-D': 5µm.

Materials and Methods

Molecular Biology and Constructs: Full length VCP (1-802aa), and truncated VCP cDNAs ΔN-VCP (186 - 802 aa), ΔN+D1-VCP (456 - 802 aa) and ΔD2-VCP (1 - 477 aa) were amplified from VCP cDNA derived from pUASt-VCP WT, a gift from Dr. Yun Nung Jan (Rumpf, Lee et al. 2011). All cDNAs were subcloned into pUASt vectors as translational fusions fused with the 6Myc tag using the Gateway cloning system (Invitrogen). To generate pUASt-Mfn-3Flag, Mfn cDNA was obtained from an EST clone (*Drosophila* Genome Research Center, RE04414), and subcloned into pUASt with the 3Flag tag. To generate VCP RNAi 2, microRNA precursors targeting the coding region of VCP transcripts were cloned into the pUASt vector. The MicroRNA-based silencing technology has been described previously (Chen, Guo et al. 2006; Ganguly, Feldman et al. 2008). All constructs generated above were verified with sequencing.

***Drosophila* strains:** UASt-VCP WT, VCP RH, AE and E2Q lines were gifts from Dr. Tzu Kang Sang (Chang, Hung et al. 2011). IFM-Gal4, UAS-Mfn RNAi, pCasper-DRP1-HA, $PINK1^{5}$, $parkin^{25}$, dpk^{21}, $parkin^{25}$ mul^{A6} were described previously (Clark, Dodson et al. 2006; Deng, Dodson et al. 2008; Yun, Puri et al. 2014). VCP RNAi line1 flies were obtained from the Vienna *Drosophila* RNAi Center (VDRC 24354). VCP RNAi 2 was generated in the lab (see above). Efficiency of RNAi knocking down was verified by Western blott. 24B-Gal4, Mef2-Gal4 and EDTP-Gal4 were obtained from the Bloomington Stock Center at Indiana University. The pCasper-Mfn-HA flies (Sandoval, Yao et al. 2014) were a kind gift from Dr. Hugo Bellen. The pCasper-Mfn-eGFP construct was a kind gift from Dr. C.K. Yao at Academia Sinica, Taipei. Flies carrying pCasper-Mfn-eGFP and pUASt-VCP RNAi 2 constructs were created through injection in a w^{1118} genetic background (pCasper-Mfn-eGFP, X chromosome; VCP RNAi line 2, 2nd chromosome, Rainbow Transgenic Flies, Inc.). vcp^{K15502}, hsFLP22, neoFRT42D, and Ubi-

mRFP.NLS, neoFRT42D were obtained from Bloomington stock center. *Drosophila* strains were maintained in a 25°C humidified incubator or at room temperature.

Generation of Germline Nurse Cell Clones: vcp^{K15502} was recombined with neoFRT42D. Female flies with the genotype: hsFLP22 / +; vcp^{K15502}, neoFRT42D / Ubi-mRFP.NLS, neoFRT42D or pCasper-Mfn-eGFP / hsFLP22; vcp^{K15502}, neoFRT42D / Ubi-mRFP.NLS, neoFRT42D were heat-shocked at 37°C for 2 hours every day from 2nd instar larvae until pupae formation. After eclosion, flies were fed with dry yeast paste for 24 hours to stimulate oogenesis. The egg chambers then were dissected and fixed in 3.7% formaldehyde/Schneider's Buffer for immunoflurescence assays.

TUNEL Assay: Fly thoraxes of the relevant genotypes were cut and fixed in 4% paraformaldehyde/Schneider's Buffer at desired time points. Indirect flight muscles were then dissected out and separated. Muscles were further blocked with blocking buffer [50mM Tris-Cl (pH 7.4), 0.1% Triton X-100, 188mM NaCl] and assayed using the In Situ Cell Death Detection Kit (Roche). 15-20 fly thoraxes are dissected for each round. For each experiment, at least three rounds were performed.

Toluidine Blue staining and Electronic Microscopy: Fly thoraxes of the relevant genotypes were fixed in 1% paraformaldehyde/1% glutaraldehyde/0.1M Phosphate Buffer, post-fixed in 1% osmium tetroxide/ddH20, dehydrated in gradient ethanol and embedded in Epon 812. After polymerization, sections were obtained using either glass knives or diamond knife (Diatome). 1.0-1.5µm sections were stained with Toluidine blue. 80-90nm sections were stained with uranyl acetate and lead citrate and examined by transmission electron microscope (UCLA Brain Research Institute Electron Microscopy Facility). At least 3 thoraxes of each genotype were examined.

Mitochondrial cross-section size quantification: Electron microscopy images (10,000X magnification) were analyzed in Image J Software (National Institute of Health). After setting the scale, each mitochondrion on the image was selected and its area calculated. An independent t test was used to test for statistical significance. At least 3 images were analyzed for each thorax and at least 3 thoraxes of each genotype were examined.

Immuofluoresence and Confocal Microscopy: For assays in indirect flight muscles, muscles of the corresponding age and genotypes were fixed in 4% paraformaldehyde/Schneider's Buffer, permeabilized in 0.3% Triton-X100/PBS. Rhodamine Phalloidin (Invitrogen, 1:500) was used for myofibrile staining. Muscle pieces were incubated with anti-TDP43 rabbit monoclonal antibody (ProteinTech, 1:100), anti-Ref(2)P/p62 rabbit polyclonal antibody (Abcam, 1:100), anti-P4D1 monoclonal antibody (ENZO,1:100) at 4°C overnight. Washes were followed by Goat anti-rabbit/mouse Alexa Fluor 546 secondary antibody (Invitrogen 1:200) at room temperature for 2 hours. For assays of egg chambers, egg chambers were fixed in 3.7% formaldehyde/Schneider's Buffer for 30 minutes and permeabilized with 0.4% Triton-X100/PBS for 4 hours. Egg chambers were incubated with anti-GFP rabbit polyclonal antibody (Invitorgen 1:100), anti-ATP5A mouse monoclonal antibody (Abcam, 1:100) at 4°C overnight and followed by goat anti-rabbit/mouse Alexa Fluor 488/546 secondary antibodies (Invitrogen 1:200) at 4°C overnight. Fibroblasts were fixed in 10% formalin for 10 minutes, 0.2% Triton-X100/PBS permeabilization for 15 minutes, 5%FBS/PBS blocking for 1 hours, anti-Tom20 mouse monoclonal antibody (BD, 1:200) at 4°C overnight and followed by goat anti-mouse Alexa Fluor 488 secondary antibodies (Invitrogen 1:200) at 4°C overnight. Images were taken using a LSM5 confocal microscope (Zeiss).

S2 Cell Culture, transfection and dsRNA treatment: S2 cells were cultured in Schneider's Buffer, 10% FBS, 1% Penicillin and Streptomycin, 50μM Tetracyclin at 25℃. Qiagen Effectene and was used as a transfection reagent according to the producer's instruction. Mfn DsRNA were designed according to a protocol from www.flyrrnai.org and synthesized using the Mega T7 kit from Ambion. Cells were harvested 96hrs after dsRNA treatment. Mfn dsDNA-F: TGA GCA AAT ACC CCC AAA AG; Mfn dsDNA-R: GAT CTG GAG CGG TGA TTT GT.

Fibroblast Cell Culture: Human primary fibroblasts from IBMPFD (GM21752) and age-matched control (GM00024) were obtained from the Coriell Institute for Medical Research (https://catalog.coriell.org) and grown in Dulbecco's Modified Eagle Medium (DMEM, Gibco) or Minimum Essential Media (MEM, Gibco) supplemented with 10% fetal bovine serum (FBS), 2 mM L-glutamine, and penicillin/streptomycin at 37˚C and 5% CO2. Primary fibroblasts were immortalized by infection with retrovirus expressing hTERT (Addgene plasmid #1771). Infected cells were selected in puromycin (1.5ug/mL) for 1 week and maintained in 1ug/ml puromycin.

Protein lysates and Western blot: S2 cells, fly thoraxes or fibroblasts were lysed in RIPA Buffer with Protease Inhibitors (Roche) and 200mM PMSF (Sigma). Protein lysates were centrifuged at 16,000g for 15mins, and the supernatants boiled with 6XSDS sample Buffer (Bioland) at 95℃ for 5 mins. Proteins were separated in SDS-PAGE Gels. Gels were transferred to PVDF membrane (Millipore) and incubated with primary antibody at 4˚C overnight. Following several washes, blots were then incubated with secondary antibodies for 2 hours at room temperature and then washed extensively. Primary antibodies used include: Anti-HA mouse monoclonal antibody (Millipore 1:1000), Anti-Myc mouse monoclonal antibody (Millipore, 1:3000), Anti-Flag rabbit polyclonal antibody (Genscript 1:2000), Anti-GFP rabbit polyclonal antibody (Invitrogen, 1:3000), Anti-Actin rabbit polyclonal antibody (Sigma 1:2000),

Anti-Tubulin mouse monoclonal antibody (Sigma 1:4000), Anti-Porin mouse monoclonal antibody (Abcam, 1:2000), Anti-VCP rabbit monoclonal antibody (Cell Signalling Technology 1:2000), Anti-Human Mfn 1 and 2 mouse monoclonal antibody (Abcam 1:2000), Anti-MnSOD rabbit polyclonal antibody (Abcam 1:2000) and Anti-NDUSF3 mouse monoclonal antibody (Abcam 1:2000). Anti-*Drosophila* Mfn Rabbit polyclonal antibody (1:3000) was a gift from Dr. Alexander Whitworth (Ziviani, Tao et al. 2010). Donkey anti-mouse and anti-rabbit HRP conjugated secondary antibodies (GE Healthcare, 1:10000 or 20000) were used.

Co-immunoprecipitation: 48 hours after transfection, S2 cells were harvested and lysed in the RIPA Buffer with protease inhibitors. Protein lysates were incubated with Dynabeads G and primary antibody (Anti-Myc mouse monoclonal antibody, Millipore 1:300) at 4˚C overnight and washed in 0.1%Tween/PBS 4 times and eluted in 2XSDS sample buffer (BioRad) and denatured at 95˚C. The samples are assayed by western blot.

***In vivo* and *in vitro* VCP Inhibitors treatment:** Powdered forms of NMS-873 (Selleckchem) and ML240 (Sigma-Aldrich) were dissolved in DMSO as stocks. Stock solution and DMSO as the vehicle control were diluted in ethanol/ddH2O and mixed with *Drosophila* food. Food Dye was added to ensure thorough mix. Parents of desired genotypes were put in DMSO or inhibitors containing food for 3 days and removed. Thus, all growth following egg laying occurred in the presence of inhibitor. Immediately after eclosion, progeny were transferred to newly prepared food vials containing the same concentration of DMSO or inhibitor. Progeny were assayed at the time points stated in the text. For human fibroblast treatment, stock solution of ML240, NMS-873 and DMSO vehicle control were diluted to the desired concentration and added to the culture media. Media were changed each day if the treatment was longer than 24 hours.

Mitochondrial fusion assay in fibroblasts: The mitochondrial fusion assay was performed using photoactivatable mitoGFP (PA-GFP) localized to the mitochondrial matrix as previously described (Karbowski, Arnoult et al. 2004; Mishra, Carelli et al. 2014). Briefly, immortalized fibroblasts were infected with retroviruses expressing matrix-tareted DsRed and matrix-targeted PA-GFP to create stable cell lines. Cells were plated on glass coverslips (LabTek) and imaged live at 37˚C on a LSM 710 confocal microscope (Carl Zeiss, Inc.). PA-GFP is activated in a region of interest (5µm x 5µm) by illumination with a 405nm laser. The activated signal is collected in z-stacks every 3 minutes over the next 30minutes. Fusion events result in the dilution of the activated signal, and the average pixel intensity (for the entire cell) over time is a measurement of fusion rates (Karbowski, Arnoult et al. 2004). P-values are calculated using a Student's t-test on the slopes of intensity versus time for individual measurements (>20 per genotype).

Mitochondrial respiration measurements: Oxygen consumption rates (OCR) were measured in immortalized fibroblasts using a Seahorse Biosciences Extracellular Flux Analyzer (Model XF96). Briefly, 10,0000 cells/well were plated the day before measurement into a 96-well culture plate. On the day of measurement, the media was exchanged for non-bicarbonate-containing DMEM (Sigma-Aldrich Cat. #D5030) media using the Seahorse PrepStation, and allowed to equilibrate for 1 hour at 37˚C in room air prior to initiating measurements. Oxygen levels were measured over 5 minute periods. Oxygen consumption rate was measured under basal and stress conditions as indicated. Oligomycin inhibits complex V and blocks ATP production dependent on respiration. CCCP uncouples oxidative phosphorylation and ATP production. It maximizes respiration without ATP synthesis. Antimycin A inhibits Complex III and thus blocks proton pumping and membrane potential formation. Drugs were injected

automatically as indicated in the figure legends (Oligomycin 5µM, CCCP 10µM, Antimycin A 1µM). For drug pre-treatment studies (Figure 2-9C-D), 5000 cells/well were plated into 96-well culture plates and pre-treated with ML240 for 4 days and NMS-873 for 6 days prior to OCR measurement. OCR values were normalized from total cellular content via sulforhodamine B measurements.

Statistical Analysis: The overall study design was a series of controlled laboratory experiments in *Drosophila* and human fibroblasts, as described in detail in the Figure legends sections. In all experiments, animals were randomly assigned to various experimental groups. The experiments were replicated at least 3 times (N was noted in each experiment) and the final analysis was presented. For *in vivo* experiments, 10-20 flies per group were used for each experiment. For the human fibroblasts experiments, details are described in the above methods sections. Data were analyzed using Statistical Package for the Social Sciences (SPSS) 16.0. The P values were assessed using a two-tailed unpaired Student's t test with P values considered significant as follows: *, $p<0.05$ and **, $p<0.01$. For seahorse assay in human fibroblasts, Welch's unpaired t test was used.

Reference

Abramzon, Y., J. O. Johnson, et al. (2012). "Valosin-containing protein (VCP) mutations in sporadic amyotrophic lateral sclerosis." Neurobiology of aging **33**(9): 2231 e2231-2231 e2236.

Ahmed, M., P. M. Machado, et al. (2016). "Targeting protein homeostasis in sporadic inclusion body myositis." Science translational medicine **8**(331): 331ra341.

Bartolome, F., H. C. Wu, et al. (2013). "Pathogenic VCP mutations induce mitochondrial uncoupling and reduced ATP levels." Neuron **78**(1): 57-64.

Brand, A. H. and N. Perrimon (1993). "Targeted gene expression as a means of altering cell fates and generating dominant phenotypes." Development **118**(2): 401-415.

Buchan, J. R., R. M. Kolaitis, et al. (2013). "Eukaryotic stress granules are cleared by autophagy and Cdc48/VCP function." Cell **153**(7): 1461-1474.

Chan, D. C. (2012). "Fusion and fission: interlinked processes critical for mitochondrial health." Annual review of genetics **46**: 265-287.

Chang, Y. C., W. T. Hung, et al. (2011). "Pathogenic VCP/TER94 alleles are dominant actives and contribute to neurodegeneration by altering cellular ATP level in a Drosophila IBMPFD model." PLoS genetics **7**(2): e1001288.

Chapman, E., N. Maksim, et al. (2015). "Inhibitors of the AAA+ chaperone p97." Molecules **20**(2): 3027-3049.

Chen, C. H., M. Guo, et al. (2006). "Identifying microRNA regulators of cell death in Drosophila." Methods in molecular biology **342**: 229-240.

Chen, H., S. A. Detmer, et al. (2003). "Mitofusins Mfn1 and Mfn2 coordinately regulate mitochondrial fusion and are essential for embryonic development." The Journal of cell biology **160**(2): 189-200.

Chen, H., S. A. Detmer, et al. (2003). "Mitofusins Mfn1 and Mfn2 coordinately regulate mitochondrial fusion and are essential for embryonic development." J Cell Biol **160**(2): 189-200.

Chou, T. F., K. Li, et al. (2013). "Structure-activity relationship study reveals ML240 and ML241 as potent and selective inhibitors of p97 ATPase." ChemMedChem **8**(2): 297-312.

Clark, I. E., M. W. Dodson, et al. (2006). "Drosophila pink1 is required for mitochondrial function and interacts genetically with parkin." Nature **441**(7097): 1162-1166.

Custer, S. K., M. Neumann, et al. (2010). "Transgenic mice expressing mutant forms VCP/p97 recapitulate the full spectrum of IBMPFD including degeneration in muscle, brain and bone." Hum Mol Genet **19**(9): 1741-1755.

Davies, V. J., A. J. Hollins, et al. (2007). "Opa1 deficiency in a mouse model of autosomal dominant optic atrophy impairs mitochondrial morphology, optic nerve structure and visual function." Hum Mol Genet **16**(11): 1307-1318.

de Bot, S. T., H. J. Schelhaas, et al. (2012). "Hereditary spastic paraplegia caused by a mutation in the VCP gene." Brain **135**(Pt 12): e223; author reply e224.

DeLaBarre, B., J. C. Christianson, et al. (2006). "Central pore residues mediate the p97/VCP activity required for ERAD." Molecular cell **22**(4): 451-462.

Deng, H., M. W. Dodson, et al. (2008). "The Parkinson's disease genes pink1 and parkin promote mitochondrial fission and/or inhibit fusion in Drosophila." Proc Natl Acad Sci U S A **105**(38): 14503-14508.

Deshaies, R. J. (2014). "Proteotoxic crisis, the ubiquitin-proteasome system, and cancer therapy." BMC biology **12**: 94.

Dobrynin, G., O. Popp, et al. (2011). "Cdc48/p97-Ufd1-Npl4 antagonizes Aurora B during chromosome segregation in HeLa cells." Journal of cell science **124**(Pt 9): 1571-1580.

Frydman, H. M. and A. C. Spradling (2001). "The receptor-like tyrosine phosphatase lar is required for epithelial planar polarity and for axis determination within drosophila ovarian follicles." Development **128**(16): 3209-3220.

Ganguly, A., R. M. Feldman, et al. (2008). "ubiquilin antagonizes presenilin and promotes neurodegeneration in Drosophila." Human molecular genetics **17**(2): 293-302.

Gonzalez, M. A., S. M. Feely, et al. (2014). "A novel mutation in VCP causes Charcot-Marie-Tooth Type 2 disease." Brain : a journal of neurology **137**(Pt 11): 2897-2902.

Guo, M. (2012). "Drosophila as a model to study mitochondrial dysfunction in Parkinson's disease." Cold Spring Harbor perspectives in medicine **2**(11).

Johnson, A. E., H. Shu, et al. (2015). "VCP-dependent muscle degeneration is linked to defects in a dynamic tubular lysosomal network in vivo." Elife **4**.

Ju, J. S., R. A. Fuentealba, et al. (2009). "Valosin-containing protein (VCP) is required for autophagy and is disrupted in VCP disease." The Journal of cell biology **187**(6): 875-888.

Karbowski, M., D. Arnoult, et al. (2004). "Quantitation of mitochondrial dynamics by photolabeling of individual organelles shows that mitochondrial fusion is blocked during the Bax activation phase of apoptosis." J Cell Biol **164**(4): 493-499.

Kim, N. C., E. Tresse, et al. (2013). "VCP is essential for mitochondrial quality control by PINK1/Parkin and this function is impaired by VCP mutations." Neuron **78**(1): 65-80.

Kimonis, V. E., E. Fulchiero, et al. (2008). "VCP disease associated with myopathy, Paget disease of bone and frontotemporal dementia: review of a unique disorder." Biochimica et biophysica acta **1782**(12): 744-748.

Kimonis, V. E., S. G. Mehta, et al. (2008). "Clinical studies in familial VCP myopathy associated with Paget disease of bone and frontotemporal dementia." American journal of medical genetics. Part A **146A**(6): 745-757.

Kimura, Y., J. Fukushi, et al. (2013). "Different dynamic movements of wild-type and pathogenic VCPs and their cofactors to damaged mitochondria in a Parkin-mediated mitochondrial quality control system." Genes to cells : devoted to molecular & cellular mechanisms **18**(12): 1131-1143.

Kitada, T., S. Asakawa, et al. (1998). "Mutations in the parkin gene cause autosomal recessive juvenile parkinsonism." Nature **392**(6676): 605-608.

Magnaghi, P., R. D'Alessio, et al. (2013). "Covalent and allosteric inhibitors of the ATPase VCP/p97 induce cancer cell death." Nat Chem Biol **9**(9): 548-556.

Manno, A., M. Noguchi, et al. (2010). "Enhanced ATPase activities as a primary defect of mutant valosin-containing proteins that cause inclusion body myopathy associated with Paget disease of bone and frontotemporal dementia." Genes to cells : devoted to molecular & cellular mechanisms **15**(8): 911-922.

Meyer, H., M. Bug, et al. (2012). "Emerging functions of the VCP/p97 AAA-ATPase in the ubiquitin system." Nature cell biology **14**(2): 117-123.

Meyer, H., M. Bug, et al. (2012). "Emerging functions of the VCP/p97 AAA-ATPase in the ubiquitin system." Nat Cell Biol **14**(2): 117-123.

Meyer, H. and C. C. Weihl (2014). "The VCP/p97 system at a glance: connecting cellular function to disease pathogenesis." Journal of cell science **127**(Pt 18): 3877-3883.

Mishra, P., V. Carelli, et al. (2014). "Proteolytic cleavage of Opa1 stimulates mitochondrial inner membrane fusion and couples fusion to oxidative phosphorylation." Cell Metab **19**(4): 630-641.

Mishra, P., V. Carelli, et al. (2014). "Proteolytic cleavage of Opa1 stimulates mitochondrial inner membrane fusion and couples fusion to oxidative phosphorylation." Cell metabolism **19**(4): 630-641.

Nalbandian, A., K. J. Llewellyn, et al. (2015). "In vitro studies in VCP-associated multisystem proteinopathy suggest altered mitochondrial bioenergetics." Mitochondrion **22**: 1-8.

Nalbandian, A., K. J. Llewellyn, et al. (2012). "The homozygote VCP(R(1)(5)(5)H/R(1)(5)(5)H) mouse model exhibits accelerated human VCP-associated disease pathology." PLoS One **7**(9): e46308.

Nalbandian, A., K. J. Llewellyn, et al. (2015). "Rapamycin and chloroquine: the in vitro and in vivo effects of autophagy-modifying drugs show promising results in valosin containing protein multisystem proteinopathy." PLoS One **10**(4): e0122888.

Niwa, H., C. A. Ewens, et al. (2012). "The role of the N-domain in the ATPase activity of the mammalian AAA ATPase p97/VCP." The Journal of biological chemistry **287**(11): 8561-8570.

Park, J., G. Lee, et al. (2009). "The PINK1-Parkin pathway is involved in the regulation of mitochondrial remodeling process." Biochemical and biophysical research communications **378**(3): 518-523.

Park, J., S. B. Lee, et al. (2006). "Mitochondrial dysfunction in Drosophila PINK1 mutants is complemented by parkin." Nature **441**(7097): 1157-1161.

Pickrell, A. M. and R. J. Youle (2015). "The roles of PINK1, parkin, and mitochondrial fidelity in Parkinson's disease." Neuron **85**(2): 257-273.

Poole, A. C., R. E. Thomas, et al. (2008). "The PINK1/Parkin pathway regulates mitochondrial morphology." Proceedings of the National Academy of Sciences of the United States of America **105**(5): 1638-1643.

Poole, A. C., R. E. Thomas, et al. (2010). "The mitochondrial fusion-promoting factor mitofusin is a substrate of the PINK1/parkin pathway." PLoS One **5**(4): e10054.

Puumalainen, M. R., D. Lessel, et al. (2014). "Chromatin retention of DNA damage sensors DDB2 and XPC through loss of p97 segregase causes genotoxicity." Nature communications **5**: 3695.

Raman, M., M. Sergeev, et al. (2015). "Systematic proteomics of the VCP-UBXD adaptor network identifies a role for UBXN10 in regulating ciliogenesis." Nature cell biology.

Ritson, G. P., S. K. Custer, et al. (2010). "TDP-43 mediates degeneration in a novel Drosophila model of disease caused by mutations in VCP/p97." The Journal of neuroscience : the official journal of the Society for Neuroscience **30**(22): 7729-7739.

Ritz, D., M. Vuk, et al. (2011). "Endolysosomal sorting of ubiquitylated caveolin-1 is regulated by VCP and UBXD1 and impaired by VCP disease mutations." Nature cell biology **13**(9): 1116-1123.

Ritz, D., M. Vuk, et al. (2011). "Endolysosomal sorting of ubiquitylated caveolin-1 is regulated by VCP and UBXD1 and impaired by VCP disease mutations." Nat Cell Biol **13**(9): 1116-1123.

Ruden, D. M., V. Sollars, et al. (2000). "Membrane fusion proteins are required for oskar mRNA localization in the Drosophila egg chamber." Developmental biology **218**(2): 314-325.

Rumpf, S., S. B. Lee, et al. (2011). "Neuronal remodeling and apoptosis require VCP-dependent degradation of the apoptosis inhibitor DIAP1." Development **138**(6): 1153-1160.

Sandoval, H., C. K. Yao, et al. (2014). "Mitochondrial fusion but not fission regulates larval growth and synaptic development through steroid hormone production." Elife **3**.

Seroude, L., T. Brummel, et al. (2002). "Spatio-temporal analysis of gene expression during aging in Drosophila melanogaster." Aging cell **1**(1): 47-56.

Shih, Y. T. and Y. P. Hsueh (2016). "VCP and ATL1 regulate endoplasmic reticulum and protein synthesis for dendritic spine formation." Nature communications **7**: 11020.

Tang, W. K. and D. Xia (2013). "Altered intersubunit communication is the molecular basis for functional defects of pathogenic p97 mutants." The Journal of biological chemistry **288**(51): 36624-36635.

Theodosiou, N. A. and T. Xu (1998). "Use of FLP/FRT system to study Drosophila development." Methods **14**(4): 355-365.

Valente, E. M., P. M. Abou-Sleiman, et al. (2004). "Hereditary early-onset Parkinson's disease caused by mutations in PINK1." Science **304**(5674): 1158-1160.

Vaz, B., S. Halder, et al. (2013). "Role of p97/VCP (Cdc48) in genome stability." Frontiers in genetics **4**: 60.

Wakabayashi, J., Z. Zhang, et al. (2009). "The dynamin-related GTPase Drp1 is required for embryonic and brain development in mice." J Cell Biol **186**(6): 805-816.

Watts, G. D., J. Wymer, et al. (2004). "Inclusion body myopathy associated with Paget disease of bone and frontotemporal dementia is caused by mutant valosin-containing protein." Nat Genet **36**(4): 377-381.

Weihl, C. C. (2011). "Valosin containing protein associated fronto-temporal lobar degeneration: clinical presentation, pathologic features and pathogenesis." Current Alzheimer research **8**(3): 252-260.

Weihl, C. C., S. Dalal, et al. (2006). "Inclusion body myopathy-associated mutations in p97/VCP impair endoplasmic reticulum-associated degradation." Human molecular genetics **15**(2): 189-199.

Weihl, C. C., A. Pestronk, et al. (2009). "Valosin-containing protein disease: inclusion body myopathy with Paget's disease of the bone and fronto-temporal dementia." Neuromuscular disorders : NMD **19**(5): 308-315.

Xu, S., G. Peng, et al. (2011). "The AAA-ATPase p97 is essential for outer mitochondrial membrane protein turnover." Mol Biol Cell **22**(3): 291-300.

Yang, Y., S. Gehrke, et al. (2006). "Mitochondrial pathology and muscle and dopaminergic neuron degeneration caused by inactivation of Drosophila Pink1 is rescued by Parkin." Proceedings of the National Academy of Sciences of the United States of America **103**(28): 10793-10798.

Yang, Y., Y. Ouyang, et al. (2008). "Pink1 regulates mitochondrial dynamics through interaction with the fission/fusion machinery." Proceedings of the National Academy of Sciences of the United States of America **105**(19): 7070-7075.

Ye, Y., H. H. Meyer, et al. (2001). "The AAA ATPase Cdc48/p97 and its partners transport proteins from the ER into the cytosol." Nature **414**(6864): 652-656.

Yu, W., Y. Sun, et al. (2011). "The PINK1/Parkin pathway regulates mitochondrial dynamics and function in mammalian hippocampal and dopaminergic neurons." Human molecular genetics **20**(16): 3227-3240.

Yun, J., R. Puri, et al. (2014). "MUL1 acts in parallel to the PINK1/parkin pathway in regulating mitofusin and compensates for loss of PINK1/parkin." Elife **3**: e01958.

Zhang, X., L. Gui, et al. (2015). "Altered cofactor regulation with disease-associated p97/VCP mutations." Proceedings of the National Academy of Sciences of the United States of America **112**(14): E1705-1714.

Zhang, X., H. Zhang, et al. (2014). "Phosphorylation regulates VCIP135 function in Golgi membrane fusion during the cell cycle." Journal of cell science **127**(Pt 1): 172-181.

Zhang, Z., X. Lv, et al. (2013). "Ter94 ATPase complex targets k11-linked ubiquitinated ci to proteasomes for partial degradation." Developmental cell **25**(6): 636-644.

Zhou, H. J., J. Wang, et al. (2015). "Discovery of a First-in-Class, Potent, Selective, and Orally Bioavailable Inhibitor of the p97 AAA ATPase (CB-5083)." Journal of medicinal chemistry **58**(24): 9480-9497.

Ziviani, E., R. N. Tao, et al. (2010). "Drosophila parkin requires PINK1 for mitochondrial translocation and ubiquitinates mitofusin." Proc Natl Acad Sci U S A **107**(11): 5018-5023.

CHAPTER THREE

A single Lysine is critical for Ubiquitination and Degradation of Mitofusion by Parkin

Ting Zhang[1], Moon Yong Cha[3], David Chan[3] and Ming Guo[1, 2 *]

[1]Department of Neurology, [2]Department of Molecular and Medical Pharmacology, David Geffen School of Medicine, University of California, Los Angeles, CA 90095;

[3]Division of Biology and Biological Engineering, California Institute of Technology, Pasadena, CA 91125

*To whom correspondence should be addressed: mingfly@g.ucla.edu

In Preparation

Abstracts:

Mitochondria, the major energy source of living organisms, undergo dynamic process of fusion and fission. Mitochondrial fuse to exchange context and facilitate mutual repair, which acts as an important step in mitochondrial quality control. Loss of mitochondrial fusion causes tissue defects in brain and heart. Mitofusin, a highly conserved GTPase, controls the critical initial step of mitochondrial outermembrane tethering. It is known Mitofusin undergoes a major form of posttranslational modification, ubiquitination. Yet to what extent ubiquitination affects the function of Mitofusin and, more importantly tissue health, is not well-understood because it has not been possible to eliminate this modification in otherwise wildtype Mfn. Here we identified critical lysine sites for Mitofusin ubiquitination in *Drosophila* as well as in mammalian cells. Flies harboring a single mutated lysine that prevents Mfn ubiquitination behaves as a gain-of-function mutant, displays excessive mitochondrial fusion defects, muscle degeneration and male sterility. These phenotypes are all rescued when lysine mutant Mfn also lacks GTPase activity. Parkin, an E3 ligase whose mutations cause familial Parkinson's disease, plays a major role in mitochondrial quality control. We found that loss of Mitofusin significantly accelerates Parkin-mediated mitophagy; lysine mutants identified delays Parkin-mediated degradation of Mitofusin and mitophagy, suggesting Mitofusins inhibit Parkin-mediated mitophagy. Our results indicate that the lysine sites we identified are critical to maintain the protein stability of Mitofusion in both *Drosophila* and mammalian cells and Mitofusin levels are critical to keep the balance of mitochondrial fusion/fission, mitophay and hence, tissue health.

Introduction:

Mitochondria are double-membrane intracellular organelles that generate ATP through oxidative phosphorylation and provide most of energy source for living organisms. Mitochondrial integrity is crucial for tissue health. One important mechanism by which this integrity is maintained is cycles of fission and fusion, a dynamic process intricately regulated by several highly conserved GTPases. Fusion is predominantly controlled by Mitofusions (Mfn) and OPA1, whereas fission by DRP1(Chan 2012). Mitofusions control the outermembrane tethering of two mitochondria, the critical initial step on fusion. Mitochondria fuse to exchange content and facilitate repair. Loss of mitochondrial fusion causes embryonic developmental defects(Chen, Detmer et al. 2003), skeletal muscle defects (Chen, Vermulst et al. 2010), neurodegeneration in cerebellum (Chen, McCaffery et al. 2007), and cardiomyocyte defects (Song, Mihara et al. 2015). Mutations in Mitofusion 2 (Mfn2) cause neurodegenerative diseases Charcot-Marie-Tooth disease (Bombelli, Stojkovic et al. 2014).

The discovery of PINK1 and Parkin and their roles in mitochondrial quality control have greatly advanced our understanding of mitochondrial and cellular integrity. Loss-of-function mutations in *PINK1* (*Park6*) and *Parkin* (*Park2*) cause familial Parkinson's disease (PD) (Kitada, Asakawa et al. 1998; Valente, Abou-Sleiman et al. 2004). *PINK1* encodes a serine/threonine kinase, whereas *Parkin* encodes an E3 ligase. Our lab and others have shown that *in vivo* PINK1 and Parkin function in the same pathway with PINK1 functions upstream of Parkin to promote mitochondrial health, with loss of either gene causing severe mitochondrial damage (Clark, Dodson et al. 2006; Park, Lee et al. 2006; Yang, Gehrke et al. 2006). These defects are linked to deregulated Mfn since decreasing levels of Mfn suppresses *PINK1/parkin* mutants phenotypes and PINK1 and Parkin negatively regulate Mitofusion (Mfn) protein levels in *Drosophila* (Ziviani, Tao et al. 2010), and increased levels of Mfn are toxic, resulting in phenotypes similar to those

associated with loss of PINK1 or Parkin,. In mammalian systems, upon mitochondrial depolarization, PINK1 is stabilized on the mitochondrial membrane. This results in recruitment of Parkin onto damaged mitochondria. Parkin ubiquitinates and promotes the elimination of a number of substrates, including Mfn1 and Mfn2 through proteasome-dependent degradation. This ultimately results in autophagy of mitochondria (Youle and Narendra 2011). At a molecular level, PINK1 has been reported to phosphorylate Mfn2 (Chen and Dorn 2013) and Parkin ubiquitinates mitofusions in mammals as well as in *Drosophila* (Ziviani, Tao et al. 2010; Chan, Salazar et al. 2011).

Mammals have two Mfn-encoding genes, Mfn1 and Mfn2. These proteins share similar domains: a GTPase domain at the N-terminus, a coiled-coiled heptad repeat domain 1(HR1), two transmembrane domains, and a coiled-coiled heptad repeat domain 2(HR2) at the C-terminus. Recent structural biology studies indicate that the inter-and intra-molecular interaction of HR1 and HR2 domains within or between Mfn1 and Mfn2 regulates mitochondrial fusion and morphology. GTPase domains of Mfn1 molecules transiently dimerize upon GTP binding, which is critical for its fusogenic activity; HR2 domains of Mfn2 molecules restrained by the HR1 domain forms fusion non-permissive state, disrupting this HR1/HR2 domain interaction promotes Mfn2-mediated fusion. (Franco, Kitsis et al. 2016; Cao, Meng et al. 2017). Mitofusions also undergo posttranslational modifications, including ubiquitination and phosphorylation. Protein ubiquitination plays several different roles, including promoting proteasome-dependent degradation of ubiquitinated proteins. In a first step, ubiquitin activated by E1; in a second step ubiquitin is conjugated by E2; in a third step ubiquitin is transferred to a target protein by an E3 ligase. E3 ligases provide for target protein specificity in the ubiquitination process (Pickart and Eddins 2004). Several E3 ligases have been identified that mediate ubiquitination of Mitofusions.

These include Huwe1 for Mfn2 (Leboucher, Tsai et al. 2012), March5 and GP78 for Mfn1 (Fu, St-Pierre et al. 2013; Park, Nguyen et al. 2014), SCF^{Mdm30} for the yeast homologue of Mitofusin, Fzo1 (Cohen, Amiott et al. 2011). Finally, Parkin targets both Mfn1 and Mfn2 in mammals, as well as Mfn in *Drosophila* (Tanaka, Cleland et al. 2010; Ziviani, Tao et al. 2010). An E3 ligase conjugates ubiquitin to specific lysine residues of target proteins. Since each E3 ubiquitinates multiple proteins, identification and mutation of key lysine residues on specific target proteins is critical for understanding the significance of ubiquitin modification of that protein. Sarraf, et al performed a quantitative diGLY capture proteomics and generated a profile of ubiquitination lysine sites on Parkin-targeted to mitochondria outer membrane proteins following mitochondrial depolarization with CCCP. Eight sites were identified on Mfn1, and ten on Mfn2 (Sarraf, Raman et al. 2013). The importance of specific modifications requires further study.

In some contexts, ubiquitination marks Mitofusion for degradation, thereby preventing mitochondrial fusion (Park, Nguyen et al. 2014). In other contexts inhibition of deubiquitinases, proteases that remove ubiquitin from modified proteins, results in more ubiquitination on Mfn and increased mitochondrial fusion, suggesting the non-proteolytic or regulatory role of ubiquitination (Anton, Dittmar et al. 2013; Yue, Chen et al. 2014). However, since neither the critical lysine residues modified by ubiquitination or deubiquitinases have been identified it is unclear exactly how ubiquitination of Mitofusion regulates mitochondrial fusion and tissue health.

Here we identified a conserved lysine site in *Drosophila* Mfn, Lysine456, that is essential for Mfn ubiquitination and degradation by Parkin. Flies harboring the mutant of this lysine site have stabilized Mfn protein levels, display excessive mitochondrial fusion, and have multiple defects associated with excessive fusion, including muscle degeneration and male sterility. Excessive mitochondrial fusion and associated defects are prevented by blocking Mfn GTPase activity,

consistent with the Lysine to Arginine (K to R) mutation bringing about a gain-of-function activity. In mammalian cells, mutations of the same conserved lysine significantly stabilize Mfn1 protein levels in the presence of Parkin, and delays Parkin-mediated degradation of Mfn1 and Mfn2 upon mitochondria depolarization in both human Hela cells and mouse embryonic fibroblasts. Moreover, we found that in MEFs lacking Mfn1 and Mfn2 Parkin-dependent mitophagy in response to CCCP-mediated depolarization is significantly accelerated, whereas mutation of the conserved Mfn 1 and 2 lysine residues delays mitophagy. These results provide direct evidence that ubiquitination of a specific lysine is critical for Mitofusin ubiquitination and degradation under basal conditions and in response to Parkin. Regulation through this lysine is essential since failure to ubiquitinate the residue results in dramatic defects in mitochondrial morphology, tissue health and male fertility

Results:

Lysine site 456 is critical for ubiquitination of Mfn in Drosophila.

In order to explore Mfn ubiquitination in *Drosophila* we utilized flies carrying a genomic rescue version of the Mfn gene, pCasper-Mfn-HA, expressed under the control of its own promoter, and including an HA tag on the Mfn C-terminus, a kind gift from Dr. C.K.Yao at Taipei (Figure 3-1B). Flies carrying this transgene are hereafter referred to as Mfn-WT genomic rescue. The presence of this transgene is sufficient to rescue the *mfn* loss-of-function mutant phenotype (Sandoval, Yao et al. 2014). When this construct is introduced into S2 cells Mfn can be detected using anti-HA and anti-endogenous Mfn antibodies, and expression can be suppressed using Mfn dsRNA (Supplementary Figure 3-1A). We and others have found that *PINK1* and *Parkin* function in linear pathway and negatively regulates Mfn protein levels. Thus, loss of *PINK1* or *parkin* in S2 cells

results in decreased Mfn ubiquitination and an increase in Mfn protein levels(Ziviani, Tao et al. 2010). Endogenous VCP, a conserved ATPase that mediates degradation of ubiquitin-modified proteins, also negatively regulates Mfn protein levels (Zhang, Mishra et al. 2017). Consistent with previous findings, using an anti-Ubiquitin (P4D1) antibody, we found that Mfn-WT genomic rescue is robustly ubiquitinated in S2 cells. Levels of ubiquitinated Mfn as visualized with anti-HA, are enhanced when VCP is knocked down, and decreased when PINK1 is knocked down (Supplementary Figure 3-1B). Together these *in vivo* and *in vitro* results show that the Mfn-WT genomic rescue transgene has wildtype activity and can therefore be used to explore Mfn ubiquitination.

Sarraf, et al. identified 8 lysine sites in human Mfn1 and 10 lysine sites in Mfn2 that can be significantly ubiquitinated in Parkin-overexpressing cells following CCCP treatment. In order to identify critical lysine residues we searched for those that are conserved in human Mfn1, Mfn2 and *Drosophila* Mfn. As shown in Figure 3-1A-B, we found 3 such lysine residues in *Drosophila* Mfn, K125, K456 and K791. K125 is located near the N-terminus, K791 is located near the C-terminus, and K456 is located in the heptad-repeat (HR1) domain. We generated HA-tagged Mfn-genomic rescue transgenes that included individual K to R mutations for each of these lysines and characterized their behavior in S2 cells. Surprisingly, K125R and K791R mutations did not affect Mfn ubiquitination, while K456R almost completely abolished Mfn ubiquitination (Figure 3-1C). In our assay, anti-HA antibody detects unmodified Mfn (indicated with black arrowhead in Figure 3-1C), as well as mono-ubiquitinated Mfn and multi/poly-ubiquitinated Mfn (higher molecular bands above the unmodified Mfn in Figure 3-1C). The anti-ubiquitin antibody robustly detects ubiquitinated forms. The K456R mutation abolished the abundant ubiquitination observed in WT

and resulted in significant stabilization of unmodified Mfn (Figure 3-1C and Figure 3-1D). These results show that K456 is a critical lysine for Mfn ubiquitination in *Drosophila.*

The Mfn KR mutant has defects indicative of excessive mitochondrial fusion, similar to those observed in parkin and PINK1 null mutants.

In order to explore the biological consequences of the Mfn-K456R mutation, we generated Mfn-K456R mutant transgenetic flies, hereafter referred to as Mfn-KR genomic rescue flies. Flies carrying a single copy of a Mfn-WT genomic rescue appear wildtype in a variety of assays (below). In contrast, Mfn-KR genomic rescue flies display a number of defects. Thus, wildtype flies and those expressing Mfn-WT have a smooth adult thorax (Figure 3-2A). In contrast Mfn-KR flies have an indentation in their thorax, similar to that observed in *parkin* and *PINK1* null mutants and Mfn-WT overexpressing flies (Yun, Puri et al. 2014) (Figure 3-2A). This indentation often reflects defects in mitochondria of the underlying flight muscle. We visualized mitochondria in the adult indirect flight muscle using mitochondria-target GFP (mitoGFP). In wildtype and Mfn-WT genomic rescue flies mitochondria are compact and well-aligned between myofibrils (Figure 3-2B-B' and 2C-C'). In contrast, in flight muscles from Mfn-KR genomic rescue transgenetic flies and *parkin*/*PINK1* null mutants, there is a general loss of mitoGFP signal associated with the presence of large GFP aggregates (Figure 3-2D-D', 2E-E' and 2F-F'). No cell death was observed in wildtype or Mfn-WT genomic rescue flies using TUNEL staining (Figure 3-2B-C"). However, high levels of TUNEL staining were observed in muscle from Mfn-KR mutant flies, and *parkin*/*PINK1* null mutants (Figure 3-2B''-F''), as observed previously (Deng, Dodson et al. 2008). Importantly, the defects in mitoGFP localization and cell death and cell death in the Mfn-KR genomic rescue flies could be robustly suppressed by knockdown of Mfn using RNAi (Figure

3-2G, G' and G''), as also previously observed for *PINK1* and *parkin* mutants (Deng, Dodson et al. 2008). Finally, *PINK1* and *parkin* mutants are also male sterile, with defects in the development of the nebenkern, a specialized mitochondrial structure (Deng, Dodson et al. 2008). Mfn-KR genomic rescue flies show similar phenotypes. They are 100% sterile (Figure 3-2H). A mechanistic basis for these phenotypes is provided by the observations that Mfn protein levels are increased in Mfn-KR mutant flies, as detected using either an anti-HA antibody (which detects only Mfn-KR), or an anti-Mfn antibody (which detects all Mfn), and that these levels are decreased by *mfn* RNAi (Figure 3-2I). These results, and those from S2 cells, demonstrate that the Mfn-KR mutant results in loss of Mfn ubiquitination, and an increase in Mfn protein levels. This results in excessive mitochondrial fusion, and phenotypes very similar to those of *parkin/PINK1* null mutants. The fact that these mitochondrial defects can be robustly rescued by *mfn* RNAi suggests that the Mfn-KR mutant is a gain-of-function allele.

Further support for this hypothesis comes from examination of mitochondrial morphology in the adult ovary. Each female fly has a pair of ovaries, and each ovary contains a linear series of egg chambers that progress from stage 1 to stage 14. Each egg chamber has three types of cells: somatic follicle cells, germline-derived nurse cells and the oocyte. Follicle cells are present in a monolayer of cells that cover the egg chambers; the 15 nurse cells and 1 oocyte are derived from 4 sequential mitotic divisions of one germline stem cell. The nurse cells provide proteins and RNAs for oocyte development and early embryonic development(Frydman and Spradling 2001). Figure 3-3A shows the diagram of a typical stage 7 egg chamber. Mitochondria have a short tubular morphology in wildtype nurse cells (Figure 3-3D). Mitochondria also have a short tubular morphology in Mfn-WT genomic rescue nurse cells (Figure 3-3B), and Mfn-WT localizes to mitochondria in these cells, as visualized using anti-HA antibody staining (Figure 3-3B-B''). Mfn-

KR also localizes to mitochondria (Figure 3-3C-C''), but the mitochondria are clumped and aggregated (Figure 3-3C-C"). As with adult flight muscle, the mitochondrial clumping and aggregation seen in Mfn-KR ovaries is similar to that observed in the ovaries of *parkin/PINK1* null mutants (Figure 3-3D-F).

Mitochondrial and tissue defects in Mfn-KR mutant flies are suppressed by loss of Mfn GTPase activity.

As an independent test the hypothesis that the Mfn-KR mutant is a gain of function allele, we characterized the effects of introducing a second mutation that prevents an essential Mfn activity, in the Mfn-KR mutant background. Mfn, and its homologs in species from yeast to humans, is a GTPase, and defects in this activity impair its pro-fusion function (Hermann, Thatcher et al. 1998). We generated a conserved GTPase mutant using the genomic rescue construct, pCasper-Mfn-T171A-HA (mammalian Mfn1 T108A mutant (Santel, Frank et al. 2003)), hereafter referred to as the Mfn-TA mutant, as well as the double mutant pCasper-Mfn-T171A/K456R-HA, hereafter referred to as the Mfn-KR/TA mutant (Figure 3-4A). GTPase defect mutations in the yeast Mfn counterpart fzo decrease fzo's ubiquitination and increase fzo protein stability (Cohen, Amiott et al. 2011). Ubiquitination of Mfn-TA expressed in S2 cells was also decreased, as compared with Mfn-WT, while Mfn-TA levels were comparatively stabilized (Figure 3-4B). Interestingly, the Mfn-KR/TA mutant had a level of stability similar to that of the Mfn-KR mutant alone (Figure 3-4B). An enhancement of Mfn protein levels was also observed in Mfn-KR/TA transgenetic flies (Figure 3-4C). Importantly, even though the levels of Mfn-KR/TA were comparable to those of Mfn-KR flies, Mfn-KR/TA flies were 100% fertile (individual male assayed, data not shown), suggesting that loss of GTPase activity eliminates Mfn-KR gain of function activity.

Further evidence that loss of GTPase activity eliminates a Mfn-KR activity comes from characterization of adult flight muscle in Mfn-TA and Mfn-KR/TA transgenics. In 2-day old Mfn-TA transgenics mitochondria were more fragmented as compared to those of similarly aged Mfn-WT transgenics as visualized using mitoGFP and Phalloidin staining (Figure 3-4D-E), and at the ultrastructural level using EM (Figure 3-4D'', D''', 4E'', E'''). No defects were observed in either genotype, as visualized using Toluidine Blue-stained plastic sections (Figure 3-4D' and 4E'). In contrast, in Mfn-KR transgenics muscle showed obvious signs of degeneration, including large vacuole formation in the muscle tissue compared to Mfn-WT flies (Figure 3-4F'), and enlarged and swollen mitochondria with broken cristae, as observed using EM (Figure 3-4F'', F'''). Consistent with our results from the male sterility assay, the Mfn-KR/TA mutant robustly suppressed the mitochondrial and muscle tissue defects in Mfn-KR mutants in all three assays (Figure 3-4G-G''').

Finally, we characterized the ability of different Mfn transgenes to rescue *mfn* loss-of-function mutant phenotypes. *mfn* mutants are third instar larvae lethal (Sandoval, Yao et al. 2014). We focused our analysis on one lethal allele, *mfn* G, which carries a Q65stop mutation. One copy of Mfn-WT genomic rescue completely rescues the lethality and male sterility in *mfn* mutant G (Figure 3-5A). One copy of Mfn-KR mutant genomic rescue also completely rescues the lethality in *mfn*G, though the rescued individual is 100% sterile. In contrast, one copy of the Mfn-TA genomic rescue cannot rescue the lethality of *mfn*G, suggesting that the GTPase activity of Mfn is critical for normal development in flies (Figure 3-5A). Importantly, the robust ability of the Mfn-KR genomic rescue to suppress the lethality associated with the *mfn* G mutation is almost eliminated in Mfn-KR/TA double mutants, with the majority of Mfn-KR/TA double mutants in

the *mfn* G background dying during. A very few individuals reach the black pupae stage, but these ultimately die and no adult progeny is ever observed (Figure 3-5A).

We further characterized mitochondrial morphology phenotypes in flight muscles of *mfn* G animals whose viability was rescued by the presence of the Mfn genomic rescue transgenes. When *mfn* G animals carry the Mfn-WT genomic rescue transgene, mitoGFP is present in mitochondria of uniform size, located throughout the muscle (Figure 3-5B, B'). In contrast, *mfn* G animals carrying the Mfn-KR genomic rescue transgene show a general loss of mitoGFP signal, associated with occasional large mitoGFP aggregates. These phenotypes are similar to those observed in Mfn-KR mutants transgenetic flies (Figure 3-2) and *PINK1/parkin* mutants (Figure 3-2) (Deng, Dodson et al. 2008). During early *Drosophila* male spermatogenesis, two mitochondria interweave with each other and form a single large mitochondrial structure known as the "nebenkern" (Figure 3-5D, black circle). This sits next to the nucleus (open white circle with dark dot) (Figure 3-5D) (Fabian and Brill 2012). Previously, we showed that in *PINK1/parkin* mutants, in which Mfn is stabilized and males are sterile, a large vacuole forms in the nebenkern (Clark, Dodson et al. 2006). While the Mfn-WT genomic rescue transgene gave rise to fertile males in the *mfn* G mutant background, the Mfn-KR genomic rescue transgene did not, and these males contained a vacuole structure similar to that seen in *PINK1/parkin* mutants (Figure 3-4H-J). Thus, the Mfn-KR mutant can not only rescue the lethality of *mfn* mutants, but also display excessive mitochondrial fusion defects in muscle and testis tissues. The mitochondrial and tissue defects of Mfn-KR mutants are completely suppressed by GTPase defective double mutants Mfn-KR/TA, again supporting the hypothesis that Mfn-KR mutants behave as a gain-of-function allele.

Lysine site 456 is critical for Parkin mediated ubiquitination and degradation of Mfn in Drosophila.

Ubiquitination is a sequential process requiring three enzymes: a ubiquitin activating enzyme or E1, a ubiquitin conjugating enzyme or E2, and a ubiquitin ligase or E3. Several E3 ligases have been identified for mammalian Mitofusins, such as Huwe1, March5, GP78, and Parkin (references). Among them, only one potential lysine site on Mitofusin 1 has been identified for March5 (Park, Nguyen et al. 2014). In other work, Parkin ubiquitylome projects have identified multiple sites on both Mitofusin 1 and Mitofusion 2, but which of these are physiologically important require further studies. One of the sites identified in these studies is lysine 456. Here we test if lysine 456 is critical for Parkin mediated ubiquitination and degradation of Mfn.

We and other groups have shown that Parkin degrades Mfn in *Drosophila*; we previously showed that Mfn overexpression leads mitochondrial defects similar to *PINK1*/parkin mutants, with loss of mitoGFP and large mitoGFP aggregates in a mitoGFP/Phalloidin assay (Figure 3-6A, A'), suggesting excessive fusion defects. Parkin overexpression can robustly rescue this phenotype (Figure 3-6B, B'). To explore the hypothesis that lysine 456 is critical for Parkin mediated degradation of Mfn we generated Uast-Mfn-WT-3XFlag and Uast-Mfn-KR-3XFlag transgenic flies and drove expression of these proteins in the indirect flight muscle using IFM-Gal4. Mfn-KR OE display similar mitochondrial defects to Mfn-WT OE (Figure 3-6C, C'). Parkin OE significantly rescues the mitochondrial defects in Mfn-WT OE but could not rescue those associated with Mfn-KR expression (Figure 3-6D, D'). To explore the basis for this behavior we expressed both proteins in S2 cells using actin GAL4. For Mfn-WT 2 strong bands were detected. The lower band represents unmodified Mfn and the upper band is mono-ubiquitinated Mfn, which is abundant in this overexpression scenario. In contrast, for Mfn-KR, overexpression is associated

with only the appearance of the band representing unmodified Mfn, which is present at a higher level than with expression of Mfn-WT. This result indicates that even when overexpressed, ubiquitination and degradation of Mfn-KR is inhibited (Figure 3-6F). Consistent with the mitochondria phenotypes observed in muscles, Parkin OE results in degradation of overexpressed Mfn-WT, while degradation of Mfn-KR is blocked (Figure 3-6F). We further performed the ubiquitination assay with Mfn-WT/KR-HA genomic rescues in S2 cells. Parkin OE enhances Mfn-WT genomic rescue's ubiquitination, but this modification is blocked in cells expressing Mfn-KR, in which Mfn protein levels are strongly stabilized Figure 3-2G). As a positive control, we also showed that Parkin OE robustly ubiquitinates the stabilized Mfn-WT in *PINK1* dsRNA treated S2 cells, further supporting the hypothesis that it is the KR mutation that specifically blocks the Parkin's ability to ubiquitinate Mfn (Supplementary Figure 3-2A). To determine if the failure of Parkin to ubiquitinate Mfn-KR reflects structural changes that prevent interaction we carried out co-immunoprecipitations from S2 cells. These assays show that Mfn-WT and the Mfn-KR mutant have comparable levels of interaction with Parkin. These results strongly suggest that lysine 456 is critical for Parkin's ubiquitination of Mfn and hence its degradation. Finally, it is interesting to note that in both genomic rescue and overexpression scenarios, Parkin overexpression results in some mono-ubiquitinated Mfn-KR, as compared with little or no polyubiquitinated protein (Figure 3-6F-H). This suggests that mono-ubiquitination and poly/multi-ubiquitination may share different lysine sites on Mfn, with poly/multi-ubiquitination being more important for regulation of Mfn protein stability.

We previously showed that Mul1 is another E3 ligase that negatively regulates Mfn protein levels in parallel with Parkin (Yun, Puri et al. 2014). Interestingly, Mul OE still suppresses mitochondria defects in Mfn-KR mutants (Figure 3-6E-E'). Mul1 OE also results in a significant

decrease in Mfn protein levels in both Mfn-WT and KR mutants, suggesting lysine 456 is not critical for Mul1-dependent degradation of Mfn (Supplementary Figure 3-2B).

The KR mutant stabilizes Mfn1 protein levels in Parkin expressing Hela cells and MEFs.

The above data demonstrate that lysine 456 is critical for Parkin's ubiquitination and degradation of Mfn in *Drosophila*. To explore whether the lysine site identified is also important for Parkin/Mitofusions interaction in mammalian systems we generated Mfn1-K395R and Mfn2-K416R mutants, hereafter Mfn1-KR and Mfn2-KR mutants. Since the KR mutant in *Drosophila* Mfn significantly stabilizes Mitofusion protein levels, we first tested whether the KR mutant resulted in a change in the stability of Mfn1 and Mfn2 in Hela cells, which lack Parkin. We expressed the Mfn1-WT and K395R mutant using pcDNA3.1 vector with an N-terminal HA tag. Protein levels were comparable (Supplementary Figure 3-3B). In contrast, when we expressed Mfn1-WT and Mfn1-KR in Hela cells stable-expressing Parkin, a kind gift from Dr. David Chan, the Mfn1-KR mutant was stabilized, as detected by the anti-HA antibody (Figure 3-7A).

As another test of the resistance of the Mfn1-KR mutant to Parkin-mediated degradation, we stably expressed mouse Mfn1-WT and Mfn1-KR in Mfn1-/- Mfn2-/- mouse embryonic fibroblasts (MEFs). These cells provide a genetic background in which potential confounding interactions between overexpressed and endogenous proteins, and between Mfn1 and Mfn2, are eliminated. As with Hela cells, MEFs do not have detectable endogenous Parkin (Supplementary Figure 3-3E). In this background, the Mfn1-KR mutant-expressing cells have comparable Mfn protein levels to those expressing Mfn-WT (Supplementary Figure 3-3A). In contrast, when Parkin is stably co-expressed, Mfn1-KR mutants display enhanced protein levels compared to Mfn-WT (Figure 3-7E). It is worth noticing that the stabilization ratios of Mfn1-KR/Mfn1-WT in Hela and

Mfn1/Mfn2 KO MEF cells are almost identical, 2.06±0.24 in Hela cells (Figure 3-7A) and 2.08±0.26 in MEFs (Figure 3-8E). Together these observations indicate that the lysine site identified in human and mouse Mfn1 is specific to their modification by Parkin. In contrast, protein stabilization of Mfn2-KR is not obvious in case of Mfn2 with or without Parkin expression in Mfn1 -/- Mfn2 -/- MEFs stable-expressing Mfn2-WT/KR mutants (Supplementary Figure 3-3C-D).

KR mutation in Mfn1 and Mfn2 delay their degradation by Parkin in Hela cells and MEFs.

In mammalian systems, Parkin ovexpression does not significantly change Mfn protein levels in unstressed cells(Sarraf, Raman et al. 2013). In contrast, when mitochondria are depolarized with CCCP, Parkin is recruited to mitochondria and degrades outermembrane proteins, including Mfn1 and Mfn2, within 6 hours (Chan, Salazar et al. 2011). Here we test the hypothesis that the lysine residues identified as regulating Mfn stability in unstressed cells also regulated parkin-dependent degradation in response to mitochondrial stress.

We first treated Hela cells stably expressing Parkin expressing Hela cells with 10μM CCCP. Under these conditions Mfn1-WT was degraded at 3 and 6 hrs. In contrast, the degradation of Mfn1-KR was significantly delayed (Figure 3-7B). Consistent with the results presented above, at time point 0, Mfn1-WT showed high levels of ubiquitination under basal Parkin OE condition, and levels of ubiquitination of the Mfn1-KR mutant were lower. The decreased ubiquitination accompanied by protein stabilization of Mfn1-KR mutants was also observed in Mfn1 -/- Mfn2 -/- MEFs that stably expressed Parkin (Figure 3-7F), consistent with our observations of decreased ubiquitination of Mfn-KR in *Drosophila* (Figure 3-1C and D). At time point 3 and 6hrs, the ubiquitination of Mfn1-WT decreases along the time points as the protein levels diminish,

ubiquitination of Mfn1-KR mutant builds up along the time points with a significantly delayed degradation of Mfn1(Figure 3-7C). This result suggests while K395 in Mfn1 is important in Parkin-mediated degradation, other lysine sites may try to compensate and degrade stabilized Mfn.

We also generated Hela cells that stable-expressed Mfn2-WT and KR mutants with an N terminal HA tag. In the absence of CCCP treatment, the Mfn2-KR mutant is not stabilized as compared with Mfn2-WT. To explore the possibility that this lysine contributes, along with others, to ubiquitin-dependent Mfn degradation we generated a K3R mutant of Mfn2 in which two additional conserved lysine surrounding K416 are also mutated to R. This Mfn2-K3R mutant also was not stabilized as compared to Mfn2-WT (Figure 3-7C-D). Interestingly, however, upon CCCP treatment, Mfn2-KR and K3R were degraded at a much slower rate than Mfn2-WT (Figure 3-7C). The fact that Mfn2-KR and K3R behaved similarly in this assay suggests that K416 is a critical lysine for modification of Mfn2 by Parkin in response to mitochondrial stress, but not under basal conditions.

We further performed Parkin-mediated Mfn1/2 degradation assays in Mfn1-/- Mfn2 -/- MEFs that stably-expressed mouse Parkin and mouse Mfn1 or Mfn2 WT/KR mutants. As shown in Figure 3-7G, at 3hrs and 6 hrs after CCCP treatment, mouse Mfn1-WT was rapidly degraded, whereas the degradation of Mfn1-KR was significantly delayed. A delay in degradation of Mfn2-KR was also observed at 6hrs and 12hrs after CCCP treatment (Figure 3-7H). Together these results suggest that the conserved K characterized here is also important in Parkin-mediated degradation of Mfn2. Homo-or heterotypic interactions between Mfn1 and Mfn2, respectively, may also be important for control of Mfn2 degradation.

Mfn1 and Mfn2 KR mutants significantly delay Parkin-mediated mitophagy in Mfn1-/- Mfn2 -/- MEFs and Hela cells

As KR mutants delay Parkin's degradation of Mfn1 and Mfn2 after CCCP treatment, we were interested to test whether these mutations also resulted in a delay in Parkin-mediated mitophagy. To explore this question, we used a cell sorting based assay that utilizes mito-mKeima, a protein that changes its fluorescence emission spectrum in response to pH. In the mitophagy process, mitochondrial will experience a pH drop from pH 7 to pH 4; mito-mKeima signal will shift correspondingly and be detected at 488nm excitation wavelength (green for pH 7) and at 561nm excitation wavelength (red for pH 4) in flowcytometry sorting. Through calculating the shift of green to red mito-mKeima signal, we could quantify the mitophagy process (Lazarou, Sliter et al. 2015). Interestingly, as compared to wildtype Parkin-expressing MEFs, Parkin-expressing Mfn1-/- Mfn2-/- MEFs showed very robust mitophagy at 3 and 6 hours after 20μM CCCP treatment (Figure 3-8A and A').

We then took these cells and expressed in them Mfn1 or Mfn2-WT/KR using retrovirus transduction. In the Mfn1/Mfn2-WT expressing cells there was a reduction in mitophagy as compared with Parkin-expressing Mfn1-/- Mfn2-/- MEFs. Expression of Mfn1/2-KR resulted in a further reduction in mitophagy as compared with Parkin-expressing Mfn1-/- Mfn2-/- MEFs (Figure 3-8B and B'). To further confirm this result, we performed the quantitative mito-mKeima assay in Hela cells that stable-expressed the Mfn2-WT/KR mutant. Compared to wildtype cells, overexpression of Mfn2-WT resulted in a delay in mitophagy, and expression of Mfn2-KR delayed this process further (Figure 3-9A).

At the early stage of mitophagy, Parkin mediates the degradation of mitochondrial outermembrane protein through proteasome pathway. At later stages of mitophagy proteins

components of the mitochondrial innermembrane and matrix are degraded through autophagy (Lazarou, Sliter et al. 2015; Shirihai, Song et al. 2015). We hypothesized that the ability of KR mutants to delay mitophagy should result in a delay in the degradation of other mitochondrial proteins. Indeed, in Hela cells stable-expressing YFP-Parkin, the presence of Mfn2-KR resulted in a significant delay in degradation of several proteins, the inner membrane protein COXII, and the matrix protein HSP60, at 16 hours and 24 hours after 10μM CCCP treatments (Figure 3-9B). Together these results argue that a delay in the degradation of Mitofusin during mitophagy can delay the entire process, identifying regulation of Mitofusin as an important component of mitochondrial quality control.

Discussion

How ubiquitination of Mitofusins regulates mitochondrial fusion and quality control is currently unclear. We identified a single conserved lysine in *Drosophila* Mfn whose mutation resulted in a dramatic inhibition of ubiquitination, stabilization of Mfn protein levels and excessive mitochondrial fusion. These observations provide direct *in vivo* evidence indicate that ubiquitination is not required for Mfn fusion capacity since stabilized Mfn is functional and requires intact GTPase activity to bring about mitochondrial fusion. The fact that Mfn-KR mutant flies display robust tissue defects indicates that regulation of Mfn levels, controlled by ubiquitination, is crucial for tissue health (Figure 3-10).

The conserved lysine site identified displayed specificity for ubiquitination by Parkin in both *Drosophila* and in mammalian cells. Thus, in Hela cells and MEFs, which have very low levels of endogenous parkin endogenous Parkin, Mfn-KR mutants are not stabilized as compared with Mfn-WT. In contrast, when Parkin is overexpressed, KR mutants are resistant to Parkin-dependent

degradation. This Parkin-dependent degradation has been reported in mammalian cells by others, but the mechanism has been unclear (Tanaka, Cleland et al. 2010). Our results identify a conserved lysine as a critical mediator of Parkin's effects on Mfn stability.

Mitofusin's activity is regulated in multiple ways including by GTPase activity, posttranslation modification, domain-domain interactions and hetero-dimerization and homo-dimerization. Previous studies have shown that single amino-acid change can exert significant effect on these events, with consequences for mitochondrial morphology. (Anton, Dittmar et al. 2013; Cao, Meng et al. 2017). We observed robust phenotypes in flies harboring a single lysine mutation. The phenotypes associated with comparable mutations in mammalian cells are significant, but weaker. The results of ubiquitination assays show that the Mfn1-KR mutant still accumulates some ubiquitin, while delaying Parkin-mediated degradation upon CCCP treatment. This result suggests that other lysine site might compensate in the effort to degrade abnormally stabilized Mfn1.

The role of Mitofusins in mitophagy is not clear. Our results provide direct evidences showing that Mitofusin 1 and 2 are critical in the mitophagy process. That loss of Mfn1 and Mfn2 significantly accelerates Parkin-mediated mitophagy after CCCP treatment suggests that Mitofusin and/or basal levels of mitochondrial fusion could function as a brake on the mitophagy machinery in cells responding to environmental stresses. One potential explanation could be that loss of Mfn1 and Mfn2 generates a subgroup of mitochondria that have decreased membrane potential and/or other features that predispose them for elimination by mitophagy in response to other cellular stress. Consistent with this possibility, selective Parkin translocation to mitochondria with decreased membrane potential in Mitofusins double knock-out cells has been reported (Narendra, Tanaka et al. 2008). Yet interestingly, the basal level mitophagy in MEFs without Mitofusins are

low, suggesting that Parkin translocation is not sufficient to trigger mitophagy. Under stimulation mitophagy levels in these cells are high, but in the presence of Mfn1 and Mfn2 KR, mitophagy is delayed, suggesting that the presence of Mitofusins acts in some way as a brake on the mitophagy process. Our data indicate that the levels of Mitofusins are critical for regulation of Parkin-dependent mitophagy (Figure 3-10). Our results argue that manipulation of Mitofusin levels could be a strategy for accelerating or decelerate mitophagy as a therapeutic strategy in various pathological settings.

Figures and Figure legends:

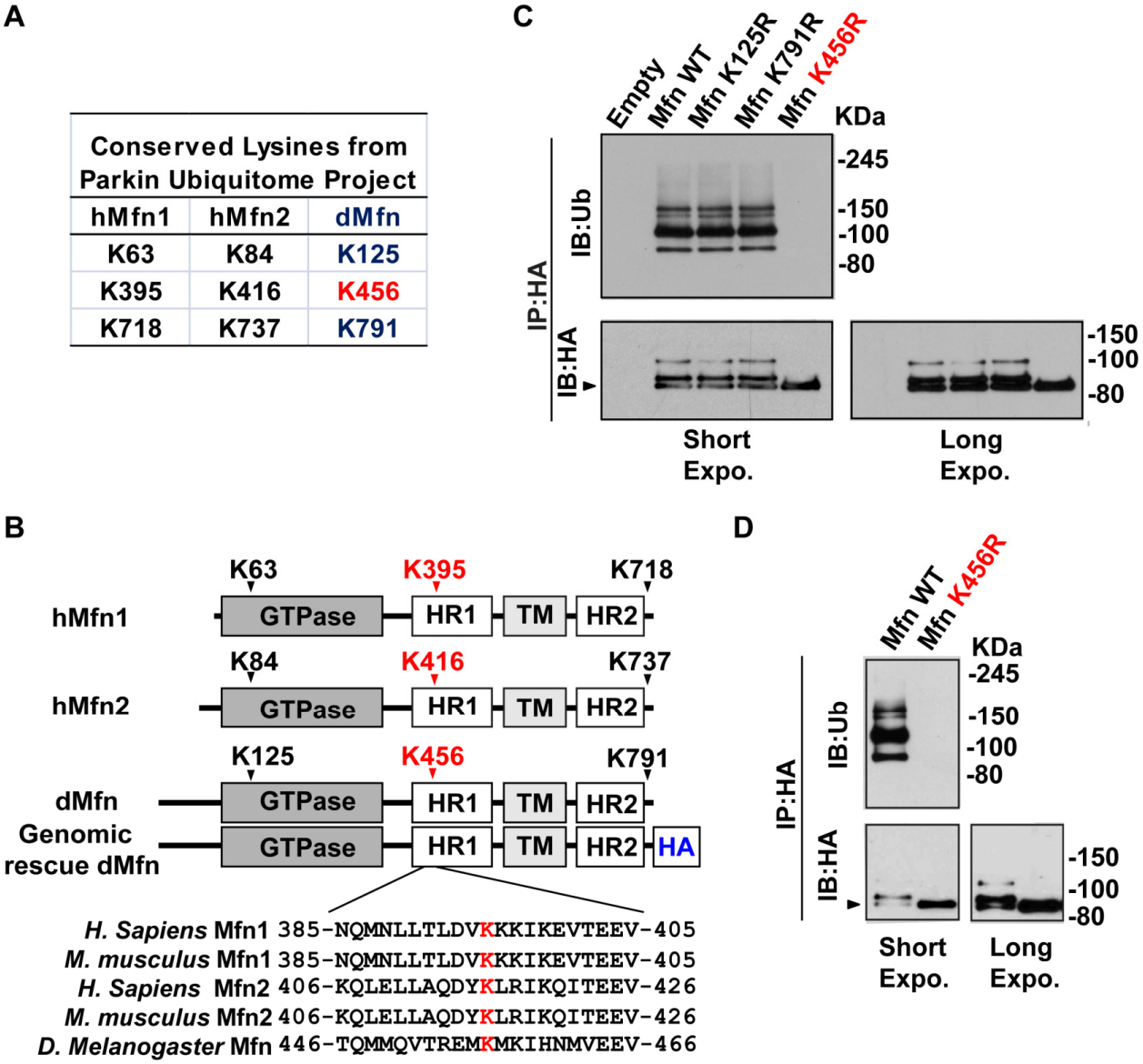

Figure 3-1: Lysine site 456 is critical for Mfn Ubiquitination in *Drosophila*.

(A): List of conserved lysine sites in *Drosophila* Mfn shared by human Mfn1 and Mfn2 identified in Parkin ubiquitylome project. **(B):** Diagram of human Mfn1, Mfn2 and *Drosophila* Mfn. The conserved lysine sites found in (A) are listed. Genomic rescue Drosophila Mfn (pCasper-Mfn-HA) encodes Mfn under the endogenous Mfn promoter and has one copy of HA at the C-terminus.

Lysine sites 395/416/456 in human Mfn1/Mfn2/Drosophila Mfn are labeled in red because they are the lysine sites will be focused. Amino acid sequence alignments flanking the lysine sites are displayed. **(C)**: Ubiquitination assay of genomic rescue *Drosophila* Mfn WT and KR mutants. 125 and 791 Lysine to Arginine mutations (pCasper-Mfn K125R-HA and pCasper-Mfn K791R-HA) do not change the Mfn ubiquitination. 456 Lysine to Arginine mutation (pCasper-Mfn K456R-HA) significantly decreases the ubiquitination detected by anti-pan ubiquitin antibody (P4D1 antibody). Unmodified Mfn is stabilized (black arrow head). **(D)**: Another independent gel confirms that K456R mutation abolish Mfn ubiquitination and stabilized unmodified Mfn (black arrow head).

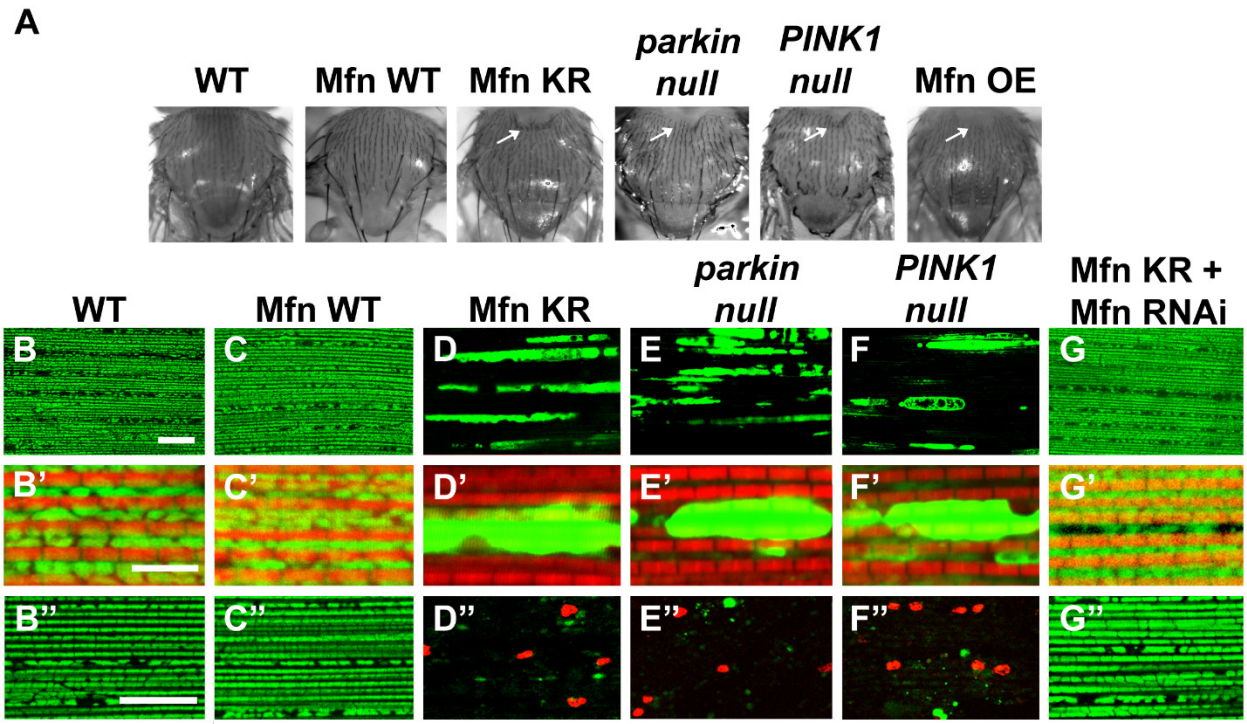

H

Genotype	Male Fertility
W-	100% N=96
WT-Mfn-HA	100% N=95
K456R-Mfn-HA	0% N=126
PINK1 mutant	0% N=90
Parkin mutant	0% N=95

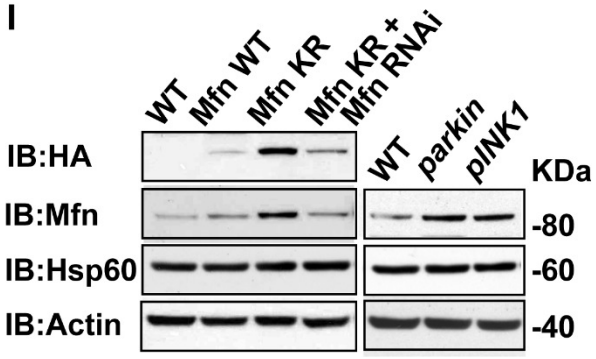

Figure 3-2: Mfn-KR mutants displays excessive mitochondrial fusion defects, similar to *PINK1* and *parkin* null mutants

(A): Compared to wildtype and Mfn WT genomic rescue transgenic (pCasper-Mfn-HA) flies, Mfn K456R genomic rescue mutant transgenetic (pCasper-Mfn K456R-HA) flies, hereafter Mfn KR mutant, display thoracic indentation phenotype, similar to that observed in *parkin*, *PINK1* null mutants and Mfn OE flies (white arrows). **(B-G'')**: In 2 days old *Drosophila* indirect flight muscle, mitoGFP assay display that wildtype (B-B') and Mfn WT (C-C') flies have similar mitochondrial morphology. Mfn KR mutant flies significant loss the mitoGFP signal with accumulation of large

GFP aggregates (D-D'), which is very similar to the mitochondrial defects shown in *parkin* (E-E') and *PINK1* (F-F') null mutants. TUNEL/mitoGFP assay that in 6 days old flies, both wildtype (B'') and Mfn WT (C'') files are TUNEL negative (red), whereas Mfn KR (D''), *parkin* (E'') and *PINK1* (F'') null mutants display strong TUNEL positive signal (red) and loss of mitoGFP (green). The mitoGFP and TUNEL positive phenotypes in Mfn KR mutants can be robustly rescued by knocking down Mfn using *mfn* RNAi (G-G''). Scale bar: 20μm in B-G, 5μm in B'-G', 10μm in B''-G''. **(H)**: Male fertility assay of single males from genotypes listed, N indicates the total animal number tested. **(I)**: Western blots assay of the Mfn levels in protein lysates from 2 day old fly thoraces. Anti-HA antibody and anti-Mfn antibody both showed that Mfn KR mutant flies have significantly enhanced Mfn protein levels as well as in *parkin* and *PINK1* mutants.

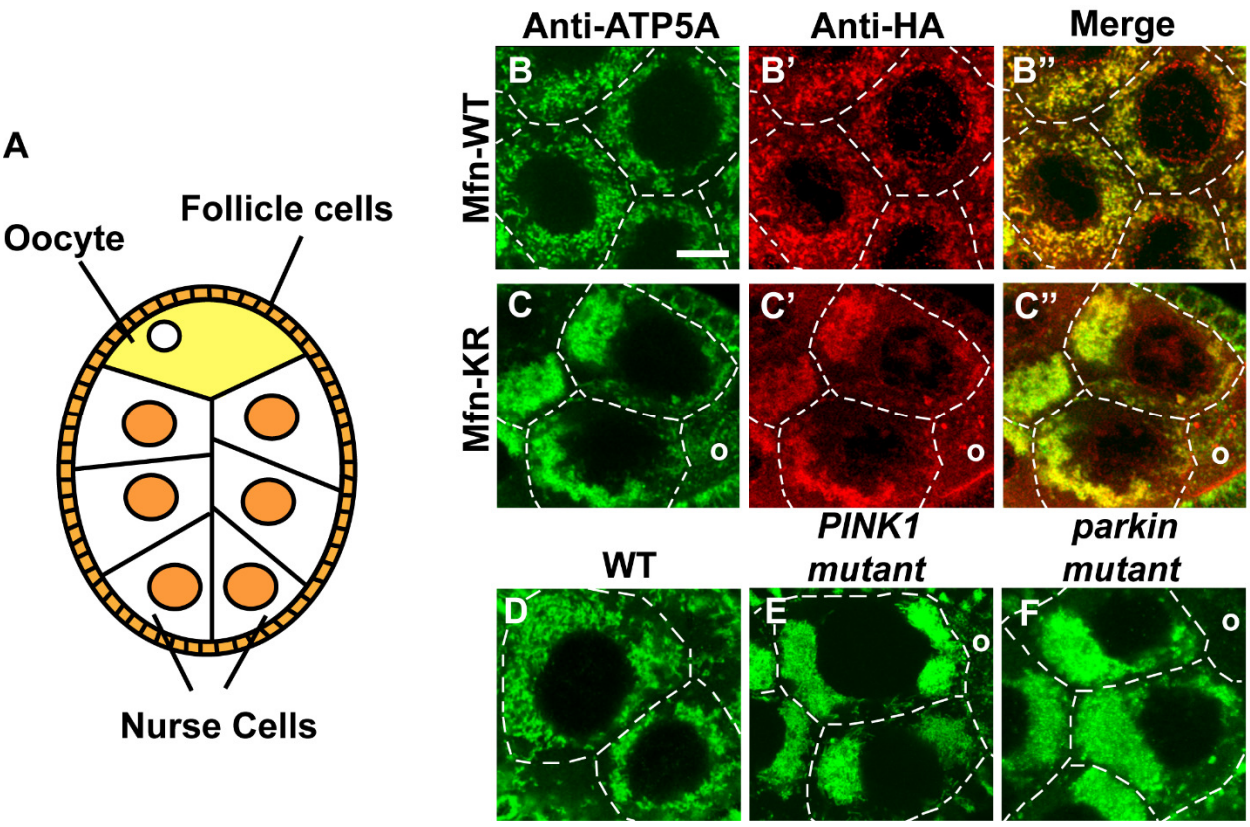

Figure 3-3: Mfn-KR mutants localize on mitochondria and lead to excessive mitochondrial fusion.

(A): Diagram of a stage 7 egg chamber in Drosophila female germline. 15 nurse cells occupy the majority of the egg chamber; oocyte, the progeny, locates in the anterior part of egg chamber where germ plasm is; a monolayer of follicle cells covers the surface of egg chamber. **(B-C'')**: In stage 7 egg chambers, mitochondria in transgenic flies with one-copy of pCasper-Mfn-WT-HA (Mfn-WT genomic rescue) display tubular shapes (B-B''); in transgenic flies with one-copy of pCasper-Mfn-KR-HA (Mfn-KR mutant genomic rescue) display clumped aggregates (C-C''). In Mfn-WT and KR mutants, Mfn signals (Anti-HA staining) locate well with mitochondrial signals (Anti-ATPase staining), suggesting both Mfn-WT and KR mutants locates on the mitochondria (B'' and C''). Scale bar: 10μm. **(D-F):** Mitochondrial morphology in wildtype (D), *PINK1* (E) and *parkin* (F) null mutants' stage 7 egg chambers using anti-ATPase antibody staining. Similar clumped

mitochondrial are observed in *PINK1* and *parkin* null mutants. Scale bar: 10µm.O stands for oocyte in C-C'', E and F.

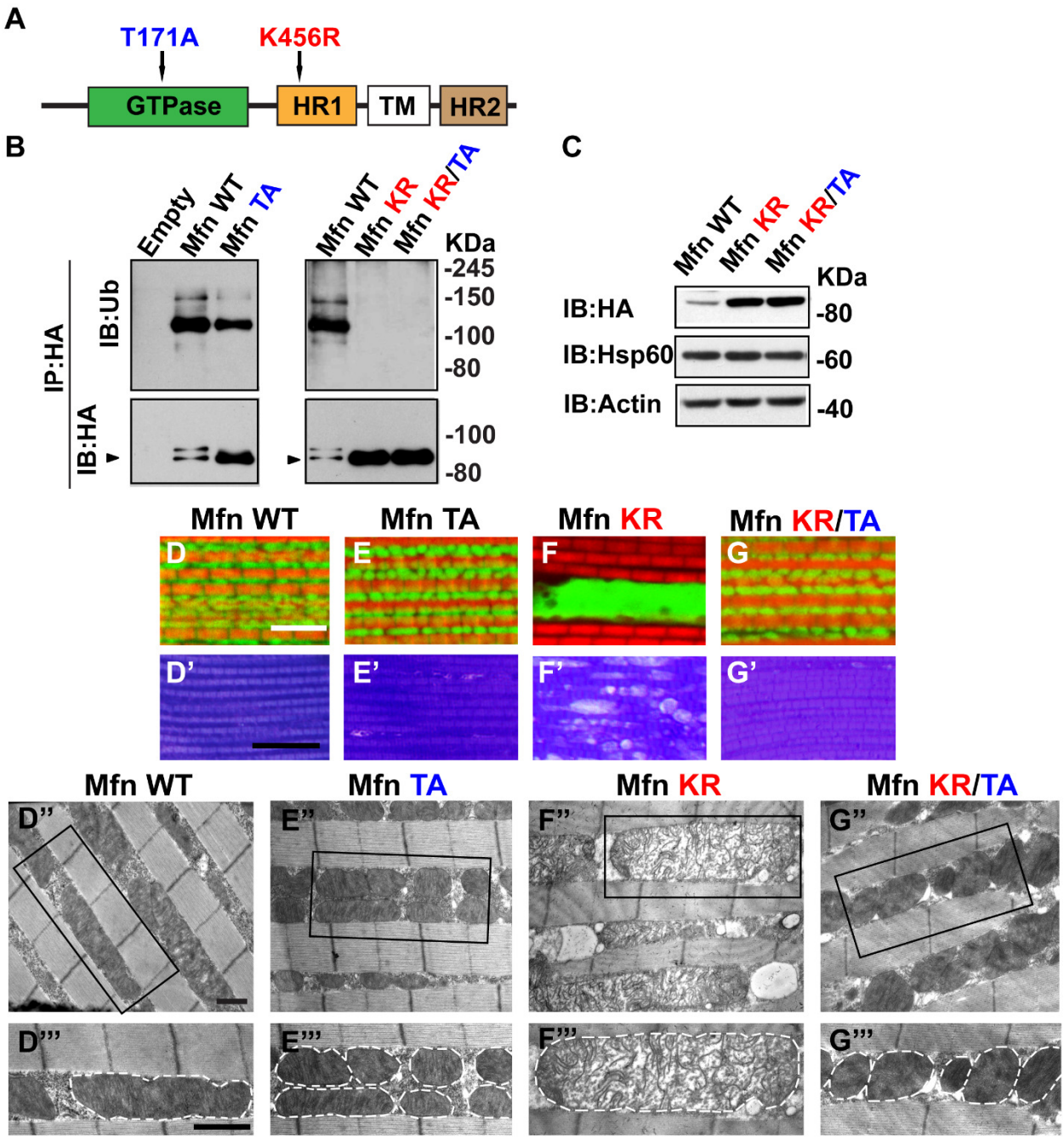

Figure 3-4: Mfn GTPase defective mutant rescues mitochondrial and tissue defects in Mfn-KR mutant flies.

(A): Diagram of the GTPase defective mutant and KR mutant's locations in *Drosophila* Mfn. T171A corresponds to human Mfn1 T109A, hereafter Mfn-TA mutant. **(B):** Ubiquitination assay

of genomic rescue *Drosophila* Mfn-WT, KR mutant, TA mutants and KR/TA mutants in S2 cells. Mfn proteins levels in significantly stabilized in Mfn-TA, KR and KR/TA mutants with decreased ubiquitination. Arrowhead points toward the stabilized unmodified Mfn. **(C):** Western blots assay of Mfn protein levels in fly thoraxes with single copy transgene of Mfn-WT, Mfn-KR mutant and Mfn-KR/TA double mutant using anti-HA antibody. Hsp60 and Actin are used as mitochondrial quantity controls and loading controls. **(D-G):** Mitochondrial phenotypes in the flies with single copy of transgenetic Mfn-WT, Mfn-KR mutant, Mfn-TA mutant and Mfn-KR/TA double mutant genomic rescues. MitoGFP/Phalloidin assay shows that Mfn-TA mutant transgene does not show significant mitochondrial morphology changes compared to Mfn-WT (D and E). Mfn-KR mutant display large mitochondrial aggregates with general loss of MitoGFP signals (F), which is robustly rescued in Mfn-KR/TA double mutants (G). Scale bar: 5μm **(D'-G'):** Toluidine Blue assay displays the muscle tissue integrity in flies with the indicated genotypes. Mfn-KR mutant genomic rescue transgene causes large vacuole formation (F') compared to Mfn-WT transgene (D'). The phenotype is significantly rescued in Mfn-KR/TA double mutants. Mfn-TA genomic rescue transgene itself does not cause tissue damage (E'). Scale bar: 30μm. **(D''-G'''):** Electronic microscopy images of mitochondria in flies with indicated genotypes. Mfn-KR mutant transgene cause swollen mitochondria with broken cristae and is rescued in Mfn-KR/TA double mutant transgene. Mfn-TA mutant transgene leads to smaller mitochondria compared to Mfn-WT transgene. Scale bar: 10μm in D''-G'' and 1μm in D'''-G'''. Flies are all 2-3 days old in B-G.

A

Rescue	*mfn mutant* +				
	-	Mfn WT	Mfn KR	Mfn KR/TA	Mfn TA
Lethal Phase	Larvae	Adult	Adult	Larvae	Larvae*
Male Sterility	N/A	0% (N=98)	100% (N=95)	N/A	N/A

*:occassion black pupae

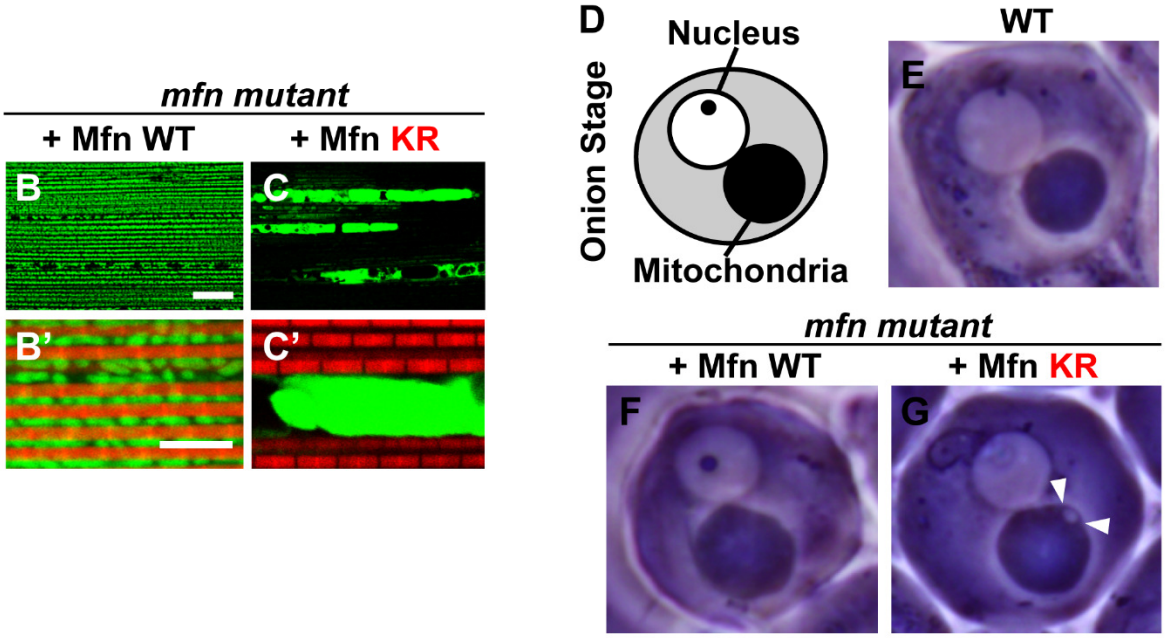

Figure 3-5: Mfn-KR mutants display mitochondrial and tissue defects in *mfn* mutants and is dependent on GTPase activity.

(A): Lethal phases and adult male sterility assay in *mfn* mutant flies (Marf G mutant) rescued by different Mfn genomic rescue. All rescue experiments are performed with one copy of the transgene. N indicates the number of single male flies used for sterility assay. **(B-C'):** Mitochondrial phenotypes in *mfn* mutants rescued by one copy of transgenetic Mfn-WT genomic rescue and Mfn-KR genomic rescue. Rhodamine phalloidin stains the myofibrils (Red), mitoGFP outlines mitochondria (Green). Scale bar: 20µm in B and C; 5µm in B' and C'. **(D)**: Diagram of a round spermatid in early *Drosophila* male spermatogenesis. Two mitochondria are interwoven with each other and form nebenkern, which resembles an onion (black filled circle); Nucleus with

condensed protein body (open white circle with dark dot) aligns next to the nebenkern. **(E-G):** Phase contrast images of onion stage in wild type male (E) and *mfn* mutant males rescued by one copy of transgenetic Mfn-WT genomic rescue (F) and Mfn-KR genomic rescue (G). White arrowheads indicate the vacuole formation in the nebenkern in G.

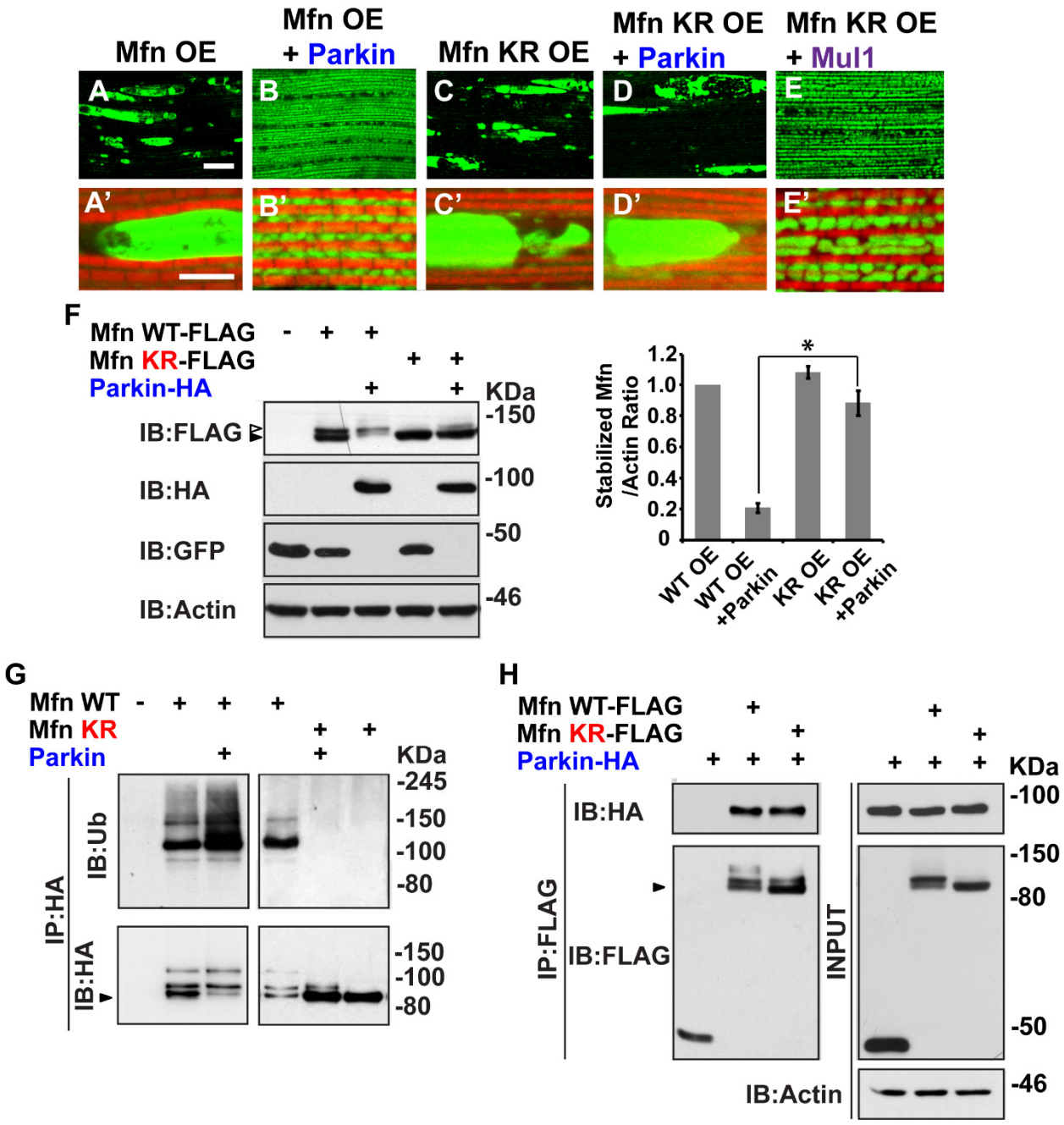

Figure 3-6: Lysine site 456 is critical for Parkin mediated ubiquitination and degradation of Mfn in *Drosophila*

(A-E'): MitoGFP/Phalloidin assay shows that muscle with Mfn-WT overexpression (IFM-Gal4>Uast-Mfn-WT-Flag) have large mitoGFP aggregates with loss of GFP signal in the

background (A and A'). *Drosophila* Parkin expression (Uast-8HA-Parkin) robustly suppresses the mitochondrial defects in Mfn OE (B and B'). Muscle overexpressed with Mfn KR mutant (IFM-Gal4>Uast-Mfn-KR-Flag) display similar phenotypes to Mfn-WT OE (C and C'). Parkin expression couldn't suppress the mitochondrial defects in Mfn-KR OE flies (D and D'). Mul1 expression can suppress the mitochondrial defects in Mfn-KR OE flies (E and E'). Scale bar: 20μm in A-E, 1μm in A'-E'. **(F):** Western blots assay of Mfn protein levels in S2 cells. Uast-Mfn-WT-Flag and Uast-Mfn-KR-Flag proteins are coexpressed with Uast-8HA-Parkin and Uast-GFP using Actin-Gal4. Anti-Flag antibody shows that Parkin significantly degrades Mfn-WT, but not Mfn-KR mutant. Note that when Mfn-WT is overexpressed, both unmodified and ubiquitinated Mfn are observed (2 bands indicated by filled and open arrowheads respectively), whereas Mfn-KR overexpression have only one band indicating unmodified Mfn. Unmodified Mfn (lower bands) are normalized with Actin. Statistically analysis shows that Mfn's degradation by Parkin is significantly blocked by KR mutation. ($p=0.025$, $N=4$, Independent t test). **(G):** Ubiquitination assay of *Drosophila* Parkin on Mfn-WT and KR mutant genomic rescues in S2 cells. Parkin can robustly build ubiquitination chains on Mfn-WT, but not on Mfn-KR mutants. Uast-Parkin-9myc is expressed under Actin-Gal4. Arrowhead indicated unmodified Mfn. **(H):** Coimmunoprecipitation assay between Parkin and Mfn-WT and KR mutants in S2 cells. Parkin binds equally with Mfn-WT and KR mutants

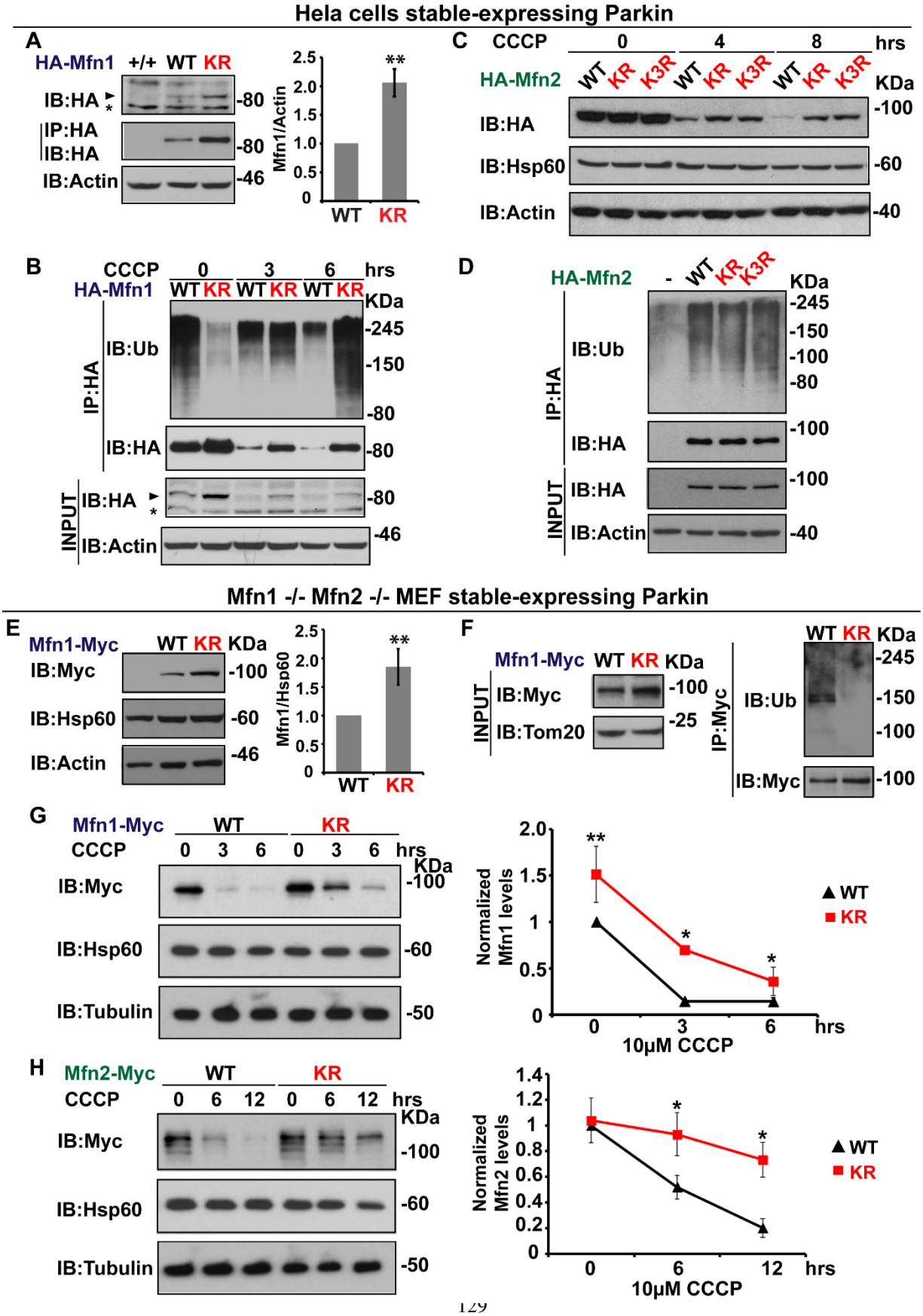
Hela cells stable-expressing Parkin
A
HA-Mfn1
+/+ WT KR
IB:HA
IP:HA
IB:HA
IB:Actin
-80
-80
-46
Mfn1/Actin
2.5
2.0
1.5
1.0
0.5
0
**
WT KR
C
CCCP
0 4 8 hrs
HA-Mfn2
WT KR K3R WT KR K3R WT KR K3R
KDa
IB:HA
IB:Hsp60
IB:Actin
-100
-60
-40
B
CCCP
0 3 6 hrs
HA-Mfn1
WT KR WT KR WT KR
KDa
IP:HA
IB:Ub
IB:HA
INPUT
IB:HA
IB:Actin
-245
-150
-80
-80
-80
-46
D
HA-Mfn2
- WT KR K3R
KDa
IP:HA
IB:Ub
IB:HA
INPUT
IB:HA
IB:Actin
-245
-150
-100
-80
-100
-100
-40
Mfn1 -/- Mfn2 -/- MEF stable-expressing Parkin
E
Mfn1-Myc
WT KR KDa
IB:Myc
IB:Hsp60
IB:Actin
-100
-60
-46
Mfn1/Hsp60
2.5
2.0
1.5
1.0
0.5
0
**
WT KR
F
Mfn1-Myc
WT KR KDa
INPUT
IB:Myc
IB:Tom20
-100
-25
IP:Myc
WT KR KDa
IB:Ub
IB:Myc
-245
-150
-100
-100
G
Mfn1-Myc
WT KR
CCCP
0 3 6 0 3 6 hrs
KDa
IB:Myc
IB:Hsp60
IB:Tubulin
-100
-60
-50
Normalized Mfn1 levels
2.0
1.5
1
0.5
0
**
*
*
0 3 6 hrs
10μM CCCP
WT
KR
H
Mfn2-Myc
WT KR
CCCP
0 6 12 0 6 12 hrs
KDa
IB:Myc
IB:Hsp60
IB:Tubulin
-100
-60
-50
Normalized Mfn2 levels
1.4
1.2
1
0.8
0.6
0.4
0.2
0
*
*
0 6 12 hrs
10μM CCCP
WT
KR

Figure 3-7: KR mutants stabilizes Mfn1 protein level and significantly delays Parkin-mediated degradation of Mfn1 and Mfn2 in Hela cells and Mfn1-/- Mfn2 -/- MEFs.

(A): In Parkin stable expressed Hela cells, equal amounts of pcDNA3.1-HA-human Mfn1-WT/KR are transfected. Anti-HA antibody displays that KR mutants have increased Mfn1 levels, both in input and immunoprecipitated pull down (P=0.019, Independent t test, N=3). **(B):** Ubiquitination assay in Hela cells stable-expressing human Parkin. Parkin-Hela cells are transfected with equal amounts of pcDNA3.1-HA-human Mfn1-WT/KR constructs treated with 25μM CCCP and harvested at 3 and 6 hours post treatment. Anti-HA antibody indicates that Mfn1-WT protein levels decrease after CCCP treatments, which is significantly delayed in Mfn1-KR mutants. Anti-P4D1 antibody indicates that Mfn1-KR mutants have decreased ubiquitination compared to Mfn1-WT at timepoint 0 and stabilized protein levels; Interestingly, Mfn1-KR mutants accumulate ubiquitination with the delayed degradation progress. **(C-D):** In Hela cells stable expressing Parkin, Mfn2-WT, KR and K3R mutants, when cells are treated with 10μM CCCP and harvested at 4 and 8 hours post treatment, anti-HA antibody indicates the degradations of Mfn2 KR and K3R mutants are significantly slower than those of WT(C). The ubiquitination of Mfn2 proteins do not change significantly between WT, KR or K3R mutants (D). **(E-G):** In Mfn1-/- Mfn2-/- MEFs stable-expressing mouse Parkin, Mfn1-WT and KR mutant, KR mutants display enhanced Mfn1 levels (p=0.005, Independent t test, N=6) (E). Ubiquitination assay shows that KR mutants has decreased ubiquitination as indicated by anti-P4D1 antibody, while the protein levels are increased in the input and anti-Myc antibody pull down (F). When cells are treated with 10μM CCCP and harvested at 3 and 6 hours post treatment, anti-Myc antibody indicates the degradations of Mfn1 KR mutants are significantly slower than those of WT(G). **(H):** Protein degradation of mouse Mfn2 protein levels in Mfn1 -/- Mfn2 -/- MEFs stable-expressing

mouse Parkin, Mfn2-WT or KR mutants. Cells are treated with 10μM CCCP and harvested at 6 and 12 hours post treatment. Anti-Myc antibody indicates the degradations of Mfn2-KR mutants are significantly slower than those of WT.

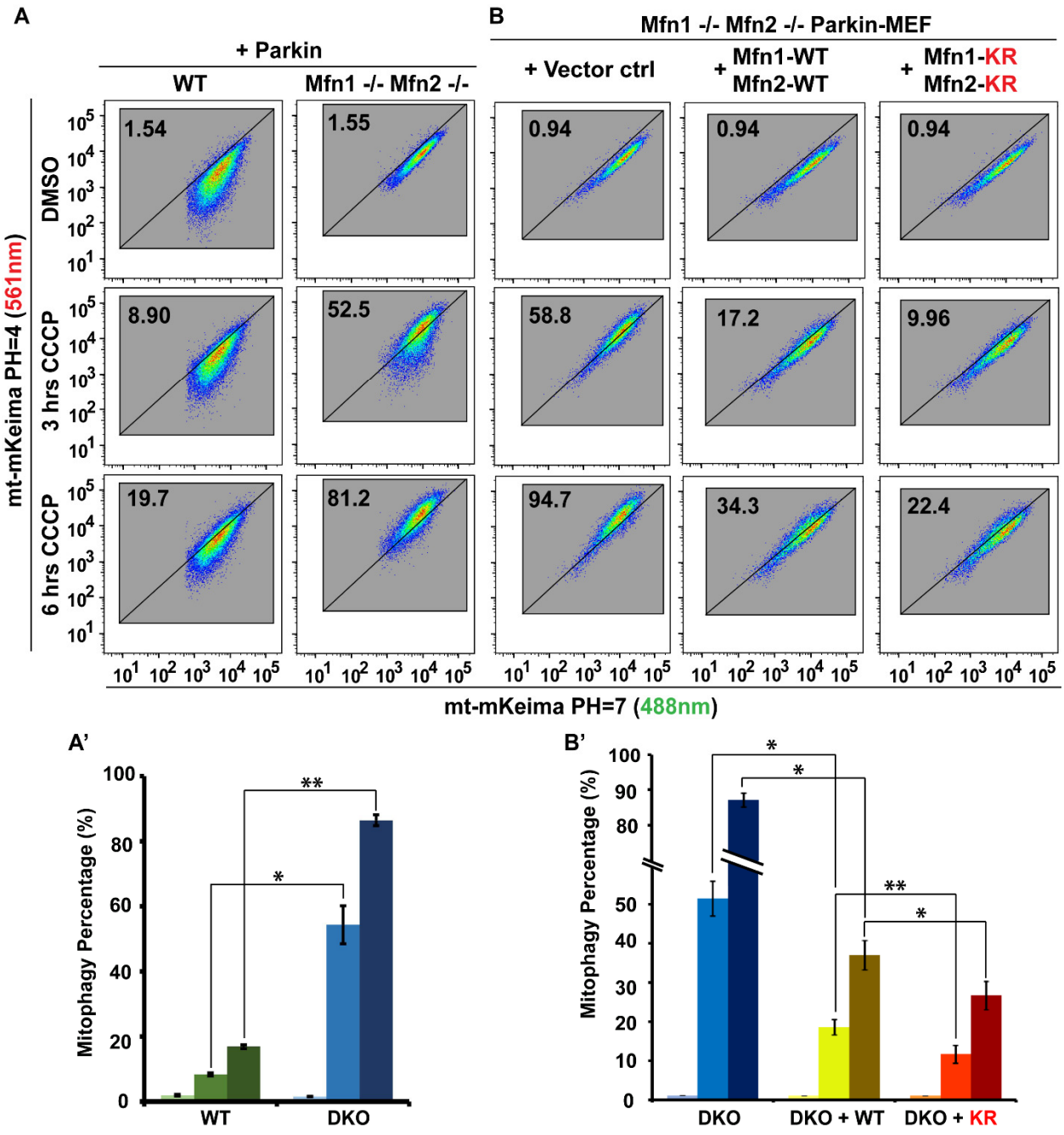

Figure 3-8: Mfn1 and Mfn2 KR mutants significantly delay mitophagy in Mfn1-/- Mfn2 -/- MEFs. Quantitative mitophagy assay in MEFs. 48 hours after infection, cells are treated with 20μM CCCP and harvested at 3 and 6 hours post treatment and undergo flowcytometry analyzer and calculate the percentage of mitophagy. **(A-A'):** Wildtype MEF and Mfn1 -/- Mfn2 -/- MEFs are infected with mouse Parkin and mito-mKeima. Compared to wildtype, Mfn1-/- Mfn2 -/- MEFs (double

knock-out, DKO) has very robust mitophagy detected at both 3 (54.30 ± 5.83% vs. WT 8.38 ± 0.42%, p=0.038, paired t test, N=4) and 6 hours (86.40 ± 1.64 vs. WT 16.90 ± 0.65%, p=0.0003, paired t test, N=4). **(B-B'):** Mfn1 -/- Mfn2 -/- MEFs stable-expressing mouse Parkin are infected with mito-mKeima, mouse Mfn1-WT-10Myc, HA-Mfn2-WT or Mfn1-KR-10myc, HA-Mfn2-KR. Mfn1+Mfn2-WT rescue groups significantly reduce the mitophagy to 19.35 ± 1.65% at 3 hours (vs. DKO 51.45 ± 4.39%, p=0.017, paired t test, N=4) and 37.05 ± 3.75% at 6 hours (vs. DKO 87.13 ± 1.92%, p=0.013, paired t test, N=4). DMSO groups between each genotype are manually set to be as equal as possible approximate to 1 or 1.5 in each experiment. CCCP treated groups are normalized to DMSO groups. Compared to Mfn1+Mfn2-WT groups, Mfn1+Mfn2-KR rescue groups further reduced the mitophagy percentage to 11.70 ± 2.27% at 3 hours (p=0.009, paired t test, N=4) and 26.7 ± 3.60% at 6 hours (p=0.010, paired t test, N=4). Representative results of one round assay are displayed and statistics are derived from four independent rounds of assays. *: $p<0.05$; **: $p<0.01$; Percentages are displayed in Mean±½ SEM.

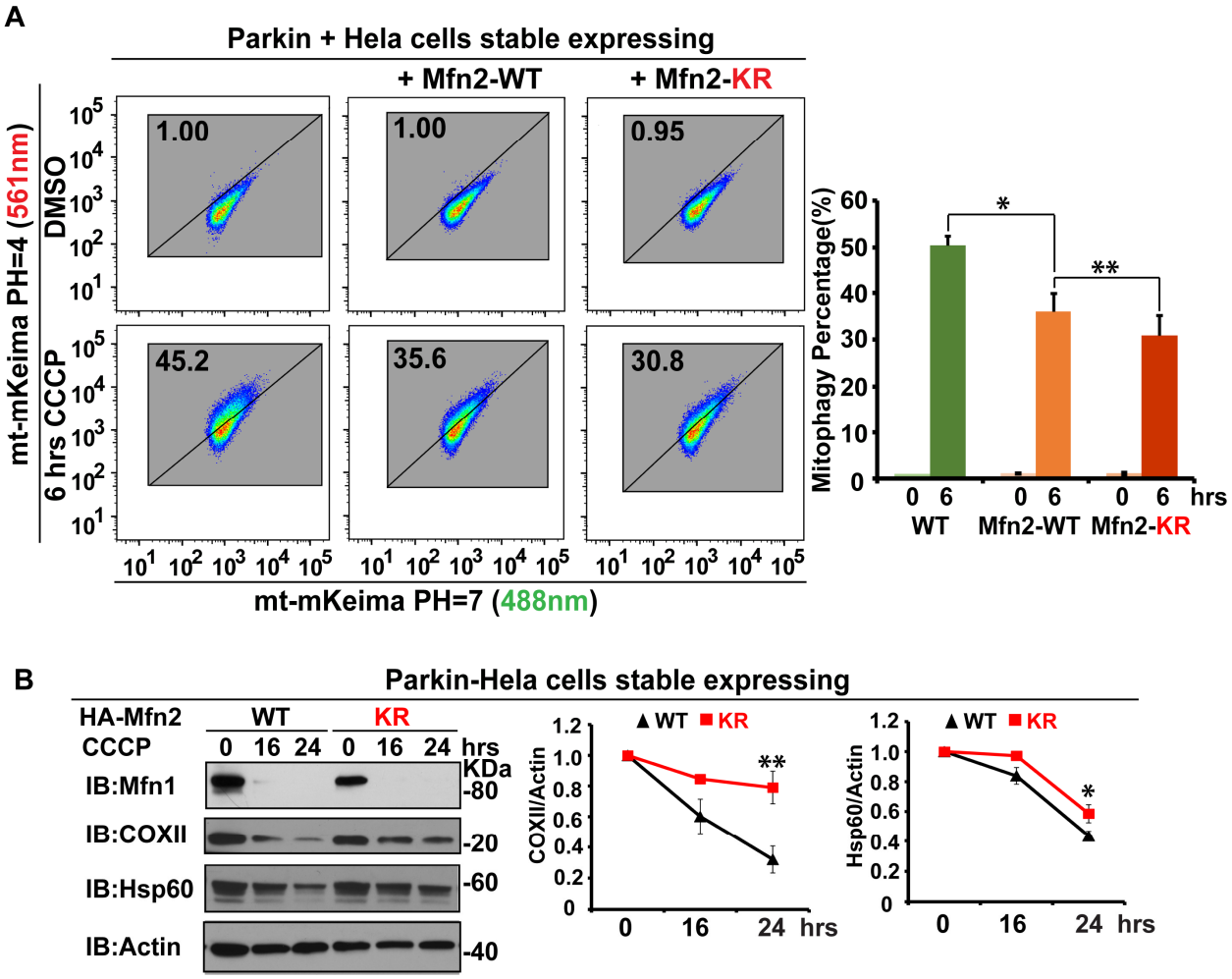

Figure 3-9: Mfn2 KR mutant significantly delays mitophagy and Parkin mediated mitochondrial protein degradation in Hela cells.

(A): Quantitative mitophagy assay in Hela cells. Wildtype Hela and Hela cells stable-expressing Mfn2-WT and Mfn2-KR mutants are infected with Parkin and mito-mKeima. 48 hours after infection, cells are treated with 20μM CCCP and harvested at 6 hours post treatment and undergo flowcytometry analyzer and mitophagy percentage are calculated. The mitophagy percentage of wildtype Hela cells are 50.44 ± 2.00% at 6 hours; Mfn2-WT expression significantly reduce the mitophagy to 36.03 ± 3.91% at 6 hours (p=0.025, paired t test, N=5). Compared to Mfn2-WT, Mfn2-KR expression further reduced the mitophagy percentage to 30.89 ± 4.33% at 6 hours (p=0.001, paired t test, N=5). Representative results of one round assay are displayed and statistics

are derived from five independent rounds of assays. Percentages are displayed in mean+½ SEM. **(B):** Mitophagic protein degradation in Hela cells stable-expressing YFP-Parkin, Mfn2-WT and KR mutant. Cells are treated with 20μM CCCP and harvested at 16 and 24 hours post treatment. Anti-COXII and Hsp60 are used to detect degradation of mitochondrial proteins. The degradation rate of each protein is normalized against Actin, which is stable in the mitophagy process. *: $p<0.05$; **: $p<0.01$; Ratio are displayed in Mean±½ STD.

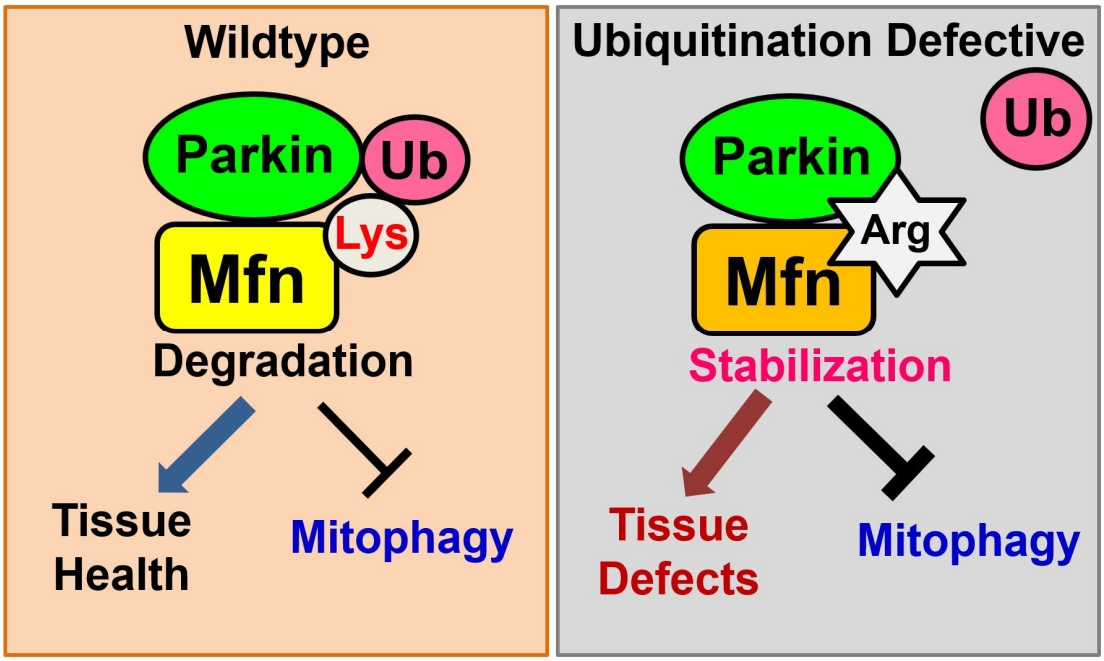

Figure 3-10: Mitofusin levels are critical to protein stability, mitochondrial quality control and tissue health.

The conserved lysine sites K456/395/316 identified in Mitofusins in *Drosophila* and mammalian cells are critical for their ubiquitination and degradation by Parkin. Loss of Ubiquitination leads to Mfn stabilization and mitochondrial and tissue defects. The fact that loss of Mitofusins accelerates Parkin-mediated mitophagy whereas accumulation of Mitofusins inhibits mitophagy suggest that Mitofusins negatively regulates mitochondrial quality control when outside perturbance presents.

Supplementary Figures and Figure Legends:

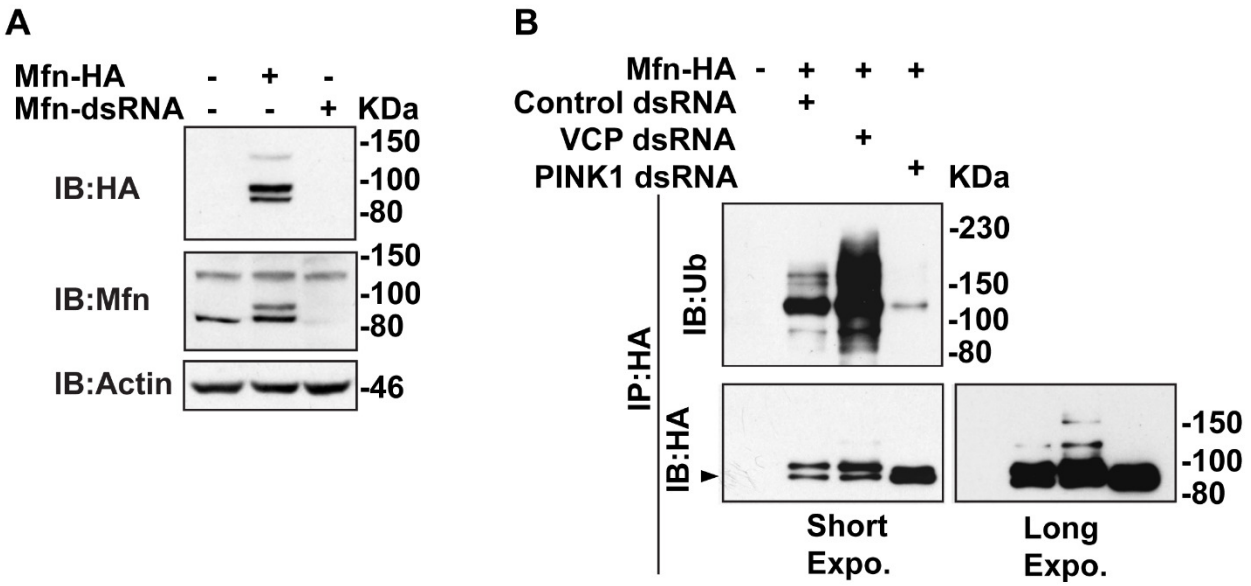

Supplementary Figure 3-1: pCasper-Mfn-HA is a valid tool for ubiquitination assay of *Drosophila* Mfn at endogenous expression level.

(A): pCasper-Mfn-HA (Mfn-WT genomic rescue) is transfected in S2 cells and its expression can be detected using either anti-HA antibody or anti-*Drosophila* Mfn antibody. When using Mfn dsDNA to knock down Mfn expression, both endogenous Mfn and Mfn-WT genomic rescue expression are completely abolished. These results suggesting pCasper-Mfn-HA well represents Mfn expression under the endogenous promoter. **(B):** Ubiquitination assay of pCasper-Mfn-HA (Mfn genomic rescue) in S2 cells. Anti-P4D1 antibody indicates that Mfn is under ubiquitnation at wildtype status; when VCP is knocking down using dsDNA, the Mfn ubiquitination significantly accumulates; when PINK1 is knocking down using dsDNA, the Mfn ubiquitination significantly decreases. Anti-HA antibody indicates that Mfn protein levels increases when VCP is knocking down; Mfn is significantly stabilized when PINK1 is knocking down. These results are consistent with previous reports, suggesting pCasper-Mfn-HA is a valid tool to explore the ubiquitination modification of *Drosophila* Mfn.

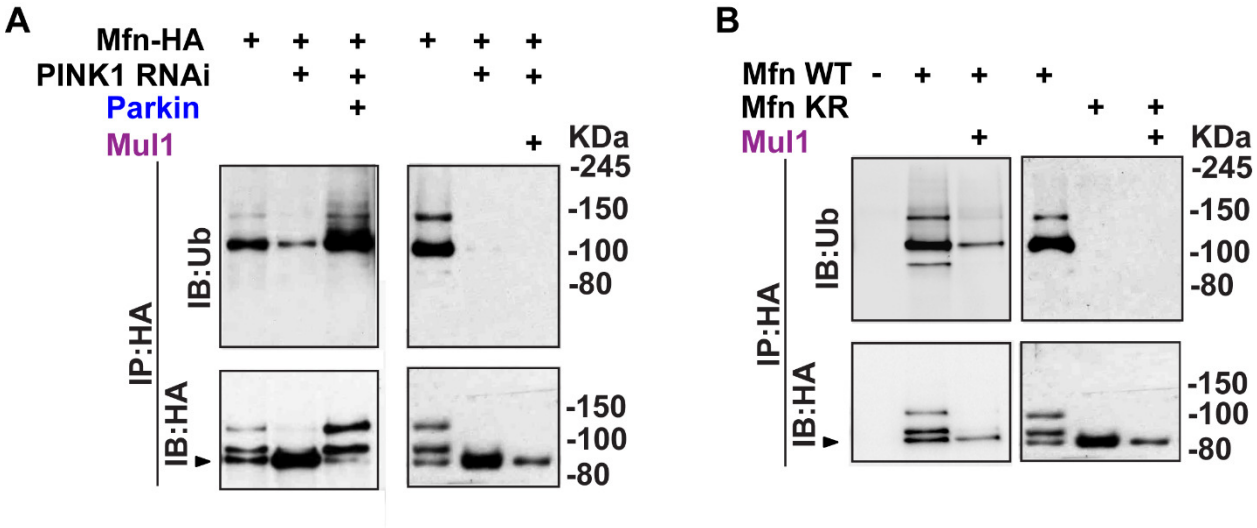

Supplementary Figure 3-2: Mul1 does not build ubiquitination chain on either Mfn WT or Mfn KR mutants as Parkin.

(A): When PINK1 is knocking down in *Drosophila* S2 cells, Mfn levels (pCasper-Mfn-HA, Mfn-WT genomic rescue) are significantly stabilized with decreased ubiquitination. Parkin overexpression can restore the ubiquitination of Mfn and decrease the levels of stabilized Mfn. This result serves as a good control for Parkin's inability to build ubiquitin chain on Mfn KR mutant, which also significantly stabilizes Mfn (Figure 3-6F). In contrast, Mul1 overexpression degrades stabilized Mfn, but no ubiquitination is detected. **(B):** Mul1 overexpression decreases Mfn-WT and KR mutant levels, suggesting Mfn K395 is not the critical site for Mul1's ability to promote degradation of Mfn.

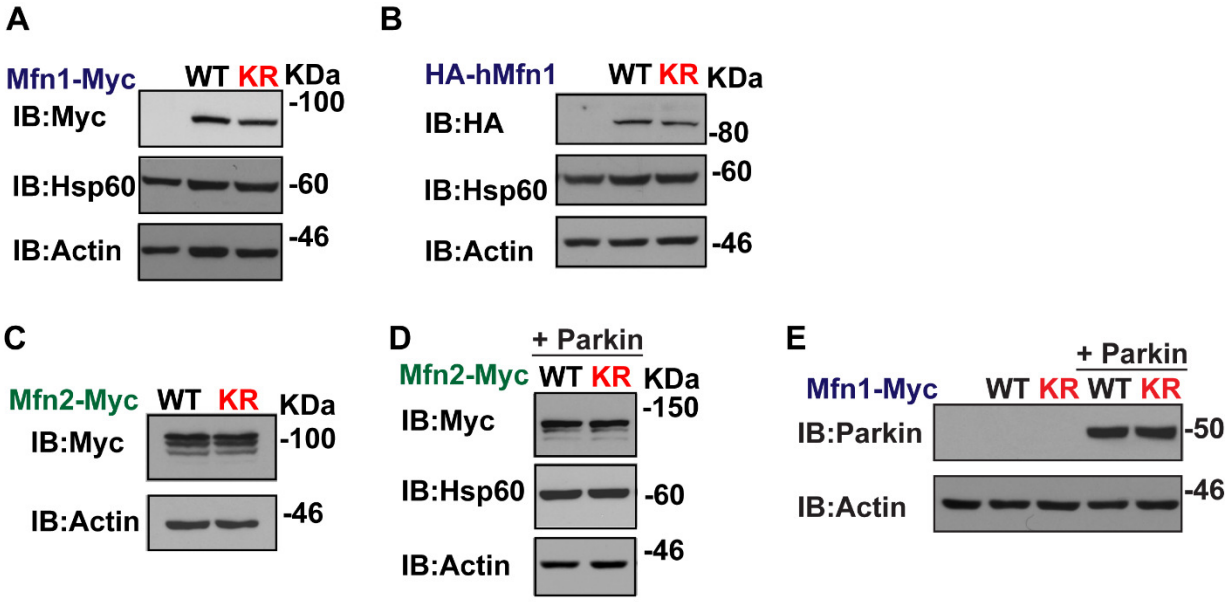

Supplementary Figure 3-3: Without Parkin, KR mutants does not change Mfn1 and Mfn2 protein levels in Hela and Mfn1 -/- Mfn2 -/- MEFs.

(A): In Mfn1 -/- Mfn2 -/- MEFs stable-expressing Mfn1-WT/KR mutants, Mfn1 protein levels do not vary significantly**. (B):** In Hela cells in equal amounts of pcDNA3.1-HA-human Mfn1-WT/KR constructs are transfected. Mfn1 levels are detected using anti-HA Without Parkin, Mfn1 KR mutants does not vary significantly. (**C-D**): In Mfn1 -/- Mfn2 -/- MEFs without (C) or with stable-expressing mouse Parkin (D), Mfn2-WT and KR mutant, KR mutant does not show significant difference compared to WT. **(E):** Anti-Parkin antibody indicates that MEF has undetectable endogenous Parkin, but comparable stably expressed in both Mfn1-WT and KR mutant stable lines.

Materials and Methods:

Molecular Biology and Constructs: pCasper-Mfn-WT-HA is a kind gift from Dr. C.K.Yao at Taipei. pUASt-8HA-Parkin, pMT-Parkin-9Myc, pUASt-Mfn-WT-3Flag was previously described (Yun, Puri et al. 2014; Zhang, Mishra et al. 2017). pCasper-Mfn-K125R/K456R/K791R/T191A-HA, pUASt-Mfn-K456R-3Flag were generated using site-mutagenesis on the genomic DNA and cDNA in the pENTRA-1A vector followed by the Gateway recombination into pCasper and pUASt target vectors (Invitrogen). Human Mfn1 cDNA was amplified from Mfn1-YFP, a kind gift from Dr. Richard Youle at NIH. Polymorphisms within the Mfn1 cDNA were corrected according to the NCBI annotation. Human Mfn2 cDNA was amplified from Mfn2-YFP (Addgene: 28010) and subcloned into pcDNA3.1-HA vector, a kind gift from Dr. William Young (UCLA). pQCXIP-mouse Mfn1-10Myc, pQCXIP-mouse Mfn2-15Myc are kind gifts from Dr. David Chan at California Institute of Technology. Mfn1-K395R/Mfn2-K416R mutants in human and mouse cDNA are all generated using site-mutagenesis. Mouse Parkin cDNA was a kind gift from Dr. David Chan and subcloned into pQCXIP vector. All constructs were verified with sequencing.

***Drosophila* strains:** The pCasper-Mfn-HA, *marf B, G* mutant flies were kind gifts from Dr. Hugo Bellen at the Baylor School of Medicine (Sandoval, Yao et al. 2014). Flies carrying pCasper-Mfn-K125R/K456R/K791R/T191A-HA, pUASt-Mfn-WT/K456R-3Flag vectors were created through injection in a w^{1118} genetic background (Rainbow Transgenic Flies, Inc.). IFM-Gal4, UASt-Mfn RNAi, UASt-Mul1, UASt-8HA-Parkin, *PINK1*^{5}, *parkin*^{25} and *dpk*^{21} were described previously (Clark, Dodson et al. 2006; Deng, Dodson et al. 2008; Yun, Puri et al. 2014). Flies with each construct are tested with insertion at difference chromosomes. *Drosophila* strains were maintained in a 25°C humidified incubator.

TUNEL Assay: Describe in (Zhang, Mishra et al. 2017). Fly thoraxes with corresponding genotypes were cut and fixed in 4% paraformaldehyde/Schneider's Buffer for 30 minutes. Indirect flight muscles were then dissected out and separated. Isolated muscles pieces were blocked with Blocking buffer and assayed using In Situ Cell Death Detection Kit by following the manufacturer's instruction (Roche). 5-10 fly thoraxes are dissected.

Toluidine Blue staining and Electronic Microscopy: Describe in (Zhang, Mishra et al. 2017). Fly thoraxes were fixed in 1% paraformaldehyde/1% glutaraldehyde/0.1M Phosphate Buffer, post-fixed in 1% osmium tetroxide/ddH20, dehydrated in gradient ethanol and embedded in Epon 812. After polymerization, sections were obtained using either glass knives or diamond knife (Diatome). 1.0-1.5μm sections were stained with Toluidine blue. 80-90nm sections were stained with uranyl acetate and lead citrate and examined by transmission electron microscope (UCLA Brain Research Institute Electron Microscopy Facility). At least 3 thoraxes of each genotype were examined.

Immunofluorescence and Confocal Microscopy: Egg chambers were fixed in 3.7% formaldehyde/Schneider's Buffer for 30 minutes and permeabilized with 0.4% Triton-X100/PBS for 4 hours. Egg chambers were incubated with anti-HA rabbit polyclonal antibody (Sigma 1:100), anti-ATP5A mouse monoclonal antibody (Abcam, 1:100) at 4°C overnight and followed by Goat anti-rabbit/mouse Alexa Fluor 488/546 secondary antibodies (Invitrogen 1:200) at 4°C overnight. Indirect Flight muscle pieces are incubated with Rhodamine Phalloidin 4°C overnight. Images were taken using a LSM5 confocal microscope (Zeiss).

S2 Cell Culture, transfection and dsRNA treatment: S2 cells were cultured in Schneider's Buffer, 10% FBS, 1% Penicillin and Streptomycin at 25°C. Qiagen Effectene transfection reagent is used according to producer's instruction. PINK1 and VCP dsRNA were designed according to

a protocol from www.flyrrnai.org and synthesized using Mega T7 kit from Ambion. Cells were assayed 72-96hrs after dsRNA treatment. PINK1 dsDNA-F: TGA GCA AAT ACC CCC AAA AG; PINK1 dsDNA-R: GAT CTG GAG CGG TGA TTT GT. VCP dsDNA-F: VCP dsDNA-R.

Hela, MEF Cell Culture, transfection and Stable Cell Lines Generation:

Cells are grown in Dulbecco's Modified Eagle Medium (DMEM, Gibco) supplemented with 10% fetal bovine serum (FBS) and penicillin/streptomycin at 37˚C and 5% CO2. Parkin stable hela cells are a kind gift from Dr. David Chan. *Mfn1, Mfn2* double knockout MEFs are infected by infection with retrovirus expressing Parkin, Mfn1-WT/KR and Mfn2-WT/KR. Infected cells were selected in puromycin (1.5µg/mL) for 1 week and maintained in 1µg/ml puromycin.

Protein lysates and Western blot: S2 cells, fly thoraxes, Hela and MEFs were lysed in RIPA Buffer with Protease Inhibitors (Roche) and 200mM PMSF (Sigma). Protein lysates were centrifuged at 10,000g for 15mins, and the supernatants boiled with 6XSDS sample Buffer (Bioland) at 95°C for 5 mins. Proteins were separated in SDS-PAGE Gels. Gels were transferred to PVDF membrane (Millipore) and incubated with primary antibody at 4˚C overnight. Following several washes, blots were then incubated with secondary antibodies for 2 hours at room temperature. Primary antibodies used include: Anti-HA mouse monoclonal antibody (Millipore 1:1000), Anti-HA rabbit polyclonal antibody (Sigma, 1:1000), Anti-Myc rabbit monoclonal antibody (Cell Signaling, 1:1500), Anti-Flag rabbit/mouse antibody (Genscript 1:2000), Anti-GFP rabbit polyclonal antibody (Invitrogen, 1:3000), Anti-Actin rabbit polyclonal antibody (Sigma 1:2000), Anti-Tubulin mouse monoclonal antibody (Sigma 1:4000), Anti-Hsp60 mouse monoclonal antibody (Abcam, 1:3000), Anti-Human Mfn1 antibody is a kind gift from Dr. David Chan. Anti-Human Mfn2 mouse monoclonal antibody (Abcam 1:2000), Anti-*Drosophila* Mfn Rabbit polyclonal antibody (1:3000) was a gift from Dr. Alexander Whitworth (Ziviani, Tao et al.

2010). Donkey anti-mouse, anti-rabbit and anti-chicken HRP conjugated secondary antibodies (GE Healthcare and Jackson Immunoresearch laboratory, 1:10000 or 20000) were used.

Coimmunoprecipitation and Ubiquitination Assay: For CO-IP, 48 hours after transfection, cells were harvested and lysed in RIPA Buffer with protease inhibitors. For Ubiquitination assay, cells are lysed in RIPA Buffer+1%SDS+Benzonuclease (Sigma) with protease inhibitors. Protein lysates were incubated with Dynabeads G and primary antibody (Anti-Myc mouse monoclonal antibody, Millipore 1:300 or Anti-HA mouse monoclonal antibody, Sigma 1:300) at 4˚C overnight and washed in 0.1%Tween/PBS 4 times and eluted in 2XSDS sample buffer (BioRad) and denatured at 95˚C. The samples are assayed by western blot.

Mito-mKeima Mitophagy Assay: H293T cells are transfected with corresponding retrovirus expressing pQCXIP-human/mouse Mfn1/2 WT and KR mutants, pQCXIP-human/mouse Parkin, pCHAC-mt-mKeima (a kind gift from Dr. Richard Youle at NIH) with packaging vectors, pCLEO for MEFs, pUMVC/VSV-G for Hela cells. 48-72hrs after transfections, serum was harvested and filtered with 0.45um filters and infected MEFs and Hela cells. 48-72hrs after infection, cells were resuspended in Flowcytometry Sorting Buffer (1xPhosphate-Buffered Saline Ca 2+ and Mg 2+ free + 1% Fetal Bovine Serum + 25μM HEPES Buffer) and subjected to flowcytometry using SORP BD LSRII (IMED) Analytic Flow Cytometer at UCLA Flowcytometry Core. Mitochondrial mKeima signals were measured using dual-excitation with emission filter 630/11nm for 488nm (pH=7) laser and 614/20 nm for 561nm laser (pH=4). Zombie UV (Biolegend) were used to gate live cells. 30,000 cells were collected for each genotype and FlowJo (v10) was used for data analysis. Representative results from a single experiment was displayed and statistics were collected from multiple rounds. DMSO treated groups are manually set approximately to 1 or 1.5 between each genotype, CCCP treated groups are normalized to the DMSO groups.

Statistical Analysis: The data were analyzed based on results repeated independently at least 3 times. N was indicated in the Figure legends. Data were analyzed using Statistical Package for the Social Sciences (SPSS) 16.0. The *P* values were assessed using a two-tailed unpaired Student's t test with P values considered significant as follows: *, $p<0.05$ and **, $p<0.01$.

Reference:

Anton, F., G. Dittmar, et al. (2013). "Two deubiquitylases act on mitofusin and regulate mitochondrial fusion along independent pathways." Molecular cell **49**(3): 487-498.

Bombelli, F., T. Stojkovic, et al. (2014). "Charcot-Marie-Tooth disease type 2A: from typical to rare phenotypic and genotypic features." JAMA neurology **71**(8): 1036-1042.

Cao, Y. L., S. Meng, et al. (2017). "MFN1 structures reveal nucleotide-triggered dimerization critical for mitochondrial fusion." Nature **542**(7641): 372-376.

Chan, D. C. (2012). "Fusion and fission: interlinked processes critical for mitochondrial health." Annual review of genetics **46**: 265-287.

Chan, N. C., A. M. Salazar, et al. (2011). "Broad activation of the ubiquitin-proteasome system by Parkin is critical for mitophagy." Hum Mol Genet **20**(9): 1726-1737.

Chen, H., S. A. Detmer, et al. (2003). "Mitofusins Mfn1 and Mfn2 coordinately regulate mitochondrial fusion and are essential for embryonic development." The Journal of cell biology **160**(2): 189-200.

Chen, H., J. M. McCaffery, et al. (2007). "Mitochondrial fusion protects against neurodegeneration in the cerebellum." Cell **130**(3): 548-562.

Chen, H., M. Vermulst, et al. (2010). "Mitochondrial fusion is required for mtDNA stability in skeletal muscle and tolerance of mtDNA mutations." Cell **141**(2): 280-289.

Chen, Y. and G. W. Dorn, 2nd (2013). "PINK1-phosphorylated mitofusin 2 is a Parkin receptor for culling damaged mitochondria." Science **340**(6131): 471-475.

Clark, I. E., M. W. Dodson, et al. (2006). "Drosophila pink1 is required for mitochondrial function and interacts genetically with parkin." Nature **441**(7097): 1162-1166.

Cohen, M. M., E. A. Amiott, et al. (2011). "Sequential requirements for the GTPase domain of the mitofusin Fzo1 and the ubiquitin ligase SCFMdm30 in mitochondrial outer membrane fusion." Journal of cell science **124**(Pt 9): 1403-1410.

Deng, H., M. W. Dodson, et al. (2008). "The Parkinson's disease genes pink1 and parkin promote mitochondrial fission and/or inhibit fusion in Drosophila." Proc Natl Acad Sci U S A **105**(38): 14503-14508.

Deng, H., M. W. Dodson, et al. (2008). "The Parkinson's disease genes pink1 and parkin promote mitochondrial fission and/or inhibit fusion in Drosophila." Proceedings of the National Academy of Sciences of the United States of America **105**(38): 14503-14508.

Fabian, L. and J. A. Brill (2012). "Drosophila spermiogenesis: Big things come from little packages." Spermatogenesis **2**(3): 197-212.

Franco, A., R. N. Kitsis, et al. (2016). "Correcting mitochondrial fusion by manipulating mitofusin conformations." Nature **540**(7631): 74-79.

Frydman, H. M. and A. C. Spradling (2001). "The receptor-like tyrosine phosphatase lar is required for epithelial planar polarity and for axis determination within drosophila ovarian follicles." Development **128**(16): 3209-3220.

Fu, M., P. St-Pierre, et al. (2013). "Regulation of mitophagy by the Gp78 E3 ubiquitin ligase." Molecular biology of the cell **24**(8): 1153-1162.

Hermann, G. J., J. W. Thatcher, et al. (1998). "Mitochondrial fusion in yeast requires the transmembrane GTPase Fzo1p." The Journal of cell biology **143**(2): 359-373.

Kitada, T., S. Asakawa, et al. (1998). "Mutations in the parkin gene cause autosomal recessive juvenile parkinsonism." Nature **392**(6676): 605-608.

Lazarou, M., D. A. Sliter, et al. (2015). "The ubiquitin kinase PINK1 recruits autophagy receptors to induce mitophagy." Nature **524**(7565): 309-314.

Leboucher, G. P., Y. C. Tsai, et al. (2012). "Stress-induced phosphorylation and proteasomal degradation of mitofusin 2 facilitates mitochondrial fragmentation and apoptosis." Molecular cell **47**(4): 547-557.

Narendra, D., A. Tanaka, et al. (2008). "Parkin is recruited selectively to impaired mitochondria and promotes their autophagy." The Journal of cell biology **183**(5): 795-803.

Park, J., S. B. Lee, et al. (2006). "Mitochondrial dysfunction in Drosophila PINK1 mutants is complemented by parkin." Nature **441**(7097): 1157-1161.

Park, Y. Y., O. T. Nguyen, et al. (2014). "MARCH5-mediated quality control on acetylated Mfn1 facilitates mitochondrial homeostasis and cell survival." Cell death & disease **5**: e1172.

Pickart, C. M. and M. J. Eddins (2004). "Ubiquitin: structures, functions, mechanisms." Biochimica et biophysica acta **1695**(1-3): 55-72.

Sandoval, H., C. K. Yao, et al. (2014). "Mitochondrial fusion but not fission regulates larval growth and synaptic development through steroid hormone production." eLife **3**.

Santel, A., S. Frank, et al. (2003). "Mitofusin-1 protein is a generally expressed mediator of mitochondrial fusion in mammalian cells." Journal of cell science **116**(Pt 13): 2763-2774.

Sarraf, S. A., M. Raman, et al. (2013). "Landscape of the PARKIN-dependent ubiquitylome in response to mitochondrial depolarization." Nature **496**(7445): 372-376.

Shirihai, O. S., M. Song, et al. (2015). "How mitochondrial dynamism orchestrates mitophagy." Circulation research **116**(11): 1835-1849.

Song, M., K. Mihara, et al. (2015). "Mitochondrial fission and fusion factors reciprocally orchestrate mitophagic culling in mouse hearts and cultured fibroblasts." Cell metabolism **21**(2): 273-285.

Tanaka, A., M. M. Cleland, et al. (2010). "Proteasome and p97 mediate mitophagy and degradation of mitofusins induced by Parkin." J Cell Biol **191**(7): 1367-1380.

Valente, E. M., P. M. Abou-Sleiman, et al. (2004). "Hereditary early-onset Parkinson's disease caused by mutations in PINK1." Science **304**(5674): 1158-1160.

Yang, Y., S. Gehrke, et al. (2006). "Mitochondrial pathology and muscle and dopaminergic neuron degeneration caused by inactivation of Drosophila Pink1 is rescued by Parkin." Proceedings of the National Academy of Sciences of the United States of America **103**(28): 10793-10798.

Youle, R. J. and D. P. Narendra (2011). "Mechanisms of mitophagy." Nature reviews. Molecular cell biology **12**(1): 9-14.

Yue, W., Z. Chen, et al. (2014). "A small natural molecule promotes mitochondrial fusion through inhibition of the deubiquitinase USP30." Cell research **24**(4): 482-496.

Yun, J., R. Puri, et al. (2014). "MUL1 acts in parallel to the PINK1/parkin pathway in regulating mitofusin and compensates for loss of PINK1/parkin." eLife **3**: e01958.

Zhang, T., P. Mishra, et al. (2017). "Valosin-containing protein (VCP/p97) inhibitors relieve Mitofusin-dependent mitochondrial defects due to VCP disease mutants." eLife **6**.

Ziviani, E., R. N. Tao, et al. (2010). "Drosophila parkin requires PINK1 for mitochondrial translocation and ubiquitinates mitofusin." Proceedings of the National Academy of Sciences of the United States of America **107**(11): 5018-5023.

Ziviani, E., R. N. Tao, et al. (2010). "Drosophila parkin requires PINK1 for mitochondrial translocation and ubiquitinates mitofusin." Proc Natl Acad Sci U S A **107**(11): 5018-5023.

CHAPTER FOUR

CONCLUSION

Mutations in *PINK1* and *parkin* cause autosomal recessive forms of Parkinson's disease. (Kitada, Asakawa et al. 1998; Valente, Abou-Sleiman et al. 2004). Loss of PINK1 and Parkin lead to severe mitochondrial defects in *Drosophila* (Clark, Dodson et al. 2006; Park, Lee et al. 2006; Yang, Gehrke et al. 2006). Utilizing this strong mitochondrial phenotype as a disease marker, we performed a targeted overexpression screening to identify molecule that could compensate the defects in both mutants. We found that **overexpression of p97/VCP, a highly conserved ATPase, suppresses the mitochondrial defects in *PINK1* and *parkin* null mutants** (Zhang, Mishra et al. 2017). Our lab and others have shown that *PINK1* and *parkin* mutants have accumulated Mitofusin (Mfn), a key molecule controls mitochondrial fusion process; Knocking down Mfn can significantly rescue the mitochondrial defects in both mutants (Deng, Dodson et al. 2008; Yang, Ouyang et al. 2008; Park, Lee et al. 2009; Yu, Sun et al. 2011). We found that **endogenous VCP negative regulates Mitofusin protein levels.** The rescue effects of VCP overexpression in *PINK1* and *parkin* mutants is achieved through its downregulation of Mfn in both mutants (Zhang, Mishra et al. 2017).

Missense mutations of p97/VCP causes multiple neurodegeneration including inclusion body myopathy, Paget disease of the bone (IBMPFD), amyotrophic lateral sclerosis (ALS), hereditary spastic paraplegia (HSP) and Charcot-Marie-Tooth (CMT2A) (Abramzon, Johnson et al. 2012; de Bot, Schelhaas et al. 2012; Gonzalez, Feely et al. 2014). **Using *Drosophila* and patients' fibroblasts, we established *in vivo* and *in vitro* IBMPFD disease models caused by the most frequent and most severe VCP mutants.** With these models, we uncovered novel disease

mechanism showing that **VCP disease mutants behave as hyperactive alleles in degrading Mfn and lead to mitochondrial defects.** Consistent with this novel mechanism, **VCP inhibitors treatment significantly reverse the disease pathology in both disease models and patients' cells**, suggesting potential therapeutic values for this devastating disease (Zhang, Mishra et al. 2017).

Parkin encodes a conserved E3 ligase and Mitofusins are key substrates of Parkin ubiquitination both *in vivo* and *in vitro* (Ziviani, Tao et al. 2010; Chan, Salazar et al. 2011; Sarraf, Raman et al. 2013; Yun, Puri et al. 2014). Yet the key lysine on which Parkin build ubiquitin chain on Mitofusin is not known. **We identified the conserved key lysine site in Mfn in *Drosophila* and in both Mfn1 and Mfn2 in mammalian cells.** Mutations of the conserved lysine to arginine significantly decrease Mitofusins' ubiquitination and degradation by Parkin both *in vivo* and *in vitro*. **Mutations of the conserved lysine site lead to stabilized Mitofusin protein levels and severe tissue defects *in vivo* and delay Parkin-mediated mitophagy in mammalian cells.** Our works uncover the important regulatory role of Mitofusins in mitochondrial quality control and tissue health.

FUTURE DIRECTIONS

1. Parkinson's disease

1.1 Mitochondria as a therapeutic target

The established clinical pharmaceutical treatment for Parkinson's disease is neuronal transmitter replacement: to supplement dopamine in various delivery forms, activate dopamine receptors, or counteract with anti-cholinergic medications (Tarsy 2018), which can slow down the progression of Parkinson's disease, but provide long-term therapeutic effects. Novel therapeutic

approaches such as gene therapy of targeted viral delivery of neurotrophic factor such as glial-derived neurotrophic factor (GDNF) and neurturin (NRTN) or dopamine-producing enzyme aromatic L-amino acid decarboxylase (AADC) and tyrosine hydroxylase (TH) in the substantia nigra in human patients did not yield satisfactory results (Bartus, Weinberg et al. 2014; Kirik, Cederfjall et al. 2017); cell replacement therapy using human pluripotent stem cell (hPSC)-derived or induced pluripotent stem cells (iPSCs)-derived dopaminergic neurons still have numerous technical barriers before clinical application (Xiao, Ng et al. 2016; Dhivya and Balachandar 2017). The rationale of these approaches is dopamine-oriented, which aims to either replace the demised dopaminergic neurons or replace the deficient neuronal transmitter due to the death of neurons that produce them.

Without understanding and tackling the key questions such as the pathological mechanism that leads to the neuronal death, it is not surprising that pure replacements will not stop or reverse the disease pathology and fundamentally cure the disease. The broad spectrum of symptoms and pathology involvement of low brain stem and neocortex strongly suggest that the pathogenesis of Parkinson's disease is beyond dopaminergic neuronal loss in substantia nigra (Braak, Del Tredici et al. 2003; Dickson 2012).

The identification of mutations in genes that critical for mitochondrial integrity accentuates the mitochondrial dysfunctions as a key mechanism of disease onset (Hu and Wang 2016). Our work has demonstrated that using *Drosophila* and patient fibroblasts, we could establish reliable *in vivo* and *in vitro* disease models with strong mitochondrial defects. Based on these phenotypes such as defects in fusion/fission dynamic (Clark, Dodson et al. 2006; Park, Lee et al. 2006; Yang, Gehrke et al. 2006) or defects in biogenesis and respiration in patient cells (Grunewald, Voges et al. 2010; Zanellati, Monti et al. 2015; Teves, Bhargava et al. 2017), genetic or compound screening

could be performed to identify potential candidates to reverse the disease pathology. The candidates identified will not only understanding the disease mechanism but also provide more specific therapeutic targets.

1.2. Parkin Ubiquitination and mitophagy modification

Upon outside perturbance such as depolarization after CCCP treatment, Parkin translocates to mitochondria, ubiquitinates and degrades mitochondrial outermembrane proteins. A large profile of outermembrane proteins have been recorded to be Parkin substrates (Chan, Salazar et al. 2011; Sarraf, Raman et al. 2013). The fact that Mitofusin is ubiquitinated by Parkin is repeatedly reported, yet the biological consequence of the posttranslational modification is not understood largely due to that the key lysine is not identified. Our data suggest Mfn ubiquintation is critical to tissue health and mitophagy process. With the presence of Mitofusin, mitophagy is suppressed; while removing Mitofusin accelerated mitophagy process, indicating the regulatory role of Mitofusin in mitochondrial quality control.

Mitophagy process is impaired in aging and disease setting, whereas promoting mitophagy is considered as a potential therapeutic approach (Fivenson, Lautrup et al. 2017). USP 30 is a deubiquintinase that counteract the Parkin-mediated mitophagy, loss of which rescue the defective mitophay caused by pathogenic mutations in *parkin* suggesting the beneficial role of promoting mitophagy (Bingol, Tea et al. 2014). Based on what we have find regarding Mitofusin, it will be interesting to identify the lysine sites of other substrates that are critical for Parkin ubiquitination to unveil other key molecules in the either drive or hinder mitophagy, which could be potential targets to manipulate in the disease and aging settings.

2. Neurodegenerative diseases by VCP mutants

2.1. VCP disease mutants and Cofactor

We provide strong evidence that mitochondrial defects are one of the key pathological mechanisms in VCP disease. Despite the robust rescue effects of VCP inhibitors, we aim to identify alternative strategies for blocking mitochondrial defects in VCP disease for the following reasons. VCP has its unique property that it interacts with substrates through various co-factors. Each substrate has its own co-factor, making it a protein with diverse functions and challenging to identify the molecular basis of phenotypes associated with disease mutations. VCP inhibition is relatively broad-ranged; identify a more specific target in mitochondrial defects caused by VCP disease mutants will help relieve the defects without affecting other pathways.

We found VCP specifically targets Mfn to regulate mitochondrial fusion and N domain of VCP is required for the interaction. Yet, the cofactor of VCP/Mfn interaction is not known. The well-established cofactors of VCP are Npl4 (nuclear protein localization homolog 4)-Ufd1 (ubiquitin fusion degradation1) hetero-dimer, p47 and UBXD1 (UBX Domain-containing Protein 1)(Meyer, Bug et al. 2012). They all have conserved *Drosophila* homologues. Because VCP disease mutants behave hyperactively degrading Mfn and cause mitochondrial defects, we hypothesize by downregulating the cofactor of VCP/Mfn interaction, we shall block excessive VCP disease mutants/Mfn interaction and hence halt mitochondrial damage and disease progress. We are currently in the process of identify VCP/Mfn cofactor.

2.2. VCP disease models and VCP inhibitors

We worked on two VCP disease mutants as R155H is the most frequent and A232E displays the most severe clinical manifestation (Kimonis, Fulchiero et al. 2008; Ritson, Custer et al. 2010). Currently there are more than 30 disease-causing mutations have been identified and cause multiple neurodegenerative disease as mentioned above. Biochemical studies have unanimously showed that VCP disease-causing mutations obtain enhanced ATPase activity in hydrolyzing ATP

(Weihl, Dalal et al. 2006; Manno, Noguchi et al. 2010; Niwa, Ewens et al. 2012; Tang and Xia 2013; Zhang, Gui et al. 2015), favoring the hyperactive nature and the potential broad clinical application of VCP inhibitors for the treatment of VCP mutants mediated degenerative disease.

Our work has demonstrated that utilizing both *Drosophila* and patients' cells, we are able to establish reliable *in vivo* and *in vitro* disease models, which provide great platforms for unravelling disease mechanism and exploring therapeutic targets. Generation of more disease models caused by VCP mutants using *Drosophila* and patients' sample and further explore the therapeutic effects of VCP inhibitors will have profound clinical value.

Reference

Abramzon, Y., J. O. Johnson, et al. (2012). "Valosin-containing protein (VCP) mutations in sporadic amyotrophic lateral sclerosis." Neurobiology of aging **33**(9): 2231 e2231-2231 e2236.

Bartus, R. T., M. S. Weinberg, et al. (2014). "Parkinson's disease gene therapy: success by design meets failure by efficacy." Mol Ther **22**(3): 487-497.

Bingol, B., J. S. Tea, et al. (2014). "The mitochondrial deubiquitinase USP30 opposes parkin-mediated mitophagy." Nature **510**(7505): 370-375.

Braak, H., K. Del Tredici, et al. (2003). "Staging of brain pathology related to sporadic Parkinson's disease." Neurobiol Aging **24**(2): 197-211.

Chan, N. C., A. M. Salazar, et al. (2011). "Broad activation of the ubiquitin-proteasome system by Parkin is critical for mitophagy." Hum Mol Genet **20**(9): 1726-1737.

Clark, I. E., M. W. Dodson, et al. (2006). "Drosophila pink1 is required for mitochondrial function and interacts genetically with parkin." Nature **441**(7097): 1162-1166.

de Bot, S. T., H. J. Schelhaas, et al. (2012). "Hereditary spastic paraplegia caused by a mutation in the VCP gene." Brain **135**(Pt 12): e223; author reply e224.

Deng, H., M. W. Dodson, et al. (2008). "The Parkinson's disease genes pink1 and parkin promote mitochondrial fission and/or inhibit fusion in Drosophila." Proc Natl Acad Sci U S A **105**(38): 14503-14508.

Dhivya, V. and V. Balachandar (2017). "Cell replacement therapy is the remedial solution for treating Parkinson's disease." Stem Cell Investig **4**: 59.

Dickson, D. W. (2012). "Parkinson's disease and parkinsonism: neuropathology." Cold Spring Harb Perspect Med **2**(8).

Fivenson, E. M., S. Lautrup, et al. (2017). "Mitophagy in neurodegeneration and aging." Neurochem Int **109**: 202-209.

Gonzalez, M. A., S. M. Feely, et al. (2014). "A novel mutation in VCP causes Charcot-Marie-Tooth Type 2 disease." Brain : a journal of neurology **137**(Pt 11): 2897-2902.

Grunewald, A., L. Voges, et al. (2010). "Mutant Parkin impairs mitochondrial function and morphology in human fibroblasts." PLoS One **5**(9): e12962.

Hu, Q. and G. Wang (2016). "Mitochondrial dysfunction in Parkinson's disease." Transl Neurodegener **5**: 14.

Kimonis, V. E., E. Fulchiero, et al. (2008). "VCP disease associated with myopathy, Paget disease of bone and frontotemporal dementia: review of a unique disorder." Biochimica et biophysica acta **1782**(12): 744-748.

Kirik, D., E. Cederfjall, et al. (2017). "Gene therapy for Parkinson's disease: Disease modification by GDNF family of ligands." Neurobiol Dis **97**(Pt B): 179-188.

Kitada, T., S. Asakawa, et al. (1998). "Mutations in the parkin gene cause autosomal recessive juvenile parkinsonism." Nature **392**(6676): 605-608.

Manno, A., M. Noguchi, et al. (2010). "Enhanced ATPase activities as a primary defect of mutant valosin-containing proteins that cause inclusion body myopathy associated with Paget disease of bone and frontotemporal dementia." Genes to cells : devoted to molecular & cellular mechanisms **15**(8): 911-922.

Meyer, H., M. Bug, et al. (2012). "Emerging functions of the VCP/p97 AAA-ATPase in the ubiquitin system." Nat Cell Biol **14**(2): 117-123.

Niwa, H., C. A. Ewens, et al. (2012). "The role of the N-domain in the ATPase activity of the mammalian AAA ATPase p97/VCP." The Journal of biological chemistry **287**(11): 8561-8570.

Park, J., G. Lee, et al. (2009). "The PINK1-Parkin pathway is involved in the regulation of mitochondrial remodeling process." Biochemical and biophysical research communications **378**(3): 518-523.

Park, J., S. B. Lee, et al. (2006). "Mitochondrial dysfunction in Drosophila PINK1 mutants is complemented by parkin." Nature **441**(7097): 1157-1161.

Ritson, G. P., S. K. Custer, et al. (2010). "TDP-43 mediates degeneration in a novel Drosophila model of disease caused by mutations in VCP/p97." The Journal of neuroscience : the official journal of the Society for Neuroscience **30**(22): 7729-7739.

Sarraf, S. A., M. Raman, et al. (2013). "Landscape of the PARKIN-dependent ubiquitylome in response to mitochondrial depolarization." Nature **496**(7445): 372-376.

Tang, W. K. and D. Xia (2013). "Altered intersubunit communication is the molecular basis for functional defects of pathogenic p97 mutants." The Journal of biological chemistry **288**(51): 36624-36635.

Teves, J. M. Y., V. Bhargava, et al. (2017). "Parkinson's Disease Skin Fibroblasts Display Signature Alterations in Growth, Redox Homeostasis, Mitochondrial Function, and Autophagy." Front Neurosci **11**: 737.

Valente, E. M., P. M. Abou-Sleiman, et al. (2004). "Hereditary early-onset Parkinson's disease caused by mutations in PINK1." Science **304**(5674): 1158-1160.

Weihl, C. C., S. Dalal, et al. (2006). "Inclusion body myopathy-associated mutations in p97/VCP impair endoplasmic reticulum-associated degradation." Human molecular genetics **15**(2): 189-199.

Xiao, B., H. H. Ng, et al. (2016). "Induced pluripotent stem cells in Parkinson's disease: scientific and clinical challenges." J Neurol Neurosurg Psychiatry **87**(7): 697-702.

Yang, Y., S. Gehrke, et al. (2006). "Mitochondrial pathology and muscle and dopaminergic neuron degeneration caused by inactivation of Drosophila Pink1 is rescued by Parkin." Proceedings of the National Academy of Sciences of the United States of America **103**(28): 10793-10798.

Yang, Y., Y. Ouyang, et al. (2008). "Pink1 regulates mitochondrial dynamics through interaction with the fission/fusion machinery." Proceedings of the National Academy of Sciences of the United States of America **105**(19): 7070-7075.

Yu, W., Y. Sun, et al. (2011). "The PINK1/Parkin pathway regulates mitochondrial dynamics and function in mammalian hippocampal and dopaminergic neurons." Human molecular genetics **20**(16): 3227-3240.

Yun, J., R. Puri, et al. (2014). "MUL1 acts in parallel to the PINK1/parkin pathway in regulating mitofusin and compensates for loss of PINK1/parkin." Elife **3**: e01958.

Zanellati, M. C., V. Monti, et al. (2015). "Mitochondrial dysfunction in Parkinson disease: evidence in mutant PARK2 fibroblasts." Front Genet **6**: 78.

Zhang, T., P. Mishra, et al. (2017). "Valosin-containing protein (VCP/p97) inhibitors relieve Mitofusin-dependent mitochondrial defects due to VCP disease mutants." Elife **6**.

Zhang, X., L. Gui, et al. (2015). "Altered cofactor regulation with disease-associated p97/VCP mutations." Proceedings of the National Academy of Sciences of the United States of America **112**(14): E1705-1714.

Ziviani, E., R. N. Tao, et al. (2010). "Drosophila parkin requires PINK1 for mitochondrial translocation and ubiquitinates mitofusin." Proceedings of the National Academy of Sciences of the United States of America **107**(11): 5018-5023.